NATIONAL ADVISORY COMMITTEE FOR AERONAUTICS

TECHNICAL NOTE 2409

SUMMARY OF METHODS FOR CALCULATING DYNAMIC LATERAL

STABILITY AND RESPONSE AND FOR ESTIMATING

LATERAL STABILITY DERIVATIVES

By John P. Campbell and Marion O. McKinney

Langley Aeronautical Laboratory
Langley Field, Va.

NACA

TABLE OF CONTENTS

NATIONAL ADVISORY COMMITTEE FOR AERONAUTICS

TECHNICAL NOTE 2409

SUMMARY OF METHODS FOR CALCULATING DYNAMIC LATERAL

STABILITY AND RESPONSE AND FOR ESTIMATING

LATERAL STABILITY DERIVATIVES

By John P. Campbell and Marion O. McKinney

S U M M A R Y

A summary of methods for making dynamic lateral stability and response calculations and for estimating the aerodynamic stability derivatives required for use in these calculations is presented. The processes of performing calculations of the time histories of lateral motions, of the period and damping of these motions, and of the lateral stability boundaries are presented as a series of simple straightforward steps. Existing methods for estimating the stability derivatives are summarized and, in some cases, simple new empirical formulas are presented. Reference is also made to reports presenting experimental data that should be useful in making estimates of the derivatives. Detailed estimation methods are presented for low-subsonic-speed conditions but only a brief discussion and a list of references are given for transonic- and supersonic-speed conditions.

I N T R O D U C T I O N

Dynamic lateral stability has not received widespread attention in the past because it has not generally been a serious problem in the design of airplanes. Consideration of dynamic lateral stability has recently become more important, however, because current design trends toward the use of low aspect ratio, sweepback, and higher wing loading have, in many cases, led to unsatisfactory dynamic lateral stability. Airplane designers are therefore finding it necessary to make such calculations in connection with the design and modification of airplanes. In many cases these calculations are difficult to perform for designers who have had no previous experience in theoretical stability work because most of the published theoretical analyses are not presented in a form that is especially suited to the computation of dynamic stability. The estimation of the stability derivatives required in dynamic stability calculations has also been found to be difficult in many cases. Although theoretical and experimental data on these derivatives have appeared in

numerous publications, no single publication has presented methods for estimating the derivatives for all types of airplanes.

One approach to a presentation of methods of calculating stability and estimating stability derivatives in a form suitable for use by designers was made by Zimmerman in reference 1. Although this report has proved to be of valuable assistance to designers in making dynamic stability calculations, recent trends in airplane design have caused its usefulness to be seriously limited. For example, the equations of reference 1 do not include the product-of-inertia terms which have been shown by recent studies to be very important in some cases. (See references 2 and 3.) Moreover, the calculation of the time histories of lateral motions, one type of calculation that has been the subject of increasing interest in the last few years (references 4 to 7), is not covered in reference 1. The methods of estimating stability derivatives presented in reference 1 are also limited because they apply only to airplanes having unswept wings with an aspect ratio of 6 operating at speeds at which compressibility effects are negligible. The purpose of the present paper is to extend the methods of reference 1 to include the methods of computation which are of current interest to designers and to include methods of estimating derivatives for configurations and flight conditions which are now being considered.

This paper summarizes and reduces to simple straightforward steps methods for computing the time histories of lateral motions, the period and damping of these motions, and the lateral stability boundaries. Existing methods of estimating stability derivatives for a variety of airplane configurations are summarized and, in some cases, simple new empirical formulas are presented. Reference is also made to reports presenting experimental data that should be useful in making estimates of these derivatives.

SYMBOLS

All forces and moments are referred to the stability system of axes which is defined in figure 1. The following definitions apply to the symbols except where they are otherwise defined:

m mass of airplane, slugs

S wing area, square feet

$\bar{c}$ wing mean chord, feet (b/A)

b wing span, feet

y_d span of that part of wing that has tip dihedral, feet

l tail length (distance from center of pressure of vertical tail to center of gravity, measured parallel to longitudinal stability axis; values of l must be calculated for each angle of attack), feet

h average fuselage height at wing root; feet

w average fuselage width at wing root, feet

z_w vertical distance of quarter chord of wing root chord from fuselage center line, positive downward, feet

s nondimensional time parameter based on span (Vt/b)

x longitudinal distance rearward from airplane center of gravity to wing aerodynamic center, feet

d longitudinal distance from leading edge of vertical tail chord to horizontal tail aerodynamic center, feet (see fig. 6)

z_H vertical distance from horizontal tail to base of vertical tail, feet (see fig. 6)

z height of center of pressure of vertical tail above longitudinal stability axis; values of z must be calculated for each angle of attack, feet

A aspect ratio

Λ sweepback of wing quarter-chord line, degrees

λ taper ratio (Tip chord/Root chord); also, differential operator in Laplace transform

Γ dihedral angle, degrees (see sketch of fig. 9)

Γ_T dihedral angle of wing tip, degrees

t time, seconds

V airspeed, feet per second

k_{X_o} radius of gyration about principal longitudinal axis of inertia, feet

k_{Z_o} radius of gyration about principal normal axis of inertia, feet

k_X radius of gyration about X axis, feet

$$\left(\sqrt{k_{X_0}{}^2\cos^2\eta + k_{Z_0}{}^2\sin^2\eta}\right)$$

k_Z radius of gyration about Z axis, feet

$$\left(\sqrt{k_{Z_0}{}^2\cos^2\eta + k_{X_0}{}^2\sin^2\eta}\right)$$

K_{X_0} k_{X_0}/b

K_{Z_0} k_{Z_0}/b

K_X k_X/b

K_Z k_Z/b

k_{XZ} product-of-inertia factor $\left(\left(k_{Z_0}{}^2 - k_{X_0}{}^2\right)\sin\eta\cos\eta\right)$

$$K_{XZ} = \frac{k_{XZ}}{b^2}$$

$$K_1 = \frac{K_{XZ}}{K_X{}^2}$$

$$K_2 = \frac{K_{XZ}}{K_Z{}^2}$$

η angle of attack of principal longitudinal axis of inertia, degrees (see fig. 2)

γ angle of climb, degrees (see fig. 2)

α angle of attack of longitudinal body axis, degrees (see fig. 2)

ϵ angle between principal longitudinal axis of inertia and longitudinal body axis, degrees (see fig. 2)

ρ air density, slugs per cubic foot

ϕ angle of bank, radians

ψ	angle of yaw, radians
β	angle of sideslip, radians
p	rolling velocity, radians per second $(d\phi/dt)$
r	yawing velocity, radians per second $(d\psi/dt)$
ϕ_o	initial angle of bank, radians
ψ_o	initial angle of yaw, radians
β_o	initial angle of sideslip, radians
$(D\phi)_o$	nondimensional initial rolling velocity $(d\phi/d\sigma)$
$(D\psi)_o$	nondimensional initial yawing velocity $(d\psi/d\sigma)$
R	Routh's discriminant or real part of complex root $R + Ii$
I	imaginary part of complex root $R + Ii$
A,B,C,D,E	coefficients of the characteristic biquadratic equation
$P_1,P_2, \ldots P_7$	factors of the B, C, and D coefficients
$\lambda_1,\lambda_2,\lambda_3,\lambda_4$	roots of characteristic biquadratic equation
D	differential operator $(d/d\sigma)$
P	period of the lateral oscillation, seconds
$T_{1/2}$	time to damp to one-half amplitude, seconds
τ	time conversion factor $(m/\rho SV)$
σ	nondimensional time factor (t/τ)
μ	relative density factor $(m/\rho Sb)$
L_c	impressed rolling moment, foot-pounds
N_c	impressed yawing moment, foot-pounds
Y_c	impressed lateral force, pounds

C_{l_c} impressed rolling-moment coefficient

C_{n_c} impressed yawing-moment coefficient

C_{Y_c} impressed lateral-force coefficient

C_L lift coefficient (Lift/qS)

C_D drag coefficient (Drag/qS)

C_l rolling-moment coefficient (Rolling moment/qSb)

C_n yawing-moment coefficient (Yawing moment/qSb)

C_Y lateral-force coefficient (Lateral force/qS)

q dynamic pressure, pounds per square foot $\left(\frac{1}{2}\rho V^2\right)$

$$C_{L_\alpha} = \frac{\partial C_L}{\partial \alpha}$$

$$\left(C_{D_o}\right)_\alpha = \frac{\partial}{\partial \alpha}\left(C_D - \frac{C_L^2}{\pi A}\right)$$

$$C_{D_o} = C_D - \frac{C_L^2}{\pi A}$$

$$C_{l_\beta} = \frac{\partial C_l}{\partial \beta}$$

$$C_{n_\beta} = \frac{\partial C_n}{\partial \beta}$$

$$C_{Y_\beta} = \frac{\partial C_Y}{\partial \beta}$$

$$C_{l_p} = \frac{\partial C_l}{\partial \frac{pb}{2V}}$$

$$C_{n_p} = \frac{\partial C_n}{\partial \frac{pb}{2V}}$$

$$C_{Y_p} = \frac{\partial C_Y}{\partial \frac{pb}{2V}}$$

$$C_{l_r} = \frac{\partial C_l}{\partial \frac{rb}{2V}}$$

$$C_{n_r} = \frac{\partial C_n}{\partial \frac{rb}{2V}}$$

$$C_{Y_r} = \frac{\partial C_Y}{\partial \frac{rb}{2V}}$$

$$C_{l_{\beta_\Gamma}} = \frac{dC_{l_\beta}}{d\Gamma}$$

$$l_\beta = \frac{\mu C_{l_\beta}}{2K_X^2}$$

$$n_\beta = \frac{\mu C_{n_\beta}}{2K_Z^2}$$

$$y_\beta = \frac{C_{Y_\beta}}{2}$$

$$l_p = \frac{C_{l_p}}{4K_X^2}$$

$$n_p = \frac{C_{n_p}}{4K_Z^2}$$

$$y_p = \frac{C_{Y_p}}{4\mu}$$

$$l_r = \frac{C_{l_r}}{4K_X^2}$$

$$n_r = \frac{C_{n_r}}{4K_Z^2}$$

$$y_r = \frac{C_{Y_r}}{4\mu}$$

$$l_c = \frac{\mu C_{l_c}}{2K_X{}^2}$$

$$n_c = \frac{\mu C_{n_c}}{2K_Z{}^2}$$

$$y_c = \frac{C_{Y_c}}{2}$$

$\left(\Delta C_{n_p}\right)_1$ increment in C_{n_p} produced by lift and induced-drag forces

$\left(\Delta C_{n_p}\right)_2$ increment in C_{n_p} produced by drag not associated with lift

H   horizontal tail

a_o section lift curve slope

Subscripts:

wing   wing

fus   fuselage

tail   used to designate vertical tail

design   used to designate design under consideration

data   used to designate design for which force-test data are available

exp   experimental

V-tail   V-tail

e   effective

H   horizontal tail

C A L C U L A T I O N   O F   L A T E R A L   S T A B I L I T Y

A N D   R E S P O N S E

Various types of calculations may be performed to indicate in some way the stability of an airplane or the response to gust disturbances and control manipulations. The calculations most commonly made are calculations of time histories of disturbed motions, period and damping of the free motions, and spiral and oscillatory stability boundaries (lines of neutral damping of the spiral mode and of the lateral oscillations). Step-by-step procedures for performing these types of calculations are explained in the text and derivations and additional pertinent material are presented in appendixes A to D.

The period and damping calculations are the easiest of the three types to perform. For this reason, and because the dynamic lateral stability of airplanes is at present specified in the flying-qualities requirements in terms of the period and damping of the lateral oscillation, period and damping calculations are probably the most commonly performed.

Recent dynamic stability work has indicated, however, that the period and damping characteristics of the free motions of an airplane are not always a sufficient indication of whether the dynamic behavior of an airplane following various types of disturbances will be considered satisfactory. For this reason the calculation of time histories of the motions of airplanes is becoming more common despite the fact that these calculations are fairly laborious. The increasing use of automatic computing machines has also made the calculation of motions more popular.

For many years, calculations of stability boundaries were the type of calculation most commonly performed. In recent years, however, stability boundaries have not been considered to give an adequate indication of stability. Since boundaries are useful in some cases, however, (for example, for quick approximation of the effects of changes in dihedral and tail area) the methods of calculating the spiral and oscillatory stability boundaries are described herein. Lines of constant period and damping of the lateral oscillation are related to stability boundaries (lines of neutral stability). In some cases these lines of constant period and damping may prove more useful than boundaries. Since no extensive use has been made of lines of constant period and damping, however, the methods of calculating these lines (presented in references 8 and 9) are not given in the present paper.

The equations and methods of calculation presented in the present paper deal specifically with the inherent motions of airplanes for the

case of three degrees of freedom (roll, yaw, and sideslip) and linear
stability derivatives. In order to perform similar calculations for
cases involving additional degrees of freedom, nonlinear derivatives,
or autopilots with time lag, special equations are required. The
methods and equations for treating these cases are presented in refer-
ences 10 to 18. Additional degrees of freedom for the case of free
controls are treated in references 16 to 18 and for the case of fuel
sloshing are treated in reference 10. The use of nonlinear derivatives
in stability calculations is covered in reference 11. Methods of
treating the effect of autopilots, including the effect of time lag in
the autopilot are presented in references 12 to 15 and 19.

For some cases the effects of aerodynamic time lag are important.
There are two different sources of such lag: (1) the time required for
an aerodynamic impulse to travel from one component of the airplane to
another (for example, the time required for a change in sidewash at the
wing to reach the tail - a phenomenon commonly referred to as lag of
sidewash); and (2) the time required for the growth and decay of the
aerodynamic loads on the airplane components. For both of these cases
the time-lag effects usually become increasingly important as the period
of the lateral oscillation decreases. The effects of the first type of
time lag can be accounted for in some cases by modification of the sta-
bility derivatives. For example, the effect of the lag of sidewash on
the derivative C_{n_r} is discussed subsequently under the section on
"Estimation of Lateral Stability Derivatives". In many cases, how-
ever, both types of time lag will require special stability equations.
No general treatment of these cases has been published but an indi-
cation of the method of treatment may be obtained from the treatments
of autopilot lag in references 13 and 15.

CALCULATION OF PERIOD AND DAMPING

As pointed out in references 1 and 2, the period and damping of the
various modes of the lateral motion may be calculated from the roots of
the characteristic equation

$$A\lambda^4 + B\lambda^3 + C\lambda^2 + D\lambda + E = 0$$

by the equations

$$P = \frac{2\pi}{I}\tau$$

and

$$T_{1/2} = -\frac{\log_e 2}{R}\tau \approx -\frac{0.693}{R}\tau$$

where R represents a real root λ or the real part of a complex root
λ = R ± Ii and I represents the imaginary part of a complex root.
Negative values of $T_{1/2}$ represent the time required to double amplitude
for unstable modes of the motion.

The values of the coefficients A, B, C, D, and E may be
obtained by the method given in steps 1, 2, and 3 of the section on
"Calculation of Motions". If the period and time to damp are to be cal-
culated for a number of related cases, however, the values of the coef-
ficients A, B, C, D, and E may be more conveniently calculated by
a tabular procedure such as that shown as table I for making boundary
calculations.

Methods of determining the roots of the biquadratic characteristic
equation are presented in appendix C.

CALCULATION OF MOTIONS

Calculation of the lateral motions of an airplane involves the
integration of three simultaneous differential equations (see
appendix A) to obtain a general solution in terms of the mass and
aerodynamic parameters of the airplane. The general equations, once
obtained, can then be used to obtain numerically the motions of any
airplane in terms of the variation with time of the angles of bank, yaw,
and sideslip or some function of these angles such as rolling or yawing
velocity. Various methods, such as those given in references 20 to 22,
are of course available for integrating the differential equations.
Since the problems met in airplane dynamics are fairly complex, however,
many of these methods are not suitable because of the difficulties of
computation that arise. The method given in reference 4 (based on the
Heaviside operational calculus) is satisfactory for calculating the
forced motions following application of external forces or moments but,
without modification, this method cannot be used to calculate the motions
resulting from initial displacements in bank, yaw, or sideslip or from
initial values of rolling or yawing angular velocity. A solution based
on the Laplace transformation is more satisfactory than that based on the
Heaviside operational calculus because it permits direct calculation of
the free motions following any initial condition, in addition to calcu-
lation of the forced motions following application of external forces and
moments. The application of the Laplace transformation to the calculation
of lateral motions is outlined in appendix B. The material presented in
this appendix is similar to the work presented in references 5 and 6
except that the mass and aerodynamic stability derivatives have been com-
bined as shown in appendix A to reduce the number of arithmetical and
algebraic processes required in numerical solutions.

The process of calculating the motions is presented as a series of simple though lengthy arithmetical and algebraic steps so that an understanding of the calculus involved in solving the differential equations is not required. The method as shown is suitable for calculating the motions as variations of ϕ, ψ, β, p, and r with time for the case of the free motions following initial angular displacements (ϕ_0, ψ_0, and β_0) and angular velocities $(D\phi)_0$ and $(D\psi)_0$ and for the case of the forced motions resulting from constant impressed forces and moments (L_c, N_c, and Y_c). These are the cases for which motions are usually calculated. It is also possible to calculate the motions resulting from impressed forces and moments which are arbitrary functions of time by the methods explained in references 6 and 7.

Motions Resulting from Initial Angular Displacements and Angular

Velocities and from Constant Impressed Forces and Moments

The six steps involved in obtaining a specific solution for the lateral motions of an airplane are:

Step 1: Determine values of the following parameters:

(a) Mass characteristics:

$$m, \quad k_{X_0}, \quad k_{Z_0}, \quad \eta, \text{ and } \rho$$

(b) Geometric characteristics:

$$S \text{ and } b$$

(c) Flight conditions:

$$V, \quad C_L, \text{ and } \gamma$$

(d) Aerodynamic stability derivatives:

$$C_{l_\beta}, \quad C_{n_\beta}, \quad C_{Y_\beta}, \quad C_{l_p}, \quad C_{n_p}, \quad C_{Y_p}, \quad C_{l_r}, \quad C_{n_r}, \text{ and } C_{Y_r}$$

The methods of determining the values of the aerodynamic stability derivatives are given in subsequent sections of this paper.

In cases where impressed forces and moments are used as disturbances, determine the values of the factors

$$C_{l_c}, \quad C_{n_c}, \quad C_{Y_c}$$

that are appropriate to the particular problem.

Step 2: From the known factors, evaluate the following parameters which are the stability derivatives in the form in which they are used in the calculation of motions:

$$K_1 = \frac{K_{XZ}}{K_X{}^2} \qquad K_2 = \frac{K_{XZ}}{K_Z{}^2} \qquad \tau = \frac{m}{\rho SV} \qquad \mu = \frac{m}{\rho Sb}$$

$$l_\beta = \frac{\mu}{2K_X{}^2} C_{l_\beta} \qquad n_\beta = \frac{\mu}{2K_Z{}^2} C_{n_\beta} \qquad y_\beta = \frac{1}{2} C_{Y_\beta}$$

$$l_p = \frac{1}{4K_X{}^2} C_{l_p} \qquad n_p = \frac{1}{4K_Z{}^2} C_{n_p} \qquad y_p = \frac{1}{4\mu} C_{Y_p}$$

$$l_r = \frac{1}{4K_X{}^2} C_{l_r} \qquad n_r = \frac{1}{4K_Z{}^2} C_{n_r} \qquad y_r = \frac{1}{4\mu} C_{Y_r}$$

Also, when impressed forces and moments are used, evaluate

$$l_c = \frac{\mu}{2K_X{}^2} C_{l_c} \qquad n_c = \frac{\mu}{2K_Z{}^2} C_{n_c} \qquad y_c = \frac{1}{2} C_{Y_c}$$

The values of $K_X{}^2$, $K_Z{}^2$, and K_{XZ} can be determined from the following expressions

$$K_X{}^2 = K_{X_0}{}^2 \cos^2\eta + K_{Z_0}{}^2 \sin^2\eta$$

$$K_Z{}^2 = K_{Z_0}{}^2 \cos^2\eta + K_{X_0}{}^2 \sin^2\eta$$

$$K_{XZ} = \left(K_{Z_0}{}^2 - K_{X_0}{}^2\right) \sin\eta \cos\eta$$

where

$$K_{X_0} = \frac{k_{X_0}}{b}$$

$$K_{Z_0} = \frac{k_{Z_0}}{b}$$

Step 3: Solve for the values of the appropriate ones of the following coefficients from equations (1) to (4):

In all cases solve for the values of A, B, C, D, and E:

$$A = 1 - K_1 K_2$$

$$B = P_1 - A y_\beta$$

$$C = -P_1 y_\beta + P_2 + P_5 y_p + P_6 y_r - P_6$$

$$D = P_5 \frac{C_L}{2} + P_6 \frac{C_L}{2} \tan \gamma + P_7$$

$$E = P_3 \frac{C_L}{2} + P_4 \frac{C_L}{2} \tan \gamma$$

$$(1)$$

where

$$P_1 = -l_p - n_r + K_1 n_p + K_2 l_r$$

$$P_2 = l_p n_r - l_r n_p$$

$$P_3 = l_\beta n_r - l_r n_\beta$$

$$P_4 = l_p n_\beta - l_\beta n_p$$

$$P_5 = K_1 n_\beta - l_\beta$$

$$P_6 = K_2 l_\beta - n_\beta$$

$$P_7 = -P_2 y_\beta + P_3 y_p + P_4 y_r - P_4$$

The quantities P_1 to P_7 are factors of the coefficients B, C, D, and E which are combinations of terms that occur frequently in calculations of motions resulting from initial angular displacements and velocities and which are consequently grouped together for convenience.

Calculate the values of a_0, a_1, . . . a_5 when solving for the angle of bank ϕ or the rolling velocity p:

$$a_0 = \phi_0 A$$

$$a_1 = \phi_0 B + (D\phi)_0 A$$

$$a_2 = \phi_0 C - \beta_0 P_5 + (D\phi)_0\left(-Ay_\beta + K_2 l_r - n_r\right) -$$
$$(D\psi)_0\left(K_1 n_r - l_r\right) + l_c - n_c K_1$$

$$a_3 = \phi_0\left(P_6 \frac{C_L}{2}\tan\gamma + P_7\right) - \psi_0 P_5 \frac{C_L}{2}\tan\gamma - \beta_0 P_3 + (D\phi)_0\left(P_6 y_r - \right.$$
$$P_6 - K_2 l_r y_\beta + n_r y_\beta\right) + (D\psi)_0\left(-P_5 y_r + P_5 + K_1 n_r y_\beta - l_r y_\beta\right) -$$
$$l_c\left(n_r + y_\beta\right) + n_c\left(K_1 y_\beta + l_r\right) - y_c P_5$$

$$a_4 = \left(\phi_0 P_4 - \psi_0 P_3 + (D\phi)_0 P_6 - (D\psi)_0 P_5\right)\frac{C_L}{2}\tan\gamma +$$
$$l_c\left(n_\beta - n_\beta y_r + n_r y_\beta\right) + \dot{n}_c\left(l_\beta y_r - l_\beta - l_r y_\beta\right) - y_c P_3$$

$$a_5 = \left(-l_c n_\beta + n_c l_\beta\right)\frac{C_L}{2}\tan\gamma$$

(2)

Calculate the values of b_0, b_1, . . ., b_5 when solving for angle of yaw ψ or the yawing velocity r:

$$b_0 = \psi_o A$$

$$b_1 = \psi_o B + (D\psi)_o A$$

$$b_2 = \psi_o C - \beta_o P_6 - (D\phi)_o \left(K_2 l_p - n_p\right) + (D\psi)_o \left(-A y_\beta + K_1 n_p - l_p\right) - l_c K_2 + n_c$$

$$b_3 = -\phi_o P_6 \frac{C_L}{2} + \psi_o \left(P_5 \frac{C_L}{2} + P_7\right) - \beta_o P_4 + (D\phi)_o \left(-P_6 y_p + K_2 l_p y_\beta - n_p y_\beta\right) + (D\psi)_o \left(P_5 y_p - K_1 n_p y_\beta + l_p y_\beta\right) + l_c \left(K_2 y_\beta + n_p\right) - n_c \left(l_p + y_\beta\right) - y_c P_6$$

$$b_4 = \left[-\phi_o P_4 + \psi_o P_3 - (D\phi)_o P_6 + (D\psi)_o P_5\right]\frac{C_L}{2} + l_c \left(n_\beta y_p - n_p y_\beta\right) + n_c \left(l_p y_\beta - l_\beta y_p\right) - y_c P_4$$

$$b_5 = \left(l_c n_\beta - n_c l_\beta\right)\frac{C_L}{2}$$

$$(3)$$

Calculate the values of c_0, c_1, ..., c_4 when solving for the angle of sideslip β:

$$c_0 = \beta_o A$$

$$c_1 = \phi_o A \frac{C_L}{2} + \psi_o A \frac{C_L}{2} \tan \gamma + \beta_o P_1 + (D\phi)_o A y_p - (D\psi)_o A(y_r - 1) + y_c A$$

$$c_2 = \phi_o P_1 \frac{C_L}{2} + \psi_o P_1 \frac{C_L}{2} \tan \gamma + \beta_o P_2 + (D\phi)_o \left[A \frac{C_L}{2} - K_2 l_p y_r + K_2 l_p + \right.$$

$$n_p y_r - n_p + \left(K_2 l_r - n_r \right) y_p \Bigg] + (D\psi)_o \left[A \frac{C_L}{2} \tan \gamma + K_1 n_p y_r - \right.$$

$$K_1 n_p - l_p y_r + l_p - \left(K_1 n_r - l_r \right) y_p \Bigg] + l_c \left(-K_2 y_r + K_2 + y_p \right) +$$

$$n_c \left(y_r - 1 - K_1 y_p \right) + y_c P_1$$

$$c_3 = \phi_o P_2 \frac{C_L}{2} + \psi_o P_2 \frac{C_L}{2} \tan \gamma + (D\phi)_o \left(-K_2 l_p \frac{C_L}{2} \tan \gamma + n_p \frac{C_L}{2} \tan \gamma + \right.$$

$$K_2 l_r \frac{C_L}{2} - n_r \frac{C_L}{2} \right) + (D\psi)_o \left(K_1 n_p \frac{C_L}{2} \tan \gamma - l_p \frac{C_L}{2} \tan \gamma - \right.$$

$$K_1 n_r \frac{C_L}{2} + l_r \frac{C_L}{2} \right) + l_c \left(n_p y_r - n_p - n_r y_p + \frac{C_L}{2} - K_2 \frac{C_L}{2} \tan \gamma \right) +$$

$$n_c \left(-l_p y_r + l_p + l_r y_p - K_1 \frac{C_L}{2} + \frac{C_L}{2} \tan \gamma \right) + y_c P_2$$

$$c_4 = l_c \left(n_p \frac{C_L}{2} \tan \gamma - n_r \frac{C_L}{2} \right) + n_c \left(l_r \frac{C_L}{2} - l_p \frac{C_L}{2} \tan \gamma \right)$$

$$\left. \right\} \quad (4)$$

Step 4: Solve for the roots λ_1, λ_2, λ_3, and λ_4 of the biquadratic equation

$$A\lambda^4 + B\lambda^3 + C\lambda^2 + D\lambda + E = 0 \qquad (5)$$

where the values of the coefficients A, B, . . ., etc. were given by
the solution of equations (1). Methods of determining the roots of the
biquadratic equation are given in appendix C.

Step 5: Use the coefficients obtained from equations (1) to (4)
and the roots of equation (5) to solve for the following coefficients:

Calculate the values of the factors A_1, A_2, . . ., A_6 when
solving for the angle of bank ϕ or the rolling velocity p:

$$A_1 = \frac{a_0\lambda_1^5 + a_1\lambda_1^4 + a_2\lambda_1^3 + a_3\lambda_1^2 + a_4\lambda_1 + a_5}{6A\lambda_1^5 + 5B\lambda_1^4 + 4C\lambda_1^3 + 3D\lambda_1^2 + 2E\lambda_1}$$

$$A_2 = \frac{a_0\lambda_2^5 + a_1\lambda_2^4 + a_2\lambda_2^3 + a_3\lambda_2^2 + a_4\lambda_2 + a_5}{6A\lambda_2^5 + 5B\lambda_2^4 + 4C\lambda_2^3 + 3D\lambda_2^2 + 2E\lambda_2}$$

$$A_3 = \frac{a_0\lambda_3^5 + a_1\lambda_3^4 + a_2\lambda_3^3 + a_3\lambda_3^2 + a_4\lambda_3 + a_5}{6A\lambda_3^5 + 5B\lambda_3^4 + 4C\lambda_3^3 + 3D\lambda_3^2 + 2E\lambda_3}$$

$$A_4 = \frac{a_0\lambda_4^5 + a_1\lambda_4^4 + a_2\lambda_4^3 + a_3\lambda_4^2 + a_4\lambda_4 + a_5}{6A\lambda_4^5 + 5B\lambda_4^4 + 4C\lambda_4^3 + 3D\lambda_4^2 + 2E\lambda_4}$$

$$A_5 = \frac{a_5}{E}$$

$$A_6 = \frac{1}{E}\left(a_4 - a_5\frac{D}{E}\right)$$

(6)

Calculate the values of the factors B_1, B_2, . . ., B_6 when solving for the angle of yaw ψ or the yawing velocity r:

$$B_1 = \frac{b_0\lambda_1{}^5 + b_1\lambda_1{}^4 + b_2\lambda_1{}^3 + b_3\lambda_1{}^2 + b_4\lambda_1 + b_5}{6A\lambda_1{}^5 + 5B\lambda_1{}^4 + 4C\lambda_1{}^3 + 3D\lambda_1{}^2 + 2E\lambda_1}$$

$$B_2 = \frac{b_0\lambda_2{}^5 + b_1\lambda_2{}^4 + b_2\lambda_2{}^3 + b_3\lambda_2{}^2 + b_4\lambda_2 + b_5}{6A\lambda_2{}^5 + 5B\lambda_2{}^4 + 4C\lambda_2{}^3 + 3D\lambda_2{}^2 + 2E\lambda_2}$$

$$B_3 = \frac{b_0\lambda_3{}^5 + b_1\lambda_3{}^4 + b_2\lambda_3{}^3 + b_3\lambda_3{}^2 + b_4\lambda_3 + b_5}{6A\lambda_3{}^5 + 5B\lambda_3{}^4 + 4C\lambda_3{}^3 + 3D\lambda_3{}^2 + 2E\lambda_3}$$

$$B_4 = \frac{b_0\lambda_4{}^5 + b_1\lambda_4{}^4 + b_2\lambda_4{}^3 + b_3\lambda_4{}^2 + b_4\lambda_4 + b_5}{6A\lambda_4{}^5 + 5B\lambda_4{}^4 + 4C\lambda_4{}^3 + 3D\lambda_4{}^2 + 2E\lambda_4}$$

$$B_5 = \frac{b_5}{E}$$

$$B_6 = \frac{1}{E}\left(b_4 - b_5\frac{D}{E}\right)$$

(7)

Calculate the values of the factors C_1, C_2, $\ldots$, C_5 when solving for the angle of sideslip β:

$$C_1 = \frac{c_0\lambda_1^5 + c_1\lambda_1^4 + c_2\lambda_1^3 + c_3\lambda_1^2 + c_4\lambda_1}{6A\lambda_1^5 + 5B\lambda_1^4 + 4C\lambda_1^3 + 3D\lambda_1^2 + 2E\lambda_1}$$

$$C_2 = \frac{c_0\lambda_2^5 + c_1\lambda_2^4 + c_2\lambda_2^3 + c_3\lambda_2^2 + c_4\lambda_2}{6A\lambda_2^5 + 5B\lambda_2^4 + 4C\lambda_2^3 + 3D\lambda_2^2 + 2E\lambda_2}$$

$$C_3 = \frac{c_0\lambda_3^5 + c_1\lambda_3^4 + c_2\lambda_3^3 + c_3\lambda_3^2 + c_4\lambda_3}{6A\lambda_3^5 + 5B\lambda_3^4 + 4C\lambda_3^3 + 3D\lambda_3^2 + 2E\lambda_3} \qquad (8)$$

$$C_4 = \frac{c_0\lambda_4^5 + c_1\lambda_4^4 + c_2\lambda_4^3 + c_3\lambda_4^2 + c_4\lambda_4}{6A\lambda_4^5 + 5B\lambda_4^4 + 4C\lambda_4^3 + 3D\lambda_4^2 + 2E\lambda_4}$$

$$C_5 = \frac{c_4}{E}$$

If equation (5) has conjugate complex roots, the values of the coefficients (equations (6) to (8)) corresponding to these roots will be conjugate complex. In order to facilitate treatment of this case it is convenient to establish some special notation. This special notation is explained in appendix D.

Step 6: · The equations of motion are written in different form depending upon the roots of equation (5). If the characteristic equation has four real roots λ_1, λ_2, λ_3, and λ_4, the general form of the equations of motion is used, as follows:

$$\left.\begin{aligned}
\phi &= A_1 e^{\sigma\lambda_1} + A_2 e^{\sigma\lambda_2} + A_3 e^{\sigma\lambda_3} + A_4 e^{\sigma\lambda_4} + A_5\sigma + A_6 \\
\psi &= B_1 e^{\sigma\lambda_1} + B_2 e^{\sigma\lambda_2} + B_3 e^{\sigma\lambda_3} + B_4 e^{\sigma\lambda_4} + B_5\sigma + B_6 \\
\beta &= C_1 e^{\sigma\lambda_1} + C_2 e^{\sigma\lambda_2} + C_3 e^{\sigma\lambda_3} + C_4 e^{\sigma\lambda_4} + C_5 \\
p &= \frac{1}{\tau}\left(A_1\lambda_1 e^{\sigma\lambda_1} + A_2\lambda_2 e^{\sigma\lambda_2} + A_3\lambda_3 e^{\sigma\lambda_3} + A_4\lambda_4 e^{\sigma\lambda_4} + A_5\right) \\
r &= \frac{1}{\tau}\left(B_1\lambda_1 e^{\sigma\lambda_1} + B_2\lambda_2 e^{\sigma\lambda_2} + B_3\lambda_3 e^{\sigma\lambda_3} + B_4\lambda_4 e^{\sigma\lambda_4} + B_5\right)
\end{aligned}\right\} \quad (9)$$

If, as is generally the case, equation (5) has two complex roots and two real roots ($R + Ii$, $R - Ii$, λ_3, and λ_4), the equations of motion may be expressed as

$$\left.\begin{aligned}
\phi &= K_A e^{\sigma R} \cos(\sigma I + \omega_A) + A_3 e^{\sigma\lambda_3} + A_4 e^{\sigma\lambda_4} + A_5\sigma + A_6 \\
\psi &= K_B e^{\sigma R} \cos(\sigma I + \omega_B) + B_3 e^{\sigma\lambda_3} + B_4 e^{\sigma\lambda_4} + B_5\sigma + B_6 \\
\beta &= K_C e^{\sigma R} \cos(\sigma I + \omega_C) + C_3 e^{\sigma\lambda_3} + C_4 e^{\sigma\lambda_4} + C_5 \\
p &= \frac{1}{\tau}\left[K_A\sqrt{R^2 + I^2}\, e^{\sigma R} \cos\left(\sigma I + \omega_A + \tan^{-1}\frac{I}{R}\right) + \right. \\
&\qquad \left. A_3\lambda_3 e^{\sigma\lambda_3} + A_4\lambda_4 e^{\sigma\lambda_4} + A_5\right] \\
r &= \frac{1}{\tau}\left[K_B\sqrt{R^2 + I^2}\, e^{\sigma R} \cos\left(\sigma I + \omega_B + \tan^{-1}\frac{I}{R}\right) + \right. \\
&\qquad \left. B_3\lambda_3 e^{\sigma\lambda_3} + B_4\lambda_4 e^{\sigma\lambda_4} + B_5\right]
\end{aligned}\right\} \quad (10)$$

where

$$K_A = 2\sqrt{R_A{}^2 + I_A{}^2} \qquad \omega_A = \tan^{-1}\frac{I_A}{R_A}$$

$$K_B = 2\sqrt{R_B{}^2 + I_B{}^2} \qquad \omega_B = \tan^{-1}\frac{I_B}{R_B} \Biggr\} \qquad (10a)$$

$$K_C = 2\sqrt{R_C{}^2 + I_C{}^2} \qquad \omega_C = \tan^{-1}\frac{I_C}{R_C}$$

and R_A and I_A are defined in appendix D.

If there are four complex roots ($R + Ii$, $R - Ii$, $R' + I'i$, and $R' - I'i$), the equations are

$$\phi = K_A e^{\sigma R}\cos(\sigma I + \omega_A) + K_A{}'e^{\sigma R'}\cos(\sigma I' + \omega_A') + A_5\sigma + A_6$$

$$\psi = K_B e^{\sigma R}\cos(\sigma I + \omega_B) + K_B{}'e^{\sigma R'}\cos(\sigma I' + \omega_B') + B_5\sigma + B_6$$

$$\beta = K_C e^{\sigma R}\cos(\sigma I + \omega_C) + K_C{}'e^{\sigma R'}\cos(\sigma I' + \omega_C') + C_5$$

$$p = \frac{1}{\tau}\left[K_A\sqrt{R^2 + I^2}\,e^{\sigma R}\cos\left(\sigma I + \omega_A + \tan^{-1}\frac{I}{R}\right) + A_5 + \right.$$
$$\left. K_A{}'\sqrt{R'^2 + I'^2}\,e^{\sigma R'}\cos\left(\sigma I' + \omega_A' + \tan^{-1}\frac{I'}{R'}\right)\right] \qquad (11)$$

$$r = \frac{1}{\tau}\left[K_B\sqrt{R^2 + I^2}\,e^{\sigma R}\cos\left(\sigma I + \omega_B + \tan^{-1}\frac{I}{R}\right) + B_5 + \right.$$
$$\left. K_B{}'\sqrt{R'^2 + I'^2}\,e^{\sigma R'}\cos\left(\sigma I' + \omega_B' + \tan^{-1}\frac{I'}{R'}\right)\right]$$

where

$$K_A' = 2\sqrt{R_A'^2 + I_A'^2} \qquad\qquad \omega_A' = \tan^{-1}\frac{I_A'}{R_A'}$$

$$K_B' = 2\sqrt{R_B'^2 + I_B'^2} \qquad\qquad \omega_B' = \tan^{-1}\frac{I_B'}{R_B'} \left.\begin{array}{c}\\\\\\\\\\\end{array}\right\} \qquad (11a)$$

$$K_C' = 2\sqrt{R_C'^2 + I_C'^2} \qquad\qquad \omega_C' = \tan^{-1}\frac{I_C'}{R_C'}$$

The coefficients K_A, K_B, K_C, ω_A, ω_B, and ω_C are defined in equations (10a) and R_A, I_A, R_A', and I_A' are defined in appendix D.

Solve the appropriate ones of these equations of motion (equations (9), (10), or (11)) by substituting values of the nondimensional time factor σ in the equations and solving for ϕ, ψ, β, p, or r.

Motions Resulting from Arbitrary Disturbances

The motions resulting from arbitrary forcing functions can be obtained from the motions resulting from constant impressed forces and moments by the methods explained in references 6 and 7.

A very useful method of obtaining the motion resulting from various abrupt gust and control disturbances is given by Jones in reference 7. In this paper it is pointed out that, although the component motions of an airplane must be calculated simultaneously (that is, by simultaneous differential equations), the effects of component disturbances may by the principle of superposition be calculated separately and later added in any desired proportion. Thus, if a given rolling moment causes a 20° bank in 1 second and if a given yawing moment causes a 5° bank in 1 second, the combined effect of both acting simultaneously will be a 25° bank in 1 second. Jones also points out a somewhat similar fact with regard to the effects of disturbances that are not applied simultaneously. This fact is that, if a given disturbance which arises at the time $t = 0$ is later augmented, the effect of the increment of disturbance will run its course independently of the effect of the original disturbance. For example, in a problem involving the correction for a gust disturbance by a manipulation of the control, the motion produced by the gust disturbance can be calculated independently and the motion caused by the assumed corrective control manipulation can be added to it at any desired point. This example is illustrated graphically in figure 3.

The principle of superposition may be applied analytically as well as graphically. The analytical application which makes use of Carson's integral or Duhamel's integral is described in references 7 and 23. This method is useful for calculating the motions resulting from impressed forces and moments which are arbitrary functions of time. By application of these methods, the solutions for constant impressed forces and moments can be used to obtain new solutions for any arbitrary variation of impressed forces and moments with time which can be expressed by a mathematical formula. Some simple variations of impressed forces and moments with time and their Laplace transforms are given in reference 6. The transforms for any other function for which transforms have been worked out may be found in tables of Laplace transforms.

CALCULATION OF STABILITY BOUNDARIES

Oscillatory Stability Boundaries

As pointed out in the preceding section of this report, the degree of stability of the uncontrolled motions of an airplane is indicated by roots of the characteristic equation

$$A\lambda^4 + B\lambda^3 + C\lambda^2 + D\lambda + E = 0$$

For stability the real roots or the real part of the complex roots of the characteristic equation must be negative. A useful discriminant for determining some of the characteristics of the roots in stability work is Routh's discriminant R ($R = BCD - AD^2 - B^2E$). The use of this discriminant in dynamic stability analyses has been pointed out in many reports, for example, references 1, 2, 3, 5, 21, and 24. Routh has shown (reference 20) that, if R and the coefficient E are finite, the necessary and sufficient conditions that the real roots and the real parts of the complex roots should be negative are that every coefficient of the biquadratic and also R should have the same sign. Routh also showed that when $R = 0$ and B and D have the same sign there are a pair of complex roots with the real parts zero. Since the value of the real part of a complex root indicates the stability of an oscillatory mode of the motion of an airplane, the lateral oscillation is neutrally stable when $R = 0$ and the coefficients B and D have the same sign. Oscillatory stability boundaries can be determined, therefore, by solving the equation $R = 0$ and checking to determine whether the signs of B and D are the same.

Since two of the most important stability derivatives affecting lateral stability are the directional stability derivative C_{n_β} and

the effective dihedral derivative C_{l_β}, boundaries for neutral oscil-
latory stability are usually calculated as a function of these two
derivatives as illustrated in figure 4. These calculations are gener-
ally carried out by the method shown in table I. This table contains a
numerical example and step-by-step instructions for using the table.
The results of this numerical example are plotted in figure 4. The
procedure illustrated in table I is first to assume values of the inde-
pendent variable C_{n_β} to cover the range for which the boundary is
required. The values of all the other mass and aerodynamic stability
derivatives except C_{l_β} are then estimated. The value of C_{n_β} is
generally assumed to have been varied by varying the size of the verti-
cal tail and consequently the tail contribution to each of the other
stability derivatives varies as C_{n_β} is varied. The values of the
coefficients A, B, C, D, and E and then R are calculated as
functions of l_β:

$$l_\beta = \frac{\mu}{4K_X^2} C_{l_\beta}$$

The values of l_β corresponding to the assumed values of C_{n_β} for the
condition of neutral oscillatory stability are next obtained by solving
the expression R = 0 which is a quadratic in l_β that is of the form

$$u_1 l_\beta^2 + v_1 l_\beta + w_1 = 0$$

Finally, the values of C_{l_β} corresponding to the assumed values of C_{n_β}
are obtained from the values of l_β.

The values of l_β which satisfy the expression R = 0 must be
checked to determine whether they satisfy the other condition for
neutral oscillatory stability - that the sign of the coefficients B
and D must be the same. This check can be performed readily by sub-
stituting the values of l_β which satisfy R = 0 into the expression
for D which is a linear equation of the form

$$D = u_2 l_\beta + v_2$$

Thus, the sign of D is determined. The sign of B is a constant for
any given value of C_{n_β} and is almost invariably positive since the
three predominant terms of B contain the derivatives C_{l_p}, C_{n_r},
and C_{Y_β} which in all practical cases contribute a positive increment
to the value of B.

Since two values of C_{l_β} satisfy the condition $R = 0$ for each value of C_{n_β}, the $R = 0$ curve has two branches. As pointed out in reference 24, one of the branches of the $R = 0$ curve generally represents an oscillatory stability boundary and the other branch represents a line of numerically equal real roots with opposite signs. (See fig. 4.) If neither of the values of C_{l_β} which satisfy the expression $R = 0$ for a particular value of C_{n_β} is found to represent a point of neutral oscillatory stability, the lateral motion has no oscillatory mode for that value of C_{n_β}. If both of the values of C_{l_β} which satisfy the expression $R = 0$ are found to represent points of neutral oscillatory stability, the lateral motion has two oscillatory modes. In this case, since the boundary $D = 0$ represents the line of infinite period, the branch of the $R = 0$ boundary which lies close to the $D = 0$ boundary is usually the boundary for neutral stability of the longer period of the two oscillatory modes. A detailed discussion of the significance of the stability boundaries and the regions formed by these boundaries is given in reference 24.

In calculating stability boundaries for a specific airplane a complete solution such as that explained in the preceding paragraphs should be made. For general studies of stability, however, approximate oscillatory stability boundaries may be calculated much more simply by the methods shown in reference 24.

As pointed out previously, methods of calculating lines of constant period and damping of the lateral oscillation are presented in references 8 and 9.

Spiral Stability Boundaries

Spiral stability boundaries, like oscillatory stability boundaries, are usually determined as a function of the directional stability derivative C_{n_β} and the effective dihedral derivative C_{l_β} as illustrated in figure 4. As pointed out in reference 1, neutral spiral stability occurs when the E coefficient of the characteristic equation is zero ($E = 0$). A spiral stability boundary can be easily obtained from this relation. If expressions for E (in terms of l_β) corresponding to several values of C_{n_β} have already been obtained in the process of calculating an oscillatory stability boundary, the equations formed by setting these expressions for E equal to zero can be solved for the values of l_β $\left(\text{and hence } C_{l_\beta}\right)$ corresponding to the assumed values of C_{n_β}. If the values of E have not already been obtained, in the process of calculating an oscillatory stability boundary, a spiral

stability boundary for the level-flight condition ($\gamma = 0$) can be calculated simply from the equation

$$C_{l_\beta} = \frac{C_{l_r}}{C_{n_r}} C_{n_\beta} \tag{12}$$

Values of C_{n_β} are assumed within the range for which the boundary is required. The values of C_{l_r} and C_{n_r} corresponding to each value of C_{n_β} are then determined. The tail contributions to these derivatives generally vary with C_{n_β} since C_{n_β} is usually assumed to be varied by changing the size of the vertical tail.

ESTIMATION OF LATERAL STABILITY DERIVATIVES

GENERAL REMARKS

Methods of estimating the lateral stability derivatives have been presented in numerous publications but no single report has contained information for estimating the contribution of all principal airplane components to all the derivatives for airplanes having any sweep angle or aspect ratio. In the present paper, an approach to such a presentation is made by the coordination of and reference to existing estimation methods, by reference to publications containing data which should be useful in making estimates, and by the suggestion in some cases of simple new empirical formulas. Detailed estimation methods are presented for low-subsonic-speed conditions but only a brief discussion and a list of references are given for transonic- and supersonic-speed conditions. In general, the estimation methods presented should be expected to yield only fairly accurate values suitable for making first approximations of dynamic stability. This limitation applies especially to the cases in which the derivatives are based completely on theory.

For convenience, the references that should be useful in estimating the stability derivatives are presented in table II. The references are grouped according to the speed range covered (subsonic or supersonic) and according to the derivatives presented in each report. The references for the subsonic case (references 1 and 25 to 94) are further divided into two groups - one including reports which contain estimation methods and the other including reports which contain experimental data that should be useful in making estimates of derivatives. The

references for the supersonic case (references 95 to 115) are sub-
divided according to wing plan form.

The following sections covering the estimation of the nine sta-
bility derivatives are divided into three groups according to the type
of derivative - sideslip derivatives $\left(C_{Y_\beta}, \ C_{n_\beta}, \ C_{l_\beta}\right)$, rolling deriva-
tives $\left(C_{n_p}, \ C_{l_p}, \ C_{Y_p}\right)$, and yawing derivatives $\left(C_{n_r}, \ C_{l_r}, \ C_{Y_r}\right)$. The
derivatives C_{Y_p} and C_{Y_r} have usually been neglected in making
dynamic lateral stability calculations because theory indicated that for
unswept wings C_{Y_p} and C_{Y_r} were zero. Recent experimental data,
however, have indicated that both swept and unswept wings produce meas-
urable values of these derivatives (references 25, 59, and 86). Since
the vertical tail contributes to C_{Y_p} and C_{Y_r}, it appears desirable
to estimate these derivatives and to use them in the calculations of
stability unless it is established that for the case in question the
effects of C_{Y_p} and C_{Y_r} on stability are negligible. For these two
derivatives, only the effect of the wing and vertical tail need to be
considered.

The methods of estimating the rolling and yawing derivatives pre-
sented herein were obtained from theoretical treatments based on the
assumption of steady rolling and yawing and from experimental data
obtained principally from tests made under conditions of steady rolling
and yawing. The only information that applies directly to the oscil-
latory case is a limited amount of data on C_{n_r} obtained by oscillation
techniques. When calculations are made in which the oscillatory mode
is the subject of interest, some consideration should be given to cor-
recting the derivatives based on steady rolling or yawing to account
for differences in the derivatives that are likely to exist as a result
of differences between the oscillatory motion and the steady rolling
and yawing motion. For example, the data of reference 82 have indi-
cated that, for flap-extended or power-on conditions, fairly large dif-
ferences might exist between the values of the tail contribution to C_{n_r}
for the steady yawing and yawing oscillation cases. At present little
information is available for correcting the values of C_{n_r} for the
steady yawing case to apply to the oscillatory case and, unfortunately,
little or no information is available for correcting the other stability
derivatives.

Since most wind-tunnel force-test data that are likely to be used
in making estimates of the stability derivatives are probably for much
lower Reynolds numbers than those for the full-scale airplane, some
adjustments to the data are usually required to account for the dif-
ferences in Reynolds number. The effects of Reynolds number should be
considered in the cases of all the derivatives, especially those which

are estimated by methods that involve the use of force-test data.
Methods of correcting for Reynolds number effects for some of the
derivatives are discussed in the following sections which cover the
estimation procedures. In the cases where the Reynolds number effects
are not discussed, it can be assumed that any abrupt variation in the
derivatives near the stall for low-scale data will also be present for
the full-scale airplane but will probably occur at a higher lift coef-
ficient because of the higher maximum lift coefficient of the airplane.
An indication of the lift-coefficient range over which the theory may
not be expected to give reliable values of stability derivatives for the
full-scale airplane can be obtained from large-scale drag data. The
analysis of reference 86 indicates that the variation of the derivatives
with lift coefficient is different from the theoretical variation at
lift coefficients above that at which the drag due to lift increases
abruptly from the ideal value $C_L^2/\pi A$.

The effects of Mach number and power are not treated in the sections
on the individual derivatives but are discussed briefly in separate
sections. A detailed treatment of these effects, including design
formulas and charts, was considered beyond the scope of this paper.

THE SIDESLIP DERIVATIVES C_{Y_β}, C_{n_β}, C_{l_β}

No satisfactory purely theoretical methods have yet been developed
for obtaining accurate estimates of the sideslip derivatives C_{Y_β}, C_{n_β},
and C_{l_β} for a complete airplane, primarily because of large inter-
ference effects between the various airplane components and because of
large, and often unpredictable, variations of the derivatives with angle
of attack. Fortunately, these derivatives can be obtained from conven-
tional wind-tunnel force-test data. Such experimental data are essential
to the accurate determination of sideslip derivatives. It is, of course,
highly desirable to have force-test data for the exact airplane design
under consideration, but reasonably accurate estimates can usually be
made by correcting the force-test data for a generally similar design.
The methods of correcting the force-test data on a similar design for
use in the case under consideration are covered in the following sec-
tions. In the formulas presented, the subscript word "design" is used
to designate the design under consideration and the subscript word "data"
is used to designate the similar design for which force-test data are
available.

Force-test data should be used to determine the effect on the side-
slip derivatives of such airplane components as leading-edge high-lift
devices, stall-control devices, trailing-edge flaps, nacelles, external

stores, canopies, and dorsal and ventral fins. The effect of leading-edge high-lift devices is usually merely to extend to a higher lift coefficient the same variation of the derivative with lift coefficient as for the plain wing. Trailing-edge flaps often have large effects on the contributions of both the wing and the vertical tail to the sideslip derivatives (references 39 and 69); and since these effects are not easily estimated, it appears that in these cases use of force-test data is essential. The addition of nacelles and external stores generally has been found to decrease the directional stability factor C_{n_β} slightly. The results of a limited amount of research to determine the effect on the sideslip derivatives of the size and shape of canopies has been reported in references 48 and 73 but these results are inadequate for making accurate predictions of the effects of canopies. The effects on the sideslip derivatives of dorsal and ventral fins are usually small at the small and moderate angles of yaw that are generally considered in stability calculations. (See references 47 and 71.)

$$C_{Y_\beta}$$

In estimates of the lateral force due to sideslip derivative C_{Y_β}, force-test data for the design under consideration should be used whenever possible. If such data are not available, data for a similar design can be used and corrected as follows:

Wing-fuselage.- Since the wing-fuselage contribution to C_{Y_β} is usually relatively small compared with that of the vertical tail, great accuracy is not required in estimating this factor. This contribution may be estimated as follows:

(1) Wing: If the wings of the two designs are generally similar the difference in $C_{Y_{\beta_{wing}}}$ can be considered negligible and no correction is necessary. The theory of reference 25 does not appear to be suitable for use in estimating $C_{Y_{\beta_{wing}}}$.

(2) Fuselage: If the two fuselages are similar in shape, the difference in $C_{Y_{\beta_{fus}}}$ can probably be estimated satisfactorily by correcting for the difference in the relative size of the fuselage and wing for the two airplanes. It appears, however, from table X of reference 69 unlikely that a reliable prediction of $C_{Y_{\beta_{fus}}}$ can be made directly from the geometry of the fuselage. Some additional data on $C_{Y_{\beta_{fus}}}$ are presented in reference 77. Experimental data from other investigations have shown that differences in fuselage cross-section can cause very large differences in the variation of $C_{Y_{\beta_{fus}}}$ with angle of attack. For example, in the case of a flat fuselage with the major cross-sectional axis horizontal, the sign of $C_{Y_{\beta_{fus}}}$ has been

found to reverse at moderate and high angles of attack. Force-test data are essential for making estimates in such cases.

(3) Wing-fuselage interference: For low-wing or high-wing configurations, wing-fuselage interference causes the value of C_{Y_β} to be greater than that obtained by adding the contributions of the wing and fuselage. (See reference 39.) If the vertical location of the wing on the fuselage is generally similar for the two designs, however, any correction for a difference in this interference factor can be neglected.

Vertical tail.- Accurate estimates of $C_{Y_{\beta_{tail}}}$ are necessary because this factor is used to estimate the tail contribution to several other derivatives. This factor is especially important at low angles of attack because in this case the tail contribution is often much greater than the wing-fuselage contribution to all derivatives except C_{l_p}. For this reason it is highly desirable to have tail-off and tail-on force-test data for the design under consideration or for a very similar design. Corrections to the data for a similar design can be made as follows:

(1) Correction for differences in wing area, tail area, and tail lift-curve slope can be made by the following formula:

$$\left(C_{Y_{\beta_{tail}}}\right)_{design} = \left(C_{Y_{\beta_{tail}}}\right)_{data} \frac{\left(C_{L_{\alpha_{tail}}} S_{tail}\right)_{design}}{\left(C_{L_{\alpha_{tail}}} S_{tail}\right)_{data}} \frac{S_{data}}{S_{design}} \tag{13}$$

The value of $C_{L_{\alpha_{tail}}}$ can be obtained from figures 5 and 6 which are based on the theory of reference 34 and on the theory and data of references 28 and 35. The chart of figure 6 can be used to estimate the change in the effective aspect ratio of the vertical tail caused by the end-plate effect of the horizontal tail. It should be emphasized that for the best accuracy the charts in figures 5 and 6 should be used in conjunction with formula (13) for correcting existing force-test data and not for making a direct estimate of $C_{Y_{\beta_{tail}}}$.

(2) In the case of V-tails, the correction for $C_{Y_{\beta_{tail}}}$ can be made as follows:

$$\left(C_{Y_{\beta_{V-tail}}}\right)_{design} = \left(C_{Y_{\beta_{V-tail}}}\right)_{data} \frac{\left(KC_{L_{\alpha_N}} S_{V-tail} \sin^2\Gamma\right)_{design}}{\left(KC_{L_{\alpha_N}} S_{V-tail} \sin^2\Gamma\right)_{data}} \frac{S_{data}}{S_{design}}$$

$$\tag{14}$$

where the terms $C_{L_{\alpha_N}}$, Γ, and K are the same as given in reference 30 and are defined as follows:

$C_{L_{\alpha_N}}$ slope of the tail lift curve in pitch measured in the plane
normal to the chord plane of each tail panel

Γ dihedral angle of tail surface measured from XY-plane of the
tail to each tail panel, degrees

K ratio of sum of lifts obtained by equal and opposite changes
in angle of attack of two semispans of tail to lifts obtained
by an equal change in angle of attack for the complete tail

Values of the term K, which are usually about 0.7, can be obtained from reference 30.

(3) Since large differences in sidewash and dynamic pressure at the tail can be caused by differences in wing plan form and wing location, use of experimental data for the specific design or at least for a design which has a closely similar wing-fuselage combination and vertical tail location is extremely desirable. No methods are available which permit accurate predictions of sidewash at the tail, but the experimental data of references 39, 49, and 69 can be used to obtain some indication of the variation in sidewash with vertical location of an unswept wing on a fuselage and the experimental data of references 36 and 77 provide additional information on sidewash at the tail. Other experimental data indicate that the sidewash fields produced by highly-swept, low-aspect-ratio wings or by fuselages of flat cross section can sometimes be strong enough at high angles of attack to reverse the effectiveness of a conventionally-located vertical tail surface. Until a reliable method is developed for predicting these large sidewash effects, force-test data appear to be the only means by which satisfactory estimates of $C_{Y_{\beta_{tail}}}$ can be obtained.

$$C_{n_\beta}$$

Although attempts have been made to develop methods for estimating the yawing moment due to sideslip (static directional stability) derivative C_{n_β} (for example, references 68 and 69) no reliable method has yet been obtained. The use of force-test data therefore seems imperative.

Force-test data for the design under consideration should be used if available. If such data are not available, use data for a similar design and correct as explained in the sections to follow.

Wing-fuselage.- The corrections for the wing-fuselage contributions are:

(1) Correction for wing - From figure 7 (taken from reference 25) the values of $\left(C_{n_\beta}/C_L^2\right)_{wing}$ for the design under consideration and for the design for which test data are available can be determined. The effect of differences in taper ratio can be neglected. (See references 60 and 66.) The difference between these values of C_{n_β}/C_L^2 should then be added (with proper regard for sign) to the experimental data for the complete model.

(2) Correction for fuselage - The formula

$$C_{n_{\beta_{fus}}} = -1.3\left(\frac{\text{Fuselage volume}}{Sb}\right)\left(\frac{h}{w}\right) \qquad (15)$$

can be used to calculate the C_{n_β} of the fuselage (per radian) for the design under consideration and for the similar design for which force-test data are available. The differences between these two values can then be added (with proper regard for sign) to the force-test data for the complete model. Formula (15) does not include the effect of fineness ratio and should not be used for fineness ratios less than 4. This formula is an approximate empirical expression which should not be used to estimate the value of $C_{n_{\beta_{fus}}}$ directly but should only be used as indicated to determine a correction for force-test data. This correction method should not be used in the cases of high angles of attack when there are large differences in fuselage configuration. Force-test data are essential in such cases.

(3) Correction for vertical location of the wing - If the designs are generally similar, the correction for the vertical location of the wing on the fuselage can be neglected. (See reference 39.)

(4) Correction for center-of-gravity position - If the center-of-gravity position for the design under consideration is appreciably different from that for the design for which force-test data are available, the value of C_{n_β} for the wing-fuselage combination can be corrected by multiplying the value of C_{Y_β} for the wing-fuselage combination by the distance between center-of-gravity positions (expressed in wing spans).

Vertical tail.- Corrections to $C_{n_{\beta_{tail}}}$ for differences in $C_{Y_{\beta_{tail}}}$ and tail length l/b can be made by the following formula:

$$\left(C_{n_{\beta_{tail}}}\right)_{design} = \left(C_{n_{\beta_{tail}}}\right)_{data} \frac{\left(C_{Y_{\beta_{tail}}} \frac{l}{b}\right)_{design}}{\left(C_{Y_{\beta_{tail}}} \frac{l}{b}\right)_{data}} \qquad (16)$$

The contribution of wing-tip fins to C_{n_β} is treated in reference 70 and 84.

$$C_{l_\beta}$$

In estimates of the rolling moment due to sideslip (effective dihedral) C_{l_β}, force-test data for the design under consideration should be used. If such data are not available, data for a similar design can be used and corrected by the methods that follow.

Wing-fuselage.- The corrections for wing-fuselage contributions are:

(1) Correction for wing - From figure 8 (based on reference 25) the theoretical values of C_{l_β}/C_L for the design under consideration and for the design for which data are available can be determined. The difference between these two theoretical values can then be added (with proper regard for sign) to the experimental data. Consideration should be given to scale effect, airfoil section, and surface roughness on the value of C_{l_β} for highly swept wings. The lift coefficient at which the experimental variation of C_{l_β} with lift coefficient departs from theory is greatest at high Reynolds numbers and for smooth wings with round leading edges. For wings with rough surfaces or sharp leading edges the effects of Reynolds number on C_{l_β} are usually small and low-scale wind tunnel data can be used. For airplanes having very smooth sweptback wings with rounded leading edges, however, some correction should be made for scale effect when estimations are made from low-scale wind-tunnel data. Since no rational method has been developed for making such corrections it is suggested that, for lift coefficients higher than that at which the experimental data departs from the theory, an average of the theoretical and low-scale experimental values be used. Conservative dynamic stability results will usually be obtained if the uncorrected theoretical values of C_{l_β} are used because these values are ordinarily greater (more negative) than measured values and because the larger negative values of C_{l_β} usually tend to decrease the dynamic lateral stability.

(2) Correction for wing dihedral - The effect of dihedral on C_{l_β} is treated in references 29, 39, 51, 58, 66, and 79. Correction for the difference in dihedral between the two designs can be made by multiplying the incremental geometric dihedral angle (in degrees) by the factor $C_{l_{\beta_\Gamma}}$ obtained from figure 9. A plot of $C_{l_{\beta_\Gamma}}$ against aspect ratio for taper ratios of 1.0, 0.5 and 0.25 (obtained from references 58 and 66) and a formula from reference 50 for correcting for sweep are presented in the upper portion of figure 9. The lower chart and formula in figure 9 (developed from reference 66) should be used in addition to the upper chart and formula of figure 9 to estimate the values of $C_{l_{\beta_\Gamma}}$ for the case of a wing with partial-span dihedral.

Although this chart and formula apply directly only to wings with one dihedral break they can be used to estimate the $C_{l_{\beta_\Gamma}}$ for wings with two or more dihedral breaks by the method described in reference 66. The effect of drooped wing tips and of wing-tip end-plates on $C_{l_{\beta_{wing}}}$ should be determined by experimental data since no reliable estimation procedure for these effects is available.

(3) Correction for wing-fuselage interference - Although the contribution of the fuselage alone to C_{l_β} is usually negligible, the interference between the wing and fuselage can greatly alter the value of C_{l_β} of the wing. This interference is such that a high location of the wing on the fuselage gives more positive effective dihedral (higher $-C_{l_\beta}$) and a low wing location gives less positive dihedral than a midwing position. This effect is treated theoretically in reference 67 and has been studied experimentally in references 38 to 42. The following simplified expression for estimating the increment in C_{l_β} caused by wing-fuselage interference has been developed from the relationships presented in reference 67 and in other sources:

$$\Delta C_{l_\beta} = 1.2\sqrt{A} \; \frac{z_w}{b} \; \frac{h + w}{b} \qquad (17)$$

This expression has been found to give reasonably good agreement with experimental data for a variety of configurations. It is suggested that values of ΔC_{l_β} be calculated from this equation for both the design under consideration and for the design for which force-test data are available. The difference between these values can then be added (with the proper regard for sign) to the force-test data.

Vertical tail.- The value of $C_{l_{\beta_{tail}}}$ determined from force-test data on a similar design can be corrected as follows to obtain $C_{l_{\beta_{tail}}}$

for the design under consideration:

$$\left(C_{l_{\beta_{tail}}}\right)_{design} = \left(C_{l_{\beta_{tail}}}\right)_{data} \frac{\left(C_{Y_{\beta_{tail}}} \frac{z}{b}\right)_{design}}{\left(C_{Y_{\beta_{tail}}} \frac{z}{b}\right)_{data}} \qquad (18)$$

The results of reference 35 indicate that $C_{l_{\beta_{tail}}}$ can also be affected by the location of the horizontal tail with respect to the vertical tail. If the two designs have approximately the same horizontal tail size and location, however, this effect can be neglected.

The value of $C_{l_{\beta_{tail}}}$ for a V-tail can be estimated from the following empirical formula:

$$\left(C_{l_{\beta_{V\text{-}tail}}}\right)_{design} = \left(C_{l_{\beta_{V\text{-}tail}}}\right)_{data} \left\{ \frac{\left[\frac{C_{Y_{\beta_{V\text{-}tail}}}}{b \sin \Gamma}\left(b_{V\text{-}tail} + 4z_{V\text{-}tail} \sin \Gamma\right)\right]_{design}}{\left[\frac{C_{Y_{\beta_{V\text{-}tail}}}}{b \sin \Gamma}\left(b_{V\text{-}tail} + 4z_{V\text{-}tail} \sin \Gamma\right)\right]_{data}} \right\}$$

$$(19)$$

where $b_{V\text{-}tail}$ is the developed (not projected) span of the V-tail, $z_{V\text{-}tail}$ is the vertical distance from the center of gravity to the chord of the V-tail (positive up, and Γ is the dihedral angle of the V-tail. More information on V-tails can be found in references 30, 61, and 62.

In the case of a vertical tail located on the wing, there is, in addition to the incremental C_{l_β} produced by the tail lateral force, an incremental C_{l_β} produced by the interference effect of the vertical tail on the wing. Since this interference effect varies greatly with spanwise and vertical position of the tail, it should be determined from force tests. Usually the interference is such that a vertical tail above the wing gives a negative increment of C_{l_β} (positive effective dihedral) and one below the wing gives a positive increment of C_{l_β}. In general, the largest interference effects are obtained with vertical tails at or near the wing tips.

THE ROLLING DERIVATIVES C_{n_p}, C_{l_p}, C_{Y_p}

C_{n_p}

The wing and vertical tail are the only airplane components that contribute appreciably to the yawing moment due to rolling derivative C_{n_p}. The contributions of the fuselage and horizontal tail can usually be neglected.

Wing.- The contribution of the wing to C_{n_p} can be estimated from the formula and charts of figure 10 which were taken from reference 86. Although these charts apply strictly only to wings having a taper ratio of 1.0, experimental data have indicated that they will also provide fairly good estimates for taper ratios of 0.50, 0.25 and 0. In the estimation formula

$$C_{n_p} = \frac{\left(\Delta C_{n_p}\right)_1}{C_L} C_L + \frac{\left(\Delta C_{n_p}\right)_2}{\left(C_{D_o}\right)_\alpha} \left(C_{D_o}\right)_\alpha \tag{20}$$

the value of $\left(C_{D_o}\right)_\alpha$ should be determined, if possible, from force-test data obtained at high Reynolds number on the wing under consideration, since low Reynolds number data might indicate values of $\left(C_{D_o}\right)_\alpha$ that are too large. For the case of smooth wings with a large leading edge radius and low or moderate sweep, it is suggested that $\left(C_{D_o}\right)_\alpha$ for the airplane be assumed to be zero at all lift coefficients up to the stall. This assumption will result in larger negative values of C_{n_p} than would be estimated from low Reynolds number data on $\left(C_{D_o}\right)_\alpha$ and consequently should lead to conservative dynamic stability results since an increase in C_{n_p} in the negative direction has been found to cause a reduction in dynamic stability. The value of $\left(C_{D_o}\right)_\alpha$ for highly swept wings is often very large at high lift coefficients, especially for wings with rough surfaces, sharp leading edges, or triangular plan form. For these cases, values of $\left(C_{D_o}\right)_\alpha$ determined even from low Reynolds number data might lead to reasonably good estimates of C_{n_p}. In all these cases, however, high-scale drag data should be used whenever it is available.

Effect of high-lift devices.- The principal effect of leading-edge high-lift devices is to extend to a higher lift coefficient the linear variation of C_{n_p} with lift coefficient. The formula and charts of figure 10 are directly applicable to this case. The effect of

trailing-edge high-lift devices is not so straightforward, but experimental data have indicated that the formula and charts of figure 10 also give reasonably good estimates in this case.

Vertical tail.- The contribution of an isolated vertical tail surface to C_{n_p} can be estimated by the following approximate formula which has also been commonly used to estimate $C_{n_{p_{tail}}}$ of a complete airplane:

$$C_{n_{p_{tail}}} = -2 \frac{l}{b} \frac{z}{b} C_{Y_{\beta_{tail}}} \tag{21}$$

The values of $C_{Y_{\beta_{tail}}}$ should be determined from force-test data as previously discussed. Instead of the geometric tail length l/b, it will usually be better to use the effective tail length $-C_{n_{\beta_{tail}}} \Big/ C_{Y_{\beta_{tail}}}$ as determined by force-test data. Formula (21) then becomes

$$C_{n_{p_{tail}}} = 2 \left(\frac{z}{b}\right) C_{n_{\beta_{tail}}} \tag{21a}$$

In the case of the conventionally located vertical tail surface, however, the rolling wing produces a sidewash at the tail which greatly alters the tail contribution to C_{n_p}. This sidewash causes the values of $C_{n_{p_{tail}}}$ to be much more negative than is indicated by formula (21). This effect is discussed more fully in reference 36 in which is also presented a method for estimating the sidewash. Some preliminary theoretical studies have indicated that the effect of the sidewash on $C_{n_{p_{tail}}}$ varies considerably with tail size and tail location and to some extent with wing plan form. A comprehensive experimental verification of this theory is planned but as yet only a few scattered checks have been obtained. For the case of the conventionally located vertical tail surface, the following formula has been found to give estimates of $C_{n_{p_{tail}}}$ that are in fairly good agreement with experimental data:

$$C_{n_{p_{tail}}} = -2 \frac{l}{b} \left[\frac{z}{b} - \left(\frac{z}{b}\right)_{\alpha=0}\right] C_{Y_{\beta_{tail}}} \tag{22}$$

or

$$C_{n_{p_{tail}}} = 2 \left[\frac{z}{b} - \left(\frac{z}{b}\right)_{\alpha=0}\right] C_{n_{\beta_{tail}}} \tag{22a}$$

This formula is based on the assumption that $Cn_{P_{tail}}$ is zero at 0° angle of attack and varies with angle of attack in the same manner as indicated by formula (21). Formula (22) or the method of reference 36 can be used satisfactorily for first approximations of $Cn_{P_{tail}}$ for most configurations with conventionally located vertical tails. For more accurate estimates, especially for configurations having an unusual tail size or tail location, experimental data should be used.

For wings of triangular plan form with vertical tails either directly above or above and slightly behind the wing, experimental data have indicated that neither formula (21) nor formula (22) gives an accurate estimate of $Cn_{P_{tail}}$ but that an average of the values obtained by the two formulas provides a fairly good estimate.

It is obvious that these methods of estimating Cn_p are only approximate and are open to question in many cases. Experimental and theoretical studies are currently being made to provide better methods of estimating $Cn_{P_{tail}}$ and, when these methods become available, the approximate methods presented herein should be discarded. At the present time, however, formula (22) and reference 36 will usually provide much more accurate estimates of $Cn_{P_{tail}}$ than formula (21) which has been in common use up until this time.

$$C_{l_p}$$

Wing-fuselage.- Most of the rolling moment due to rolling (damping-in-roll derivative) C_{l_p} of an airplane is produced by the wing. The effect of the fuselage can be neglected unless the ratio of the diameter of the fuselage to the wing span is relatively large (greater than about 0.3). For large values of this ratio, the value of C_{l_p} will be smaller than that for the wing alone by an amount that can be estimated from a consideration of the area and lateral center of pressure of the wing area included within the fuselage. (See references 103, 108, and 112.)

Wing.- The damping in roll of wings has been the subject of many experimental and theoretical investigations. (See references on C_{l_p} in table II.) As a result, some methods of estimating C_{l_p} have been developed which have been found to give reasonably good agreement with experimental results. The method presented in reference 79 appears to give sufficiently accurate estimates of C_{l_p} for zero lift. This

method is extended in reference 89 to permit the estimation of C_{l_p} over the normal flight range of lift coefficient. Estimation charts and formulas from reference 89 are presented in figure 11.

High-lift devices.- Experimental data have indicated that the damping in roll of wings at low and moderate lift coefficients is not greatly affected by the addition of high-lift devices such as trailing-edge flaps, leading-edge flaps, slats, and slots. The principal effect of such devices is to increase the lift coefficient at which the sharp decrease in C_{l_p} occurs. The charts and formulas of figure 11 can be used to estimate the C_{l_p} of wings with either full-span or partial-span high-lift devices with fair accuracy despite the fact that the method is not strictly applicable to partial-span high-lift devices. (See reference 89.)

Wing-tip fuel tanks.- The use of wing-tip fuel tanks usually increases the damping in roll of the wing. The experimental data of reference 91 for unswept wings indicate that the magnitude of the increase varies with angle of attack and depends upon the wing taper ratio and on the size and location of the tanks. Unpublished experimental data indicate similar effects of wing-tip tanks on sweptback wings. The following approximate formula for estimating the increment in C_{l_p} produced by wing-tip tanks at low lift coefficients is based on the limited amount of available experimental data and should not be expected to yield very close quantitative estimates:

$$\left(\Delta C_{l_p}\right)_{tanks} = \left(C_{l_p}\right)_{tanks\ off} \left(\frac{Maximum\ tank\ diameter}{Wing\ span}\right)(K_T) \quad (23)$$

where, for symmetrically mounted tip tanks,

$$K_T = 6$$

for tanks mounted below the wing tip or forward on the wing tip,

$$K_T = 3$$

and for pylon-mounted tip tanks,

$$K_T = 1$$

Experimental data for both unswept and swept wings indicate that $\left(\Delta C_{l_p}\right)_{tanks}$ usually becomes smaller with increasing angle of attack and, in some cases, actually reverses sign at high angles of attack so that the tanks are decreasing rather than increasing the damping in roll.

The data of reference 91 can be used to obtain an approximate estimate of the effect of angle of attack for unswept wings.

Tail surfaces.- The contribution to C_{l_p} of conventional type horizontal and vertical tail surfaces is usually very small and, in most cases, negligible. When an airplane rolls, the wing produces a rotation of flow at the tail surfaces which reduces the already small damping moments of the isolated surfaces, except in the case of the vertical tail at high angles of attack where the tail center of pressure is below the center of gravity.

The contribution of an extremely large horizontal tail to C_{l_p} might not be negligible and can be estimated by multiplying the value of C_{l_p} for the particular tail plan form obtained from the charts and formulas of figure 11 by the factor $0.5 \frac{S_t}{S}\left(\frac{b_t}{b}\right)^2$ in which the factor 0.5 is included to account for the rotation of flow produced by the wing.

The contribution of an isolated vertical tail surface to C_{l_p} is given by the following approximate formula:

$$C_{l_{p_{tail}}} = 2\left(\frac{z}{b}\right)^2 C_{Y_{\beta_{tail}}} \qquad (24)$$

As in the case of $C_{n_{p_{tail}}}$ this formula can be modified to provide an approximate correction for the effect of the wing on the damping in roll of conventionally located vertical tail surfaces:

$$C_{l_{p_{tail}}} = 2\left(\frac{z}{b}\right)\left[\frac{z}{b} - \left(\frac{z}{b}\right)_{\alpha=0}\right] C_{Y_{\beta_{tail}}} \qquad (25)$$

An analysis of this expression indicates that the value of $C_{l_{p_{tail}}}$ is negligible at low and moderate angles of attack where z/b is positive but that it might be fairly important at very high angles of attack where z/b is a large negative value. As in the case of C_{n_p}, experimental data indicate that, for a vertical tail located either directly above or slightly behind a wing of triangular plan form, the value of $C_{l_{p_{tail}}}$ can be estimated with better accuracy by an average of formulas (24) and (25) than by formula (25) alone. For conventional tail arrangements, however, formula 25 gives better correlation with experimental data.

$$C_{Y_p}$$

<u>Wing</u>.- The following formula for the derivative C_{Y_p} (lateral force due to rolling) from reference 86 is based on experimental data and is the same as that presented in reference 25 except for an additional correction to account for tip suction:

$$\frac{C_{Y_p}}{C_L} = \frac{A + \cos \Lambda}{A + 4 \cos \Lambda} \tan \Lambda + \frac{1}{A} \tag{26}$$

The data of reference 86 show that this formula applies only for lift coefficients below that at which the drag factor $C_D - \dfrac{C_L^2}{\pi A}$ begins to increase. At higher lift coefficients the experimental data indicate smaller values of C_{Y_p} than given by formula (26). For these cases an approximation of the value of C_{Y_p} can be obtained from the experimental data of reference 86. As in the case of C_{n_p}, the break in the variation of C_{Y_p} with lift coefficient should be expected to occur at lower lift coefficients for wings having sharp leading edges or rough surfaces and for wings tested at low Reynolds numbers.

<u>Vertical tail</u>.- The discussion concerning $C_{n_{p_{tail}}}$ and $C_{l_{p_{tail}}}$ is also applicable to $C_{Y_{p_{tail}}}$. The value of $C_{Y_{p_{tail}}}$ for an isolated tail surface is given by the formula:

$$C_{Y_{p_{tail}}} = 2\left(\frac{z}{b}\right) C_{Y_{\beta_{tail}}} \tag{27}$$

This formula can be modified as follows to account approximately for the effects of wing sidewash in the case of a conventionally located vertical tail:

$$C_{Y_{p_{tail}}} = 2\left[\frac{z}{b} - \left(\frac{z}{b}\right)_{\alpha=0}\right] C_{Y_{\beta_{tail}}} \tag{28}$$

An average of formulas (27) and (28) can be used for tails located either directly above or above and slightly behind the wing.

THE YAWING DERIVATIVES C_{n_r}, C_{l_r}, AND C_{Y_r}

C_{n_r}

Wing-fuselage.- In the past, the contribution of the wing-fuselage combination to yawing moment due to yawing (damping in yaw) derivative C_{n_r} has usually been found to be small compared to the contribution of the vertical tail. The fuselage contribution to the damping in yaw depends, of course, on the relative size of the fuselage and wing. In the past, the relative size of these components has generally been such that the fuselage contribution could be neglected. (See references 82 and 83.) For some recent designs which have a large fuselage relative to the wing, however, the fuselage contribution to C_{n_r} is important. In the case of fuselages having flat sides or having a flattened cross section with the major axis vertical the fuselage contribution may also be important and some fuselage contribution to C_{n_r} should be assumed, especially at high angles of attack. On the other hand, experimental data have shown that a flattened cross-section fuselage with the major axis horizontal can have negative damping in yaw at moderate and high angles of attack.

The contribution of the wing to C_{n_r} can be estimated from the formula and charts of figure 12 which were taken from reference 25. Values of C_{D_0} for the wing should be estimated from force-test data. For values of $\bar{x}/\bar{c}$ greatly different from zero, the charts of reference 25 can be used. The formula and charts of figure 12 are not considered reliable at high angles of attack, especially for swept wings. The use of experimental data from the references on C_{n_r} listed in table II is recommended in this case.

The effect of partial-span inboard flaps on C_{n_r} can usually be neglected. (See reference 82.) The effect of full-span trailing-edge or leading-edge high-lift devices can be estimated satisfactorily from the formula and charts of figure 12. Values of C_{D_0} in this case are, of course, for the wing with the high-lift device installed.

Vertical tail.- The contribution of a conventional-type vertical tail to C_{n_r} can be estimated from the formula

$$C_{n_{r_{tail}}} = 2\left(\frac{l}{b}\right)^2 C_{Y_{\beta_{tail}}} \qquad (29)$$

or, with the effective tail length $-C_{n_{\beta_{tail}}}/C_{Y_{\beta_{tail}}}$ substituted for the geometric tail length l/b,

$$C_{n_{r_{tail}}} = 2\frac{\left(C_{n_{\beta_{tail}}}\right)^2}{C_{Y_{\beta_{tail}}}}. \qquad (29a)$$

The experimental values for $C_{n_{r_{tail}}}$ presented in reference 82 for power-on or flap-down configurations are 30 to 40 percent greater than values predicted by formulas (29) or (29a). These differences are attributed to lag of sidewash effects in the free-oscillation tests used in measuring C_{n_r}. In estimations of $C_{n_{r_{tail}}}$ for stability calculations, similar lag of sidewash effects should be assumed if the oscillatory mode is of primary importance but no lag of sidewash should be assumed if the aperiodic mode is most important.

Methods for estimating the $C_{n_{r_{tail}}}$ for wing-tip vertical tails are presented in references 70 and 82.

$$C_{l_r}$$

The wing and vertical tail are the only airplane components that contribute appreciably to rolling-moment-due-to-yawing derivative C_{l_r} of an airplane. The contributions of the fuselage and horizontal tail can usually be neglected. A semiempirical method for estimating C_{l_r} is presented in reference 85. This method involves the use of experimental data on the parameter C_{l_β} to correct the theoretical values of $C_{l_{r_{wing}}}$ given in reference 25 and to estimate the value of $C_{l_{r_{wing}}}$.

Wing.- The formula of reference 85 and the charts of C_{l_r}/C_L from reference 25 for estimating $C_{l_{r_{wing}}}$ are given in figure 13. The values of C_{l_β}/C_L to be used in the charts can be obtained from figure 8. For taper ratios less than 0.25, values of C_{l_r}/C_L and C_{l_β}/C_L for a taper ratio of 0.25 can be used. The value of $C_{l_{\beta_{exp}}}$ used in the formula should be the same as the value of $C_{l_{\beta_{wing}}}$ estimated from experimental data by the method indicated in the section on C_{l_β}. In the case of C_{l_r}, however, (unlike the case of C_{l_β}) conservative

dynamic stability results will usually be obtained if the smaller values of the derivative (based on low-scale experimental data) are used instead of the larger (theoretical) values. This difference is a result of the fact that either an increase in the normally negative value of C_{l_β} or a decrease in the normally positive value of C_{l_r} can cause reduction in dynamic stability. As pointed out in reference 85 the estimation procedure shown in figure 13 appears to account satisfactorily for the effects of high-lift devices, wing, dihedral, and airfoil section.

Vertical tail.- The contribution of the vertical tail to C_{l_r} is usually estimated by the formula

$$C_{l_{r_{tail}}} = -2\left(\frac{l}{b}\right)\left(\frac{z}{b}\right)C_{Y_{\beta_{tail}}} \qquad (30)$$

where $C_{Y_{\beta_{tail}}}$ is preferably obtained from force-test data. When experimental data on $C_{l_{\beta_{tail}}}$ are available, the following formula from reference 85 can be used and will probably be more reliable than equation (30) because it takes into account any interference effects that might cause the effective vertical location of the center of pressure of the tail to be different from the location determined by geometrical procedures:

$$C_{l_{r_{tail}}} = -2\left(\frac{l}{b}\right)C_{l_{\beta_{tail}}} \qquad (31)$$

or with the effective tail length $-C_{n_{\beta_{tail}}}/C_{Y_{\beta_{tail}}}$ substituted for the geometric tail length l/b,

$$C_{l_{r_{tail}}} = 2\left(\frac{C_{n_{\beta_{tail}}}}{C_{Y_{\beta_{tail}}}}\right)C_{l_{\beta_{tail}}} \qquad (31a)$$

$$C_{Y_r}$$

Wing.- The theory of reference 25 gives values of the derivative C_{Y_r} (lateral force due to yawing) for the wing for a taper ratio of 1.0. The experimental data of references 25 and 59 indicate that this theory is inadequate for making reliable estimates of $C_{Y_{r_{wing}}}$. It is recommended therefore that the experimental data given in references 25, 58, 59, and 60 be used in making estimates of $C_{Y_{r_{wing}}}$.

Vertical tail.- The value of $C_{Y_{r_{tail}}}$ can be estimated by the formula

$$C_{Y_{r_{tail}}} = -2 \frac{l}{b} C_{Y_{\beta_{tail}}} \tag{32}$$

or by the formula in which the effective tail length $-C_{n_{\beta_{tail}}}/C_{Y_{\beta_{tail}}}$ is substituted for the geometric tail length l/b:

$$C_{Y_{r_{tail}}} = 2C_{n_{\beta_{tail}}} \tag{32a}$$

The discussion of lag-of-sidewash effects for $C_{n_{r_{tail}}}$ apply also to $C_{Y_{r_{tail}}}$.

EFFECTS OF MACH NUMBER

The effects of Mach number on the lateral stability derivatives have been treated theoretically in many investigations (see table II) but very little experimental data have been obtained to verify this theoretical work. Moreover, only a small part of this experimental work has been covered in published reports (reference 111) because most of it is classified at the present time. It appears, therefore, that estimates of the lateral-stability derivatives for the time being will have to be based largely on theoretical work.

The effects of Mach number on the stability derivatives can be usually considered negligible for all airplane components except the wing and vertical tail. For the low-lift-coefficient condition in the case of many high-speed airplanes, the vertical tail contributes more than the wing to all the stability derivatives except C_{l_p}. For this reason, in calculations for transonic or supersonic speed conditions it is especially important to know the effects of Mach number on the vertical-tail lift-curve slope or $C_{Y_{\beta_{tail}}}$.

Wing.- The effects of compressibility on the subsonic stability derivatives of the wing can be estimated by the formulas of reference 26. The values of the supersonic stability derivatives for some wing plan forms can be estimated by the references tabulated in table II. In this table the derivatives are grouped according to the type of wing plan form and to the particular derivatives covered. A helpful summary and discussion of the effects of Mach number on the derivatives for several different wing plan forms is presented in reference 103. A summary of

the theoretical lift-curve slope, damping in roll, and center-of-pressure characteristics of various wing plan forms is presented in reference 107. In the cases in which the theory shows large or abrupt changes in a stability derivative with changes in Mach number (for example, fig. 10 of reference 103) special care should be taken in estimating the derivative in that particular Mach number range. The abrupt changes should be smoothed or faired out in a manner similar to that suggested in the following section for estimating $C_{Y_{\beta_{tail}}}$.

In some cases, experimental data for supersonic speeds will be available on the sideslip derivatives and on the damping-in-roll derivative C_{l_p}. In such cases the experimental data should be used in preference to the theory. Some experimental results have indicated that the effect of the vertical location of the wing on the fuselage on the derivative $C_{l_{\beta}}$ might be greatly different at supersonic speeds from that at subsonic speeds. Since no methods are presently available for estimating this effect for the supersonic case, it appears that, at least in the case of high-wing and low-wing designs, force-test data are necessary for obtaining an accurate estimate of $C_{l_{\beta}}$.

Vertical tail.- The sideslip derivatives produced by the vertical tail at transonic and supersonic speeds can be estimated theoretically but should be obtained from force-test data whenever possible. These sideslip derivatives can be used to estimate the tail contributions to the other derivatives as pointed out previously. In estimates of the value of $C_{Y_{\beta_{tail}}}$ for transonic and supersonic speeds, corrections must be made for the effect of Mach number on the lift-curve slope of the tail, and these corrections should account for any differences in the end-plate effect of the horizontal tail on the vertical tail.

For Mach numbers below about 0.8 or 0.9 and above about 1.6 or 1.8 the effect of Mach number on the lift-curve slope of the vertical tail can be estimated satisfactorily from the theoretical values of references 26, 34, and 107. Since experimental data indicate that theoretical values of lift-curve slope are usually too high for Mach numbers from about 0.8 or 0.9 to about 1.6 or 1.8, the empirically determined fairings shown in figure 14 are recommended for use as a guide in the use of the theory to obtain approximate estimates in this Mach number range when force-test data are not avilable.

Experimental data have indicated that for vertical-tail configurations which have a tail length (distance from the center of gravity to the tail center of pressure) that is relatively short in terms of tail chords, the rearward shift of the tail center of pressure at supersonic speeds can cause an appreciable increase in the tail length and

consequently an appreciable increase in the magnitude of some of the tail derivatives. Theoretical center-of-pressure positions for various plan forms at supersonic speeds are given in reference 107.

EFFECTS OF POWER

On the basis of existing information, the effects of power on the lateral stability derivatives appear to be negligible in the case of jet-propelled airplanes but these effects are often very large in the case of single-engine propeller-driven airplanes. Methods are available for estimating some of these power effects but in most cases experimental data are necessary for making a satisfactory estimate. The effects of power can be broken down into two general classes:

(1) The effects of the lateral force produced by the propeller itself

(2) The effects of the propeller slipstream on the wing, fuselage, and vertical tail of the airplane

Effects of propeller lateral force.- A method of estimating the propeller-lateral-force derivative C_{Y_β} is presented in reference 31 which is based on the work of references 32 and 33. The contribution of the propeller lateral force to the other stability derivatives can be estimated from this derivative by assuming that the propeller is effectively a vertical tail surface and by using the expressions for the tail contribution to the various derivatives presented in the preceding sections. Some experimental data on the effect of windmilling propeller on all of the derivatives are presented in reference 65.

Effects of propeller slipstream.- The effects of propeller slipstream on the lateral-stability derivatives are usually much greater than the effects of propeller lateral force in the case of single-engine tractor airplanes. The slipstream effects on the wing, the fuselage, and the vertical tail can be considered as three independent effects.

The slipstream effects on the wing can usually be neglected except for the derivatives C_{l_β} and C_{l_r}. Experimental data showing the decrease in effective dihedral $\left(-C_{l_\beta}\right)$ with power for single-engine airplanes are presented in references 54, 55, 56, 74, and 80. It appears highly desirable to determine this effect of power experimentally because interference effects make accurate estimations of the effect very difficult. The effect of the slipstream on the value of $C_{l_{r_{wing}}}$ cannot be estimated from the data on $C_{l_{\beta_{wing}}}$ as described in the

section on C_{l_r}. In fact, this procedure would probably give the wrong sign for the increment of $C_{l_{r_{wing}}}$ contributed by the slipstream. An approximation of this increment might be obtained by estimating the slipstream velocity and the lateral displacement of the slipstream caused by yawing. Usually the power effects on $C_{l_{\beta_{wing}}}$ and $C_{l_{r_{wing}}}$ will be greatest for the flap-extended configuration.

In the case of the single-engine airplane the effect of the slipstream on the fuselage is usually to increase negatively the values of C_{n_β} and C_{Y_β}. (See references 54, 55, 56, 71, 74, and 76.) Since no accurate methods of estimating these slipstream effects on C_{n_β} and C_{Y_β} are available, it is necessary to determine them from force-test data.

The effects of the slipstream on the vertical tail are often very important and should also be determined from experimental data, if possible. The increase in dynamic pressure at the tail caused by the slipstream is treated theoretically in reference 116 and is illustrated by the experimental data of references 50, 54, 55, 56, 71, 74, and 76. The experimental data of reference 76 also show that the propeller slipstream can cause a destabilizing sidewash at the tail which will tend to reduce the stabilizing effect of the increased dynamic pressure at the tail. Since these data indicate that slipstream effects on the vertical tail vary greatly with airplane configuration and propeller arrangement (single or dual rotation), use of experimental data appears to be the only satisfactory estimation procedure at present.

Suggested estimation procedure for power effects.- The following procedure is suggested for estimating power effects. Obtain force-test data for tail off and tail on. Use tail-on data directly for C_{Y_β}, C_{n_β}, and C_{l_β}. Estimate rolling and yawing derivatives as follows:

(1) Estimate $C_{Y_{\beta_{propeller}}}$ from reference 31 and use this derivative and proper linear dimensions to estimate other propeller derivatives (rolling and yawing derivatives) in the same manner as tail derivatives.

(2) Subtract tail-on data from tail-off data to get values of $C_{Y_{\beta_{tail}}}$, $C_{n_{\beta_{tail}}}$, and $C_{l_{\beta_{tail}}}$ for the power-on condition and use these values to estimate the tail contribution to the other derivatives.

(3) For tail-off values of rolling and yawing derivatives, use same values as for power-off for all derivatives except C_{l_r}. Estimate C_{l_r} as suggested in preceding section.

(4) Add the values obtained in steps 1, 2, and 3 to get the rolling and yawing derivatives for the complete airplane.

INADEQUACIES IN PRESENT INFORMATION AND METHODS

In the course of summarizing the estimation methods for the various stability derivatives, the need for much additional information on all the derivatives became apparent. In particular, information is needed to aid in the estimation of the derivatives in the transonic and supersonic speed ranges. Additional work also needs to be done in correlating and analyzing existing subsonic data and in obtaining new experimental data for the development of semiempirical methods of estimating the subsonic derivatives without resort to force-test data. Another important need is for full-scale experimental results at all speeds for checking both low-scale data and the existing methods of estimating derivatives. Details of the need for additional work along these lines are discussed in the following sections. Studies should also be made to determine the conditions for which the use of steady-state stability derivatives in conventional stability equations is inadequate and to determine satisfactory methods of treating such conditions.

Transonic and Supersonic Speeds

Additional theoretical work is needed on the estimation of stability derivatives in the transonic and supersonic speed ranges to cover the range of wing plan forms for all the derivatives. In particular, more work is needed on plan forms currently under consideration, such as wings having moderate sweepback and taper. This need is illustrated by table II which indicates that very little material is available on the stability derivatives for such plan forms except, perhaps, for the derivative C_{l_p}. It appears from the table that this derivative and the triangular plan form have, in the past, received a disproportionate share of attention, probably because of the greater ease with which they could be treated theoretically.

The greatest need for work on stability derivatives at the present time is probably in the measurement of the derivatives at transonic and supersonic speeds. Experimental data on wings are urgently needed for checking the theoretical work and for use in the development of empirical corrections to the theory wherever necessary. Such corrections are particularly needed for fairing out abrupt variations of the derivatives with Mach number and for fairing through the Mach number range for which theory predicts infinite values. Examples of such discontinuities as indicated by theory are shown in figures 8 to 13 of reference 103.

Since experimental data obtained at supersonic speeds on wing-fuselage combinations and on complete models have revealed interference effects that are different from those obtained at subsonic speeds, it appears highly desirable to obtain at least a limited amount of experimental data at transonic and supersonic speeds to evaluate these interference effects. For example, investigations should be undertaken to determine the effect of wing-fuselage interference on the derivative C_{l_β} and the end-plate effect of the horizontal tail on the lift-curve slope of the vertical tail.

Most of the experimental data on stability derivatives at transonic and supersonic speeds will of necessity be obtained at Reynolds numbers considerably less than full-scale values and under test conditions which might render the results open to question in some cases. Full-scale checks in flight of the low-scale data and of the estimation methods therefore appear to be desirable. Consequently the methods of measuring stability derivatives in flight now being developed by the Cornell Aeronautical Laboratory, the Massachusetts Institute of Technology, and the NACA should be extended to transonic and supersonic speeds when the methods appear to be developed to a satisfactory degree of reliability for the subsonic case. Some preliminary considerations involved in the use of these flight techniques are discussed in references 117 to 120.

<center>Subsonic Speeds</center>

The methods presented in this paper for estimating the stability derivatives at subsonic speeds depend either directly or indirectly on the use of force-test data. These methods are probably more reliable than methods which do not involve the use of force-test data on the particular design under consideration or on a similar design. Methods which do not rely on such data are desirable in some cases, however, because the necessary data will not always be available.

In the case of sideslip derivatives, empirical methods can probably be developed largely from existing information. In some cases it will be necessary to augment the existing information with new results since much of the available force-test data were not obtained in a manner that would make the data readily usable for developing general estimation procedures.

In the case of rolling and yawing derivatives, considerably less information is available than in the case of the sideslip derivatives. Most of the information now available was obtained in the Langley stability tunnel, principally on wing configurations and to a limited extent on complete airplane models and airplane components other than the wing. Considerably more work is required, especially for components

in combination, before satisfactory methods can be developed for estimating rolling and yawing derivatives without the use of force-test data on the particular design under consideration or on a similar design.

In discussing the work necessary for developing new procedures for estimating the stability derivatives without the use of force-test data on the design under consideration or on a similar design, it is useful to break the problem down into two parts: (1) effect of individual components and (2) the effect of interference of the components on each other.

The principal components to be considered are the fuselage, wing, vertical tail, and propeller. For the isolated fuselage, the main problem is the development of methods for the estimation of C_{n_β} and then, perhaps, of C_{n_r} and C_{Y_β}. For the isolated wing, the main problem is to estimate the derivatives at lift coefficients above that at which separation begins. Such estimations can be made with reasonable accuracy for some of the derivatives by existing methods which make use of force-test data, but the development of methods which do not involve the use of force-test data will probably be very difficult. For the isolated vertical tail, the problem is to establish the effective tail area and aspect ratio from the geometry of the tail so that the lift-curve slope $\left(\text{or } C_{Y_\beta}\right)$ of the tail can be calculated. Solutions to this seemingly simple problem have in the past become involved with interference effects so that, as yet, no reliable methods have been published for estimating C_{Y_β} of the vertical tail from its geometry. For the isolated propellers, the work that is needed at present is a systematic check of existing methods of estimating the lateral force on the propeller to determine the accuracy of these methods.

The principal interference effects to be considered are mutual interference of the wing and fuselage; wing-fuselage interference on the vertical tail; horizontal-tail interference on the vertical tail; propeller-slipstream interference on the wing, fuselage, and vertical tail. The mutual-interference effects of the wing and fuselage are probably important only for the derivatives C_{l_β}, C_{n_β}, and C_{l_r}. A large amount of experimental data is available for the sideslip derivatives but no procedures for estimating the interference effects on these derivatives have been reported. Wing-fuselage interference has very important effects on C_{Y_β} of the vertical tail, and consequently on all of the stability derivatives for some flight conditions. These effects result from the sidewash and change in dynamic pressure at the tail which may result from sideslipping, rolling, or yawing. Although considerable data which show these interference effects are available, particularly for the case of sideslipping, no reliable methods exist

for estimating the interference effects. Horizontal-tail interference also has an important effect on C_{Y_β} of the vertical tail for some horizontal-tail positions. Some work on a limited number of configurations has been done toward developing methods of estimating this effect but data are required on more configurations before the generally applicable methods can be evolved. The propeller slipstream can cause important effects on C_{l_β} and C_{l_r} of the wing, on C_{n_β} and C_{Y_β} of the fuselage, and on C_{Y_β} of the tail (and consequently on the tail contribution to all the derivatives). Some data are available for the effect of the slipstream on the sideslip derivatives but, because of the complexity of this problem, considerable additional data may be required before a satisfactory method of estimating the slipstream effects can be developed.

As mentioned in the preceding section, full-scale checks of low-scale data and of the estimation methods are desirable. For the subsonic case some of the checks can be obtained from large-scale wind-tunnel tests but some checks in full-scale flight tests should also be obtained when the various methods of measuring stability derivatives in flight have been developed to a satisfactory degree of accuracy.

Langley Aeronautical Laboratory
        National Advisory Committee for Aeronautics
                Langley Field, Va., December 13, 1950

APPENDIX A

EQUATIONS OF MOTION

The dimensional equations for the lateral motions of an airplane are

$$mk_X{}^2 \frac{d^2\phi}{dt^2} - \frac{\partial L}{\partial p} \frac{d\phi}{dt} + mk_{XZ} \frac{d^2\psi}{dt^2} - \frac{\partial L}{\partial r} \frac{d\psi}{dt} - \frac{\partial L}{\partial v} v - L_c = 0 \qquad (A1)$$

$$mk_{XZ} \frac{d^2\phi}{dt^2} - \frac{\partial N}{\partial p} \frac{d\phi}{dt} + mk_Z{}^2 \frac{d^2\psi}{dt^2} - \frac{\partial N}{\partial r} \frac{d\psi}{dt} - \frac{\partial N}{\partial v} v - N_c = 0 \qquad (A2)$$

$$-\frac{\partial Y}{\partial p} \frac{d\phi}{dt} - (\text{Lift})\phi + mV \frac{d\psi}{dt} - \frac{\partial Y}{\partial r} \frac{d\psi}{dt} - (\text{Lift})(\tan\gamma)\psi + m \frac{dv}{dt} - \frac{\partial Y}{\partial v} v - Y_c = 0$$

$$(A3)$$

If equations (A1) and (A2) are divided by $\frac{1}{2}\rho V^2 Sb$ and equation (A3) is divided by $\frac{1}{2}\rho V^2 S$ the equations of motion may be expressed in the conventional nondimensional form in which they have generally been presented in NACA reports (for example, see reference 2):

$$2\mu K_X{}^2 \frac{d^2\phi}{ds^2} - \frac{1}{2} C_{l_p} \frac{d\phi}{ds} + 2\mu K_{XZ} \frac{d^2\psi}{ds^2} - \frac{1}{2} C_{l_r} \frac{d\psi}{ds} - C_{l_\beta}\beta - C_{l_c} = 0$$

$$2\mu K_{XZ} \frac{d^2\phi}{ds^2} - \frac{1}{2} C_{n_p} \frac{d\phi}{ds} + 2\mu K_Z{}^2 \frac{d^2\psi}{ds^2} - \frac{1}{2} C_{n_r} \frac{d\psi}{ds} - C_{n_\beta}\beta - C_{n_c} = 0 \qquad (A4)$$

$$-\frac{1}{2} C_{Y_p} \frac{d\phi}{ds} - C_L\phi + 2\mu \frac{d\psi}{ds} - \frac{1}{2} C_{Y_r} \frac{d\psi}{ds} - C_L(\tan\gamma)\psi + 2\mu \frac{d\beta}{ds} -$$

$$C_{Y_\beta}\beta - C_{Y_c} = 0$$

In order to convert these equations into a form which will reduce the number of arithmetical and algebraic steps in performing stability calculations, equations (A4) are multiplied by $m/\rho Sb$ and written in the following form:

$$\left(D^2 - l_p D\right)\phi + \left(K_1 D^2 - l_r D\right)\psi - l_\beta \beta - l_c = 0$$

$$\left(K_2 D^2 - n_p D\right)\phi + \left(D^2 - n_r D\right)\psi - n_\beta \beta - n_c = 0 \quad\Bigg\} \quad (A5)$$

$$\left(-y_p D - \frac{C_L}{2}\right)\phi + \left(D - y_r D - \frac{C_L}{2}\tan\gamma\right)\psi + \left(D - y_\beta\right)\beta - y_c = 0$$

where

$$\mu = \frac{m}{\rho Sb} \qquad \tau = \frac{m}{\rho SV} \qquad \sigma = \frac{t}{\tau} \qquad D = \frac{d}{d\sigma}$$

$$K_1 = \frac{K_{XZ}}{K_X{}^2} \qquad K_2 = \frac{K_{XZ}}{K_Z{}^2}$$

$$l_\beta = \frac{\mu}{2K_X{}^2}C_{l_\beta} \qquad n_\beta = \frac{\mu}{2K_Z{}^2}C_{n_\beta} \qquad y_\beta = \frac{1}{2}C_{Y_\beta}$$

$$l_p = \frac{1}{4K_X{}^2}C_{l_p} \qquad n_p = \frac{1}{4K_Z{}^2}C_{n_p} \qquad y_p = \frac{1}{4\mu}C_{Y_p}$$

$$l_r = \frac{1}{4K_X{}^2}C_{l_r} \qquad n_r = \frac{1}{4K_Z{}^2}C_{n_r} \qquad y_r = \frac{1}{4\mu}C_{Y_r}$$

$$l_c = \frac{\mu}{2K_X{}^2}C_{l_c} \qquad n_c = \frac{\mu}{2K_Z{}^2}C_{n_c} \qquad y_c = \frac{1}{2}C_{Y_c}$$

APPENDIX B

APPLICATION OF THE LAPLACE TRANSFORMATION TO CALCULATING MOTIONS

The application of the Laplace transformation to the calculation of the lateral motions of airplanes is presented in order to illustrate the development of the equations of motion in the form in which they are presented in the present paper. This work is similar to that presented in references 5 and 6. In fact, it follows the presentation in reference 5 very closely. Reference 6 presents a brief explanation of the Laplace transformation and its application to solution of the equations of motion of an airplane. This paper also makes reference to detailed explanations of the Laplace transformation. In cases where modification of the equations presented in the present paper are necessary, reference should be made to these texts for an understanding of the mathematics involved. Applying the Laplace transforms

$$L(1) = \frac{1}{\lambda} \qquad L(D\phi) = \lambda\phi_\lambda - \phi_0$$

$$L(\phi) = \phi_\lambda \qquad L(D^2\phi) = \lambda^2\phi_\lambda - \lambda\phi_0 - (D\phi)_0$$

$$\cdot \quad \cdot \quad \cdot \quad \cdot \quad \cdot$$

and multiplying each of the equations by λ transforms equations (A5) from appendix A to

$$\left.\begin{aligned}
\left(\lambda^3 - l_p\lambda^2\right)\phi_\lambda + \left(K_1\lambda^3 - l_r\lambda^2\right)\psi_\lambda - l_\beta\lambda\beta_\lambda &= r_1 \\[2ex]
\left(K_2\lambda^3 - n_p\lambda^2\right)\phi_\lambda + \left(\lambda^3 - n_r\lambda^2\right)\psi_\lambda - n_\beta\lambda\beta_\lambda &= r_2 \\[2ex]
\left(-y_p\lambda^2 - \frac{C_L}{2}\lambda\right)\phi_\lambda + \left[\lambda^2 - y_r\lambda^2 - \frac{C_L}{2}(\tan\gamma)\lambda\right]\psi_\lambda + \left(\lambda^2 - y_\beta\lambda\right)\beta_\lambda &= r_3
\end{aligned}\right\} \quad (B1)$$

where

$$r_1 = (\lambda^2 - l_p\lambda)\phi_0 + (K_1\lambda^2 - l_r\lambda)\psi_0 + \lambda(D\phi)_0 + K_1\lambda(D\psi)_0 + l_c$$

$$r_2 = (K_2\lambda^2 - n_p\lambda)\phi_0 + (\lambda^2 - n_r\lambda)\psi_0 + K_2\lambda(D\phi)_0 + \lambda(D\psi)_0 + n_c$$

$$r_3 = -y_p\lambda\phi_0 + (\lambda - y_r\lambda)\psi_0 + \lambda\beta_0 - y_c$$

Solving equations (B1) by determinants gives

$$\phi_\lambda = \frac{\begin{vmatrix} -l_\beta\lambda & r_1 & K_1\lambda^3 - l_r\lambda^2 \\[2mm] -n_\beta\lambda & r_2 & \lambda^3 - n_r\lambda^2 \\[2mm] \lambda^2 - y_\beta\lambda & r_3 & \lambda^2 - y_r\lambda^2 - \frac{C_L}{2}(\tan\gamma)\lambda \end{vmatrix}}{\begin{vmatrix} -l_\beta\lambda & \lambda^3 - l_p\lambda^2 & K_1\lambda^3 - l_r\lambda^2 \\[2mm] -n_\beta\lambda & K_2\lambda^3 - n_p\lambda^2 & \lambda^3 - n_r\lambda^2 \\[2mm] \lambda^2 - y_\beta\lambda & -y_p\lambda^2 - \frac{C_L}{2}\lambda & \lambda^2 - y_r\lambda^2 - \frac{C_L}{2}(\tan\gamma)\lambda \end{vmatrix}}$$

which may be expressed as

$$\phi_\lambda = \frac{a_0\lambda^5 + a_1\lambda^4 + a_2\lambda^3 + a_3\lambda^2 + a_4\lambda + a_5}{\lambda^2\left(A\lambda^4 + B\lambda^3 + C\lambda^2 + D\lambda + E\right)} \tag{B2}$$

Similarly, the expressions for ψ_λ and β_λ are

$$\psi_\lambda = \frac{b_0\lambda^5 + b_1\lambda^4 + b_2\lambda^3 + b_3\lambda^2 + b_4\lambda + b_5}{\lambda^2\left(A\lambda^4 + B\lambda^3 + C\lambda^2 + D\lambda + E\right)} \tag{B3}$$

$$\beta_\lambda = \frac{c_0\lambda^4 + c_1\lambda^3 + c_2\lambda^2 + c_3\lambda + c_4}{\lambda\left(A\lambda^4 + B\lambda^3 + C\lambda^2 + D\lambda + E\right)} \tag{B4}$$

where the expressions for the coefficients in equations (B2) to (B4) are
given in terms of the mass and aerodynamic stability derivatives by
equations (1) to (4) in the main body of this paper.

In order to obtain the actual variables from the transformed
variables, an inverse Laplace transformation must be applied. The
expressions for ϕ_λ, ψ_λ, and β_λ are of the form u_λ/v_λ where u_λ

and v_λ are polynomials, the degree of v_λ being higher than that of u_λ. The inverse transform of a function of this type is

$$L^{-1}\left(\frac{u_\lambda}{v_\lambda}\right) = \sum_{n=1}^{m} \frac{u(\lambda_n)}{v'(\lambda_n)} e^{\sigma\lambda_n} \tag{B5}$$

In this equation all of the roots λ of $v_\lambda = 0$ are assumed to be distinct. This assumption is valid for β_λ; but for ϕ_λ and ψ_λ, $v_\lambda = 0$ has two zero roots. (See equations (B2), (B3), and (B4).) The terms in the equations for ϕ and ψ resulting from the two zero roots are

$$\frac{d\Omega}{d\sigma}(0) + \Omega(0)\sigma \tag{B6}$$

where

$$\Omega = \frac{u_\lambda}{v_\lambda}\lambda^2$$

The inverse transforms of ϕ_λ, ψ_λ, and β_λ are from equations (B5) and (B6)

$$\phi = A_1 e^{\sigma\lambda_1} + A_2 e^{\sigma\lambda_2} + A_3 e^{\sigma\lambda_3} + A_4 e^{\sigma\lambda_4} + A_5\sigma + A_6 \tag{B7}$$

$$\psi = B_1 e^{\sigma\lambda_1} + B_2 e^{\sigma\lambda_2} + B_3 e^{\sigma\lambda_3} + B_4 e^{\sigma\lambda_4} + B_5\sigma + B_6 \tag{B8}$$

$$\beta = C_1 e^{\sigma\lambda_1} + C_2 e^{\sigma\lambda_2} + C_3 e^{\sigma\lambda_3} + C_4 e^{\sigma\lambda_4} + C_5 \tag{B9}$$

The equations for the rolling velocity p and the yawing velocity r can be obtained from equations (B7) and (B8) by differentiation

$$p = \frac{1}{\tau}\left(A_1\lambda_1 e^{\sigma\lambda_1} + A_2\lambda_2 e^{\sigma\lambda_2} + A_3\lambda_3 e^{\sigma\lambda_3} + A_4\lambda_4 e^{\sigma\lambda_4} + A_5\right) \tag{B10}$$

$$r = \frac{1}{\tau}\left(B_1\lambda_1 e^{\sigma\lambda_1} + B_2\lambda_2 e^{\sigma\lambda_2} + B_3\lambda_3 e^{\sigma\lambda_3} + B_4\lambda_4 e^{\sigma\lambda_4} + B_5\right) \tag{B11}$$

where the expressions for the coefficients of equations (B7) to (B11) are given by equations (6) to (8) in the section "Calculation of Motions."

APPENDIX C

SOLUTION OF BIQUADRATIC EQUATION

Many methods are available, of course, for solving for the roots of a biquadratic equation. For example, there are Horner's, Ferrari's, Bernoulli's, Descartes', and Hitchcock's methods; various methods of solution by trial; and also various graphical methods such as that given in reference 1. Solution by trial in which synthetic division is used, however, is recommended as being the simplest method for most lateral stability work. The characteristic equation for the lateral motions of an airplane

$$A\lambda^4 + B\lambda^3 + C\lambda^2 + D\lambda + E = 0$$

generally has two real roots and a pair of conjugate complex roots. For these cases the two real roots can be factored out easily and the remaining quadratic solved for the conjugate complex roots. In the few cases for which all four of the roots of the characteristic equation are complex, Descartes' method can be used to factor the biquadratic equation into two quadratics. When there are real roots, solution by Descartes' method requires more time than factoring out the real roots singly and consequently is not recommended for general use. These methods of solution are explained in the following sections.

Solution by Trial by Means of Synthetic Division

Solution for real roots by trial by means of synthetic division consists of successive approximations of a root and checking by synthetic division until the root is determined to the desired degree of accuracy. This check by synthetic division is based on the fact that if a is a root of a polynomial f(x) then x - a is a factor of f(x) and consequently no remainder is left when f(x) is divided by x - a.

The method of solving the stability biquadratic equation by trial with synthetic division is explained in three steps in the following sections. First, the rule for synthetic division and a numerical example are given. Second, the specific use of synthetic division for factoring a biquadratic is illustrated by a simplified example for which the roots are known. This example shows how the cubic and then the quadratic factors of the biquadratic are obtained. Third, the use of synthetic division in extracting the roots of a representative

characteristic stability biquadratic is illustrated with special refer-
ence to methods of making the first approximations of the real roots.

   Explanation of synthetic division.- Synthetic division is explained
in almost all algebra text books but is presented herein for the con-
venience of the reader. The rule for synthetic division may be given
as follows:

   Assume that a polynomial in x (f(x)) is to be divided by x - a;
write the coefficients of the polynomial in order, supplying 0 when
a coefficient is lacking.

   Multiply a by the first coefficient, and add (algebraically) the
product to the next coefficient.

   Multiply this sum by a, add to the next coefficient, and proceed
until all the coefficients are used. The last sum is the remainder and
also the value of the polynomial when a is substituted for the
variable x.

   For example, divide $x^4 + 3x^3 + 3x^2 - x - 6$ by x - 3.

$$
\begin{array}{l}
1 + 3 + 3 - 1 - 6 \,\big| \\
\underline{+ 3 + 18 + 63 + 186} \,\big| 3 \\
1 + 6 + 21 + 62 + 180
\end{array}
$$

   Use of synthetic division in factoring out roots.- The use of
synthetic division to factor out two known rational roots of a biquadratic
equation is illustrated by the following simple example. These two
rational roots represent the two real roots of the characteristic sta-
bility equation which, of course, are not normally known but can be
approximated by the method given in the next section of this paper.

   One factor of the biquadratic is x - 1 so there is no remainder
when the biquadratic is divided by the root 1

$$
\begin{array}{l}
1 + 3 + 3 - 1 - 6 \,\big| \\
\underline{+ 1 + 4 + 7 + 6} \,\big| 1 \\
1 + 4 + 7 + 6 \quad 0
\end{array}
$$

Since the remainder is 0, x - 1 is one factor of the biquadratic
equation and $x^3 + 4x^2 + 7x + 6$ is another factor. Inasmuch as a
cubic equation must have at least one real root, a second real root of

the biquadratic equation can be factored out of the cubic. For
example x + 2 is a factor so divide the cubic by the root -2.

$$1 + 4 + 7 + 6 \quad\Big|$$
$$\underline{- 2 - 4 - 6 \Big| -2}$$
$$1 + 2 + 3 \quad 0$$

The factors of the biquadratic then are x - 1, x + 2, and $x^2 + 2x + 3$.
The quadratic factor can be solved for its roots by the quadratic
formula. For example

$$x = \frac{-2 \pm \sqrt{4 - 12}}{2} = -1 \pm i \sqrt{2}$$

Example of application to characteristic equation.- Reasonably
accurate first approximations to the real roots of the characteristic
equation can be obtained from simple formulas. Successively closer
approximations can then be obtained by interpolating from the remainders.
The following example illustrates the application of this method to
obtaining the roots of the stability biquadratic. The biquadratic

$$\lambda^4 + 10.43\lambda^3 + 16.32\lambda^2 + 68.6\lambda - 9.10 = 0$$

is of the form

$$A\lambda^4 + B\lambda^3 + C\lambda^2 + D\lambda + E = 0$$

Since the coefficient E is generally much smaller than coefficient D
in lateral stability work, one of the real roots (usually the smaller
of the two) is approximately equal to -E/D or it may be more closely
approximated by the equation

$$\lambda = - \frac{E}{D - \dfrac{CE}{D}}$$

or for the particular case

$$\lambda = - \frac{-9.10}{68.6 - \dfrac{(16.32)(-9.10)}{68.6}} = 0.129$$

Approximating the root by synthetic division

$$1 + 10.43 + 16.32 + 68.6 - 9.10 \quad | \quad \text{Approximation}$$

				Approximation
$1 + 10.43 + 16.32 + 68.6 - 9.10$				Approximation
$+ \quad .13 + 1.36 + 2.3 + 9.10$	.1284	2
$+ \quad .13 + 1.36 + 2.3 + 9.14$	.129	1
$1 + 10.56 + 17.68 + 70.9 + .04$		1
$1 + 10.56 + 17.68 + 70.9 + 0$		2

For this root, the second approximation was determined by dividing the coefficient E by the fourth sum from the quotient

$$- \frac{-9.10}{70.9}$$

This procedure generally provides a good second approximation for the small real root.

The cubic equation obtained by setting

$$\lambda^3 + 10.56\lambda^2 + 17.68\lambda + 70.9$$

equal to zero is of the form

$$a\lambda^3 + b\lambda^2 + c\lambda + d = 0$$

In most lateral-stability work, a real root of this equation will be approximately equal to $-b$ or it may be more closely approximated by the equation

$$\lambda = - \frac{b^3 + d}{b^2 + c}$$

or for the particular case

$$\lambda = - \frac{(10.56)^3 + 70.9}{(10.56)^2 + 17.68} = -9.65$$

Approximating the root by synthetic division

		Approximation
1 + 10.56 + 17.68 + 70.9		
- 9.48 - 10.20 - 70.9	-9.485	6
- 9.49 - 10.16 - 71.4	-9.49	5
- 9.48 - 10.25 - 70.4	-9.48	4
- 9.45 - 10.50 - 67.9	-9.45	3
- 9.55 - 9.64 - 76.8	-9.55	2
- 9.65 - 8.78 - 85.9	-9.65	1
1 + 0.91 + 8.90 - 15.0		1
1 + 1.01 + 8.04 - 5.9		2
1 + 1.11 + 7.18 + 3.0		3
1 + 1.08 + 7.43 + 0.5		4
1 + 1.07 + 7.52 - 0.5		5
1 + 1.075 + 7.48 0		6

For this large real root there is no simple method of determining the second approximation as there was in the case of the smaller real root. The magnitude of the estimated root in this case is arbitrarily increased or decreased slightly from the first approximation. From the remainders determined from the first two approximations, a fairly close third approximation can then be made.

Factoring the quadratic equation obtained by setting

$$\lambda^2 + 1.075\lambda + 7.48$$

equal to zero by use of the quadratic formula gives the final two roots of the biquadratic equation.

$$\lambda' = -\frac{1.075 \pm \sqrt{1.16 - 29.92}}{2}$$

$$= -0.538 \pm i\sqrt{\frac{28.76}{4}}$$

$$= -0.538 \pm 2.68i$$

The roots of the biquadratic equation may be checked by multiplying the four factors to determine whether their product equals the original biquadratic

$$(\lambda - 0.1284)(\lambda + 9.485)(\lambda + 0.538 + 2.68i)(\lambda + 0.538 - 2.68i) = (\lambda^2 + 9.457\lambda -$$

$$1.220)(\lambda^2 + 1.07\lambda + 7.47) = \lambda^4 + 10.43\lambda^3 + 16.32\lambda^2 + 68.6\lambda - 9.10$$

Solution by Descartes' Method

Descartes' method of solving a biquadratic equation is particularly useful for solving equations which do not have any real roots. This method is explained in most text books on advanced algebra and theory of equations. In general, the method consists of reducing the biquadratic equation to a cubic equation which can be solved easily. One root of the cubic equation is used to form two quadratic equations the roots of which are used to obtain the roots of the biquadratic equation.

Method.- Reduce the general biquadratic equation

$$A\lambda^4 + B\lambda^3 + C\lambda^2 + D\lambda + E = 0$$

to the form

$$\lambda^4 + b\lambda^3 + c\lambda^2 + d\lambda + e = 0$$

by dividing by A.

Obtain the values of q, r, and s from the following equations:

$$q = c - \frac{3}{8} b^2$$

$$r = d - \frac{bc}{2} + \frac{1}{8} b^3$$

$$s = e - \frac{bd}{4} + \frac{b^2 c}{16} - \frac{3}{256} b^4$$

and form the equation

$$x^6 + \frac{1}{2} qx^4 + \left(\frac{1}{16} q^2 - \frac{1}{4} s\right)x^2 - \frac{1}{64} r^2 = 0$$

and solve this cubic equation in x^2 for one of its roots $x^2 \neq 0$. Solution by trial by means of synthetic division is recommended. Determine the values of l and m from the equation

$$l = \frac{q}{2} + 2x^2 - \frac{r}{4x}$$

$$m = \frac{q}{2} + 2x^2 + \frac{r}{4x}$$

Substitute the values of l and m and the value of x used in obtaining l and m in the equations

$$y^2 + 2xy + l = 0$$

$$y^2 - 2xy + m = 0$$

and solve these quadratic equations for their roots y from which the roots of the biquadratic equation may be obtained from the following relation:

$$\lambda = y - \frac{b}{4}$$

APPENDIX D

SPECIAL NOTATION USED IN CALCULATING MOTIONS WHEN

THE CHARACTERISTIC EQUATION HAS COMPLEX ROOTS

When two of the roots λ_1 and λ_2 are conjugate complex, the coefficients A_1 and A_2, B_1 and B_2, C_1 and C_2 will be conjugate complex. If $R + Ii$ is one of the roots λ_1 and if the powers of λ_1 are expressed as

$$\lambda_1{}^k = R_k + I_k i$$

then

$$\lambda_1 = R_1 + I_1 i$$

$$\lambda_1{}^2 = R_2 + I_2 i$$

$$\lambda_1{}^3 = R_3 + I_3 i$$

$$\lambda_1{}^4 = R_4 + I_4 i$$

$$\lambda_1{}^5 = R_5 + I_5 i$$

Substitution of the root $R + Ii$ in the expression for A_1 gives

$$A_1 = \frac{\left(a_0 R_5 + a_1 R_4 + a_2 R_3 + a_3 R_2 + a_4 R_1 + a_5\right) + \left(a_0 I_5 + a_1 I_4 + a_2 I_3 + a_3 I_2 + a_4 I_1\right) i}{\left(6A R_5 + 5B R_4 + 4C R_3 + 3D R_2 + 2E R_1\right) + \left(6A I_5 + 5B I_4 + 4C I_3 + 3D I_2 + 2E I_1\right) i}$$

The division of these complex numbers is indicated by the equation

$$\frac{x_1 + y_1 i}{x_2 + y_2 i} = \frac{x_1 x_2 + y_1 y_2}{x_2{}^2 + y_2{}^2} + \frac{x_2 y_1 - x_1 y_2}{x_2{}^2 + y_2{}^2} i$$

It is evident from these relations that A_1 is a complex number. In this case new symbols are used to represent the real and imaginary parts of A_1 as follows:

$$A_1 = R_A + I_A i$$

A_2 is the conjugate of A_1 and will be referred to as

$$A_2 = R_A - I_A i$$

By procedures similar to those for the A coefficients,

$$B_1 = \frac{\left(b_0 R_5 + b_1 R_4 + b_2 R_3 + b_3 R_2 + b_4 R_1 + b_5\right) + \left(b_0 I_5 + b_1 I_4 + b_2 I_3 + b_3 I_2 + b_4 I_1\right) i}{\left(6AR_5 + 5BR_4 + 4CR_3 + 3DR_2 + 2ER_1\right) + \left(6AI_5 + 5BI_4 + 4CI_3 + 3DI_2 + 2EI_1\right) i}$$

which may be referred to as

$$B_1 = R_B + I_B i$$

and

$$B_2 = R_B - I_B i$$

Also,

$$C_1 = \frac{\left(c_0 R_5 + c_1 R_4 + c_2 R_3 + c_3 R_2 + c_4 R_1\right) + \left(c_0 I_5 + c_1 I_4 + c_2 I_3 + c_3 I_2 + c_4 I_1\right) i}{\left(6AR_5 + 5BR_4 + 4CR_3 + 3DR_2 + 2ER_1\right) + \left(6AI_5 + 5BI_4 + 4CI_3 + 3DI_2 + 2EI_1\right) i}$$

which may be referred to as

$$C_1 = R_C + I_C i$$

and

$$C_2 = R_C - I_C i$$

Similar analysis shows that, if the roots λ_3 and λ_4 are also conjugate complex quantities $\left(\lambda_3 = R' + I'i \quad \text{and} \quad \lambda_4 = R' - I'i\right)$, then

$$A_3 = R'_A + I'_A i$$

and

$$A_4 = R'_A - I'_A i$$

where

$$A_3 = \frac{\left(a_0 R'_5 + a_1 R'_4 + a_2 R'_3 + a_3 R'_2 + a_4 R'_1 + a_5\right) + \left(a_0 I'_5 + a_1 I'_4 + a_2 I'_3 + a_3 I'_2 + a_4 I'_1\right)i}{\left(6AR'_5 + 5BR'_4 + 4CR'_3 + 3DR'_2 + 2ER'_1\right) + \left(6AI'_5 + 5BI'_4 + 4CI'_3 + 3DI'_2 + 2EI'_1\right)i}$$

Also,

$$B_3 = R'_B + I'_B i$$

and

$$B_4 = R'_B - I'_B i$$

where

$$B_3 = \frac{\left(b_0 R'_5 + b_1 R'_4 + b_2 R'_3 + b_3 R'_2 + b_4 R'_1 + b_5\right) + \left(b_0 I'_5 + b_1 I'_4 + b_2 I'_3 + b_3 I'_2 + b_4 I'_1\right)i}{\left(6AR'_5 + 5BR'_4 + 4CR'_3 + 3DR'_2 + 2ER'_1\right) + \left(6AI'_5 + 5BI'_4 + 4CI'_3 + 3DI'_2 + 2EI'_1\right)i}$$

Similarly,

$$C_3 = R'_C + I'_C i$$

and

$$C_4 = R'_C - I'_C i$$

where

$$C_3 = \frac{\left(c_0 R'_5 + c_1 R'_4 + c_2 R'_3 + c_3 R'_2 + c_4 R'_1\right) + \left(c_0 I'_5 + c_1 I'_4 + c_2 I'_3 + c_3 I'_2 + c_4 I'_1\right)i}{\left(6AR'_5 + 5BR'_4 + 4CR'_3 + 3DR'_2 + 2ER'_1\right) + \left(6AI'_5 + 5BI'_4 + 4CI'_3 + 3DI'_2 + 2EI'_1\right)i}$$

REFERENCES

1. Zimmerman, Charles H.: An Analysis of Lateral Stability in Power-Off Flight with Charts for Use in Design. NACA Rep. 589, 1937.

2. Sternfield, Leonard: Effect of Product of Inertia on Lateral Stability. NACA TN 1193, 1947.

3. McKinney, Marion O., Jr., and Drake, Hubert M.: Correlation of Experimental and Calculated Effects of Product of Inertia on Lateral Stability. NACA TN 1370, 1947.

4. Jones, Robert T.: A Simplified Application of the Method of Operators to the Calculation of Disturbed Motions of an Airplane. NACA Rep. 560, 1936.

5. Murray, Harry E., and Grant, Frederick C.: Method of Calculating the Lateral Motions of Aircraft Based on the Laplace Transform. NACA TN 2129, 1950.

6. Mokrzycki, G. A.: Application of the Laplace Transformation to the Solution of the Lateral and Longitudinal Stability Equations. NACA TN 2002, 1950.

7. Jones, Robert T.: Calculation of the Motion of an Airplane under the Influence of Irregular Disturbances. Jour. Aero. Sci., vol. 3, no. 12, Oct. 1936, pp. 419-425.

8. Sternfield, Leonard, and Gates, Ordway B., Jr.: A Method of Calculating a Stability Boundary that Defines a Region of Satisfactory Period-Damping Relationship of the Oscillatory Mode of Motion. NACA TN 1859, 1949.

9. Brown, W. S.: A Simple Method of Constructing Stability Diagrams. R. & M. No. 1905, British A.R.C., 1942.

10. Schy, Albert A.: A Theoretical Analysis of the Effects of Fuel Motion on Airplane Dynamics. NACA TN 2280, 1951

11. Sternfield, Leonard: Some Effects of Nonlinear Variation in the Directional-Stability and Damping-in-Yawing Derivatives on the Lateral Stability of an Airplane. NACA TN 2233, 1950.

12. Greenberg, Harry: Frequency-Response Method for Determination of Dynamic Stability Characteristics of Airplanes with Automatic Controls. NACA Rep. 882, 1947. (Formerly NACA TN 1229.)

13. Sternfield, Leonard, and Gates, Ordway B., Jr.: A Theoretical
    Analysis of the Effect of Time Lag in an Automatic Stabilization
    System on the Lateral Oscillatory Stability of an Airplane. NACA
    TN 2005, 1950.

14. Jones, Arthur L., and Briggs, Benjamin R.: A Survey of Stability
    Analysis Techniques for Automatically Controlled Aircraft. NACA
    TN 2275, 1951.

15. Gates, Ordway B., Jr., and Schy, Albert A.: A Theoretical Method of
    Determining the Control Gearing and Time Lag Necessary for a
    Specified Damping of an Aircraft Equipped with a Constant-Time-Lag
    Autopilot. NACA TN 2307, 1951.

16. McKinney, Marion O., Jr., and Maggin, Bernard: Experimental Verifi-
    cation of the Rudder-Free Stability Theory for an Airplane Model
    Equipped with Rudders Having Negative Floating Tendency and
    Negligible Friction. NACA ARR L4J05a, 1944.

17. Greenberg, Harry, and Sternfield, Leonard: A Theoretical Investiga-
    tion of the Lateral Oscillations of an Airplane with Free Rudder
    with Special Reference to the Effect of Friction. NACA Rep. 762,
    1943. (Formerly NACA ARR, March 1943.)

18. Cohen, Doris: A Theoretical Investigation of the Rolling Oscilla-
    tions of an Airplane with Ailerons Free. NACA Rep. 787, 1944.
    (Formerly NACA ARR 4A06.)

19. Sternfield, Leonard: Effect of Automatic Stabilization on the
    Lateral Oscillatory Stability of a Hypothetical Airplane at
    Supersonic Speeds. NACA TN 1818, 1949.

20. Routh, Edward John: Dynamics of a System of Rigid Bodies. Part I.
    Eighth ed., MacMillan and Co., Ltd., 1913. (Reprinted 1930.)

21. Hunsaker, J. C., and Wilson, E. B.: Report on Behavior of Aeroplanes
    in Gusts. NACA Rep. 1, 1915.

22. Wilson, Edwin Bidwell: Theory of an Airplane Encountering Gusts.
    Part II. NACA Rep. 21, 1917. Part III. NACA Rep. 27, 1918.

23. Mazelsky, Barnard, and Diederich, Franklin W.: Two Matrix Methods
    for Calculating Forcing Functions from Known Responses. NACA
    TN 1965, 1949.

24. Sternfield, Leonard, and Gates, Ordway B., Jr.: A Simplified Method
    for the Determination and Analysis of the Neutral-Lateral-
    Oscillatory-Stability Boundary. NACA Rep. 943, 1949. (Formerly
    NACA TN 1727.)

25. Toll, Thomas A., and Queijo, M. J.: Approximate Relations and
    Charts for Low-Speed Stability Derivatives of Swept Wings. NACA
    TN 1581, 1948.

26. Fisher, Lewis R.: Approximate Corrections for the Effects of Com-
    pressibility on the Subsonic Stability Derivatives of Swept Wings.
    NACA TN 1854, 1949.

27. Katzoff, S., and Mutterperl, William: The End-Plate Effect of a
    Horizontal-Tail Surface on a Vertical-Tail Surface. NACA
    TN 797, 1941.

28. Murray, Harry E.: Wind-Tunnel Investigation of End-Plate Effects
    of Horizontal Tails on a Vertical Tail Compared with Available
    Theory. NACA TN 1050, 1946.

29. Shortal, Joseph A.: Effect of Tip Shape and Dihedral on Lateral-
    Stability Characteristics. NACA Rep. 548, 1935.

30. Purser, Paul E., and Campbell, John P.: Experimental Verification
    of a Simplified Vee-Tail Theory and Analysis of Available Data
    on Complete Models with Vee Tails. NACA Rep. 823, 1945.
    (Formerly NACA ACR L5A03.)

31. Ribner, Herbert S.: Notes on the Propeller and Slipstream in
    Relation to Stability. NACA ARR L4I12a, 1944.

32. Ribner, Herbert S.: Formulas for Propellers in Yaw and Charts of
    the Side-Force Derivative. NACA Rep. 819, 1945. (Formerly
    NACA ARR 3E19.)

33. Ribner, Herbert S.: Propellers in Yaw. NACA Rep. 820, 1945.
    (Formerly NACA ARR 3L09.)

34. DeYoung, John: Theoretical Additional Span Loading Characteristics
    of Wings with Arbitrary Sweep, Aspect Ratio, and Taper Ratio.
    NACA TN 1491, 1947. (Also included in NACA Rep. 921, 1948.)

35. Brewer, Jack D., and Lichtenstein, Jacob H.: Effect of Horizontal
    Tail on Low-Speed Static Lateral Stability Characteristics of a
    Model Having 45° Sweptback Wing and Tail Surfaces. NACA TN 2010,
    1950.

36. Michael, William H., Jr.: Analysis of the Effects of Wing Inter-
    ference on the Tail Contributions to the Rolling Derivatives.
    NACA TN 2332, 1951.

37. Bamber, M. J., and House, R. O.: Wind-Tunnel Investigation of
    Effect of Yaw on Lateral-Stability Characteristics. I - Four
    N.A.C.A. 23012 Wings of Various Plan Forms with and without
    Dihedral. NACA TN 703, 1939.

38. Bamber, M. J., and House, R. O.: Wind-Tunnel Investigation of
    Effect of Yaw on Lateral-Stability Characteristics. II -
    Rectangular N.A.C.A. 23012 Wing with a Circular Fuselage and a
    Fin. NACA TN 730, 1939.

39. House, Rufus O., and Wallace, Arthur R.: Wind-Tunnel Investigation
    of Effect of Interference on Lateral-Stability Characteristics of
    Four NACA 23012 Wings, an Elliptical and a Circular Fuselage, and
    Vertical Fins. NACA Rep. 705, 1941.

40. Recant, Isidore G., and Wallace, Arthur R.: Wind-Tunnel Investiga-
    tion of Effect of Yaw on Lateral-Stability Characteristics.
    III - Symmetrically Tapered Wing at Various Positions on Circular
    Fuselage with and without a Vertical Tail. NACA TN 825, 1941.

41. Recant, I. G., and Wallace, Arthur R.: Wind-Tunnel Investigation
    of Effect of Yaw on Lateral-Stability Characteristics.
    IV - Symmetrically Tapered Wing with a Circular Fuselage Having
    a Wedge-Shaped Rear and a Vertical Tail. NACA ARR, March 1942.

42. Wallace, Arthur R., and Turner, Thomas R.: Wind-Tunnel Investiga-
    tion of Effect of Yaw on Lateral-Stability Characteristics.
    V - Symmetrically Tapered Wing with a Circular Fuselage Having a
    Horizontal and a Vertical Tail. NACA ARR 3F23, 1943.

43. Teplitz, Jerome: Effects of Small Angles of Sweep and Moderate
    Amounts of Dihedral on Stalling and Lateral Characteristics of
    a Wing-Fuselage Combination Equipped with Partial- and Full-Span
    Double Slotted Flaps. NACA Rep. 800, 1944. (Formerly NACA
    ACR L4E20.)

44. Hollingworth, Thomas A.: Investigation of Effect of Sideslip on
    Lateral Stability Characteristics. II - Rectangular Midwing on
    Circular Fuselage with Variations in Vertical-Tail Area and
    Fuselage Length with and without Horizontal Tail Surface.
    NACA ARR L5C13, 1945.

45. Hollingworth, Thomas A.: Investigation of Effect of Sideslip on
    Lateral Stability Characteristics. III - Rectangular Low Wing
    on Circular Fuselage with Variations in Vertical-Tail Area and
    Fuselage Length with and without Horizontal Tail Surface.
    NACA ARR L5C13a, 1945.

46. Fehlner, Leo F., and MacLachlan, Robert: Investigation of Effect
    of Sideslip on Lateral Stability Characteristics. I - Circular
    Fuselage with Variations in Vertical-Tail Area and Tail Length
    with and without Horizontal Tail Surface. NACA ARR L4E25,
    1944.

47. Hoggard, H. Page, Jr.: Wind-Tunnel Investigation of Fuselage
    Stability in Yaw with Various Arrangements of Fins. NACA TN 785,
    1940.

48. Donlan, C. J., and Letko, W.: The Effect of Cowling Shape on the
    Stability Characteristics of an Airplane. NACA ARR, Sept. 1942.

49. Recant, Isidore G., and Wallace, Arthur R.: Wind-Tunnel Investiga-
    tion of the Effect of Vertical Postion of the Wing on the Side
    Flow in the Region of the Vertical Tail. NACA TN 804, 1941.

50. Neely, R. H., Fogarty, L. E., and Alexander, S. R.: Comparison of
    Yaw Characteristics of a Single-Engine Airplane Model with Single-
    Rotating and Dual-Rotating Propellers. NACA ACR L4D19, 1944.

51. Maggin, Bernard, and Shanks, Robert E.: The Effect of Geometric
    Dihedral on the Aerodynamic Characteristics of a 40° Swept-Back
    Wing of Aspect Ratio 3. NACA TN 1169, 1946.

52. Stüper, J.: Effect of Propeller Slipstream on Wing and Tail.
    NACA TM 874, 1938.

53. Rogallo, Francis M., and Swanson, Robert S.: Wind-Tunnel Tests of a
    Twin-Engine Model to Determine the Effect of Direction of Propeller
    Rotation on the Static-Stability Characteristics. NACA ARR,
    Jan. 1943.

54. Tamburello, Vito, and Weil, Joseph: Wind-Tunnel Investigation of
    the Effect of Power and Flaps on the Static Lateral Characteristics
    of a Single-Engine Low-Wing Airplane Model. NACA TN 1327, 1947.

55. Hagerman, John R.: Wind-Tunnel Investigation of the Effect of Power
    and Flaps on the Static Lateral Stability and Control Character-
    istics of a Single-Engine High-Wing Airplane Model. NACA TN 1379,
    1947.

56. Purser, Paul E., and Spear, Margaret F.: Tests to Determine Effects
    of Slipstream Rotation on the Lateral Stability Characteristics
    of a Single-Engine Low-Wing Airplane Model. NACA TN 1146, 1946.

57. Tosti, Louis P.: Low-Speed Static Stability and Damping-in-Roll
    Characteristics of Some Swept and Unswept Low-Aspect-Ratio Wings.
    NACA TN 1468, 1947.

58. Queijo, M. J., and Jaquet, Byron M.: Investigation of Effects of
    Geometric Dihedral on Low-Speed Static Stability and Yawing
    Characteristics of an Untapered 45° Sweptback-Wing Model of Aspect
    Ratio 2.61. NACA TN 1668, 1948.

59. Goodman, Alex, and Brewer, Jack D.: Investigation at Low Speeds of
    the Effect of Aspect Ratio and Sweep on Static and Yawing
    Stability Derivatives of Untapered Wings. NACA TN 1669, 1948.

60. Letko, William, and Cowan, John W.: Effect of Taper Ratio on Low-
    Speed Static and Yawing Stability Derivatives of 45° Sweptback
    Wings with Aspect Ratio of 2.61. NACA TN 1671, 1948.

61. Schade, Robert O.: Effect of Geometric Dihedral on the Aerodynamic
    Characteristics of Two Isolated Vee-Tail Surfaces. NACA TN 1369,
    1947.

62. Polhamus, Edward C., and Moss, Robert J.: Wind-Tunnel Investigation
    of the Stability and Control Characteristics of a Complete Model
    Equipped with a Vee Tail. NACA TN 1478, 1947.

63. Letko, William, and Goodman, Alex: Preliminary Wind-Tunnel Investi-
    gation at Low Speed of Stability and Control Characteristics of
    Swept-Back Wings. NACA TN 1046, 1946.

64. Lockwood, Vernard E., and Watson, James M.: Stability and Control
    Characteristics at Low Speed of an Airplane Model Having a 38.7°
    Sweptback Wing with Aspect Ratio 4.51, Taper Ratio 0.54, and
    Conventional Tail Surfaces. NACA TN 1742, 1948.

65. Bird, John D., and Jaquet, Byron M.: A Study of the Use of Experi-
    mental Stability Derivatives in the Calculation of the Lateral
    Disturbed Motions of a Swept-Wing Airplane and Comparison with
    Flight Results. NACA TN 2013, 1950.

66. Pearson, Henry A., and Jones, Robert T.: Theoretical Stability and
    Control Characteristics of Wings with Various Amounts of Taper
    and Twist. NACA Rep. 635, 1938.

67. Multhopp, H.: Aerodynamics of the Fuselage. NACA TM 1036, 1942.

68. Imlay, Frederick H.: The Estimation of the Rate of Change of
    Yawing Moment with Sideslip. NACA TN 636, 1938.

69. Pass, H. R.: Analysis of Wind-Tunnel Data on Directional Stability and Control. NACA TN 775, 1940.

70. Garbell, Maurice A.: Theoretical Principles of Wing-Tip Fins for Tailless Airplanes and their Practical Application. Jour. Aero. Sci., vol. 13, no. 10, Oct. 1946, pp. 525-536.

71. Shortal, Joseph A., and Draper, John W.: Free-Flight-Tunnel Investigation of the Effect of the Fuselage Length and the Aspect Ratio and Size of the Vertical Tail on Lateral Stability and Control. NACA ARR 3D17, 1943.

72. Bishop, Robert C., and Lomax, Harvard: A Simplified Method for Determining from Flight Data the Rate of Change of Yawing-Moment Coefficient with Sideslip. NACA TN 1076, 1946.

73. MacLachlan, Robert, and Levitt, Joseph: Wind-Tunnel Investigation of Effect of Canopies on Directional Stability Characteristics of a Single-Engine Airplane Model. NACA TN 1052, 1946.

74. Harper, Charles W., and Wick, Bradford H.: A Comparison of the Effects of Four-Blade Dual- and Single-Rotation Propellers on the Stability and Control Characteristics of a High-Powered Single-Engine Airplane. NACA ARR 4F17, 1944.

75. Paulson, John W., and Bennett, Charles V.: Stability and Control Characteristics of a Fighter Airplane in Inverted Flight Attitude as Determined by Model Tests. NACA ARR L5F25a, 1945.

76. Sweberg, Harold H., Guryansky, Eugene R., and Lange, Roy H.: Langley Full-Scale Tunnel Investigation of the Factors Affecting the Directional Stability and Trim Characteristics of a Fighter-Type Airplane. NACA ARR L5H09, 1945.

77. Queijo, M. J., and Wolhart, Walter D.: Experimental Investigation of the Effect of Vertical-Tail Size and Length and of Fuselage Shape and Length on the Static Lateral Stability Characteristics of a Model with 45° Sweptback Wing and Tail Surfaces. NACA TN 2168, 1950.

78. Johnson, Harold I.: Flight Investigation of the Effect of Various Vertical-Tail Modifications on the Directional Stability and Control Characteristics of a Propeller-Driven Fighter Airplane. NACA Rep. 973, 1950. (Formerly NACA RM L6J07.)

79. Bird, John D.: Some Theoretical Low-Speed Span Loading Characteristics of Swept Wings in Roll and Sideslip. NACA Rep. 969, 1950. (Formerly NACA TN 1839.)

80. Pitkin, Marvin, and Schade, Robert O.: Tests of a Linked Differential Flap System Designed to Minimize the Reduction in Effective Dihedral Caused by Power. NACA ARR L5F25, 1945.

81. Harmon, Sidney M.: Determination of the Damping Moment in Yawing for Tapered Wings with Partial-Span Flaps. NACA ARR 3H25, 1943.

82. Cotter, William E., Jr.: Summary and Analysis of Data on Damping in Yaw and Pitch for a Number of Airplane Models. NACA TN 1080, 1946.

83. Campbell, John P., and Mathews, Ward O.: Experimental Determination of the Yawing Moment Due to Yawing Contributed by the Wing, Fuselage, and Vertical Tail of a Midwing Airplane Model. NACA ARR 3F28, 1943.

84. Langley Stability Research Division (Compiled by Charles J. Donlan): An Interim Report on the Stability and Control of Tailless Airplanes. NACA Rep. 796, 1944. (Formerly NACA ACR L4H19.)

85. Campbell, John P., and Goodman, Alex: A Semiempirical Method for Estimating the Rolling Moment Due to Yawing of Airplanes. NACA TN 1984, 1949.

86. Goodman, Alex, and Fisher, Lewis R.: Investigation at Low Speeds of the Effect of Aspect Ratio and Sweep on Rolling Stability Derivatives of Untapered Wings. NACA Rep. 968, 1950. (Formerly NACA TN 1835.)

87. Queijo, M. J., and Jaquet, Byron M.: Calculated Effects of Geometric Dihedral on the Low-Speed Rolling Derivatives of Swept Wings. NACA TN 1732, 1948.

88. Swanson, Robert S., and Priddy, E. LaVerne: Lifting-Surface-Theory Values of the Damping in Roll and of the Parameter Used in Estimating Aileron Stick Forces. NACA ARR L5F23, 1945.

89. Goodman, Alex, and Adair, Glenn H.: Estimation of the Damping in Roll of Wings through the Normal Flight Range of Lift Coefficient. NACA TN 1924, 1949.

90. Polhamus, Edward C.: A Simple Method of Estimating the Subsonic Lift and Damping in Roll of Sweptback Wings. NACA TN 1862, 1949.

91. Murray, Harry E., and Wells, Evalyn G.: Wind-Tunnel Investigation of the Effect of Wing-Tip Fuel Tanks on Characteristics of Unswept Wings in Steady Roll. NACA TN 1317, 1947.

92. Bennett, Charles V., and Johnson, Joseph L.: Experimental Determina-
    tion of the Damping in Roll and Aileron Rolling Effectiveness of
    Three Wings Having 2°, 42°, and 62° Sweepback. NACA TN 1278, 1947.

93. MacLachlan, Robert, and Letko, William: Correlation of Two Experi-
    mental Methods of Determining the Rolling Characteristics of
    Unswept Wings. NACA TN 1309, 1947.

94. Maggin, Bernard, and Bennett, Charles V.: Low-Speed Stability and
    Damping-in-Roll Characteristics of Some Highly Swept Wings.
    NACA TN 1286, 1947.

95. Harmon, Sidney M.: Stability Derivatives at Supersonic Speeds of
    Thin Rectangular Wings with Diagonals ahead of Tip Mach Lines.
    NACA Rep. 925, 1949. (Formerly NACA TN 1706.)

96. Ribner, Herbert S.: The Stability Derivatives of Low-Aspect-Ratio
    Triangular Wings at Subsonic and Supersonic Speeds. NACA TN 1423,
    1947.

97. Ribner, Herbert S., and Malvestuto, Frank S., Jr.: Stability
    Derivatives of Triangular Wings at Supersonic Speeds. NACA
    Rep. 908, 1948. (Formerly NACA TN 1572.)

98. Spreiter, John R.: Aerodynamic Properties of Cruciform-Wing and
    Body Combinations at Subsonic, Transonic, and Supersonic Speeds.
    NACA TN 1897, 1949.

99. Malvestuto, Frank S., Jr., and Margolis, Kenneth: Theoretical
    Stability Derivatives of Thin Sweptback Wings Tapered to a Point
    with Sweptback or Sweptforward Trailing Edges for a Limited Range
    of Supersonic Speeds. NACA Rep. 971, 1950. (Formerly NACA
    TN 1761.)

100. Margolis, Kenneth: Effect of Thickness on the Lateral Force and
     Yawing Moment of a Sideslipping Delta Wing at Supersonic Speeds.
     NACA TN 1798, 1949.

101. Lampert, Seymour: Rolling and Yawing Moments for Swept-Back Wings
     in Sideslip at Supersonic Speeds. NACA TN 2262, 1951.

102. Jones, Arthur L., and Alksne, Alberta: The Yawing Moment Due to
     Sideslip of Triangular, Trapezoidal, and Related Plan Forms in
     Supersonic Flow. NACA TN 1850, 1949.

103. Jones, Arthur L.: The Theoretical Lateral-Stability Derivatives
     for Wings at Supersonic Speeds. Jour. Aero. Sci., vol. 17, no. 1,
     Jan. 1950, pp. 39-46.

104. Jones, Arthur L., Spreiter, John R., and Alksne, Alberta: The
     Rolling Moment Due to Sideslip of Triangular, Trapezoidal, and
     Related Plan Forms in Supersonic Flow. NACA TN 1700, 1948.

105. Harmon, Sidney M., and Martin, John C.: Theoretical Calculations
     of the Lateral Force and Yawing Moment Due to Rolling at Super-
     sonic Speeds for Sweptback Tapered Wings with Streamwise Tips.
     Supersonic Leading Edges. NACA TN 2156, 1950.

106. Margolis, Kenneth: Theoretical Calculations of the Lateral Force
     and Yawing Moment Due to Rolling at Supersonic Speeds for
     Sweptback Tapered Wings with Streamwise Tips. Subsonic Leading
     Edges. NACA TN 2122,1950.

107. Piland, Robert O.: Summary of the Theoretical Lift, Damping-in-
     Roll, and Center-of-Pressure Characteristics of Various Wing
     Plan Forms at Supersonic Speeds. NACA TN 1977, 1949.

108. Tucker, Warren A., and Piland, Robert O.: Estimation of the Damping
     in Roll of Supersonic-Leading-Edge Wing-Body Combinations.
     NACA TN 2151, 1950.

109. Harmon, Sidney M., and Jeffreys, Isabella: Theoretical Lift and
     Damping in Roll of Thin Wings with Arbitrary Sweep and Taper at
     Supersonic Speeds. Supersonic Leading and Trailing Edges.
     NACA TN 2114, 1950.

110. Jones, Arthur L., and Alksne, Alberta: The Damping Due to Roll
     of Triangular, Trapezoidal, and Related Plan Forms in Supersonic
     Flow. NACA TN 1548, 1948.

111. Brown, Clinton E., and Adams, Mac C.: Damping in Pitch and Roll
     of Triangular Wings at Supersonic Speeds. NACA Rep. 892, 1948.
     (Formerly NACA TN 1566.)

112. Lomax, Harvard, and Heaslet, Max A.: Damping-in-Roll Calculations
     for Slender Swept-Back Wings and Slender Wing-Body Combinations.
     NACA TN 1950, 1949.

113. Walker, Harold J., and Ballantyne, Mary B.: Pressure Distribution
     and Damping in Steady Roll at Supersonic Mach Numbers of Flat
     Swept-Back Wings with Subsonic Edges. NACA TN 2047, 1950.

114. Malvestuto, Frank S., Jr., Margolis, Kenneth, and Ribner, Herbert S.:
     Theoretical Lift and Damping in Roll at Supersonic Speeds of Thin
     Sweptback Tapered Wings with Streamwise Tips, Subsonic Leading
     Edges, and Supersonic Trailing Edges. NACA Rep. 970, 1950.
     (Formerly NACA TN 1860.)

115. Margolis, Kenneth: Theoretical Lift and Damping in Roll of Thin
     Sweptback Tapered Wings with Raked-In and Cross-Stream Wing Tips
     at Supersonic Speeds. Subsonic Leading Edges. NACA TN 2048,
     1950.

116. Goett, Harry J., and Pass, H. R.: Effect of Propeller Operation
     on the Pitching Moments of Single-Engine Monoplanes. NACA
     ACR, May 1941.

117. Milliken, William F., Jr.: Progress in Dynamic Stability and
     Control Research. Jour. Aero. Sci., vol. 14, no. 9, Sept. 1947,
     pp. 493-519.

118. Seamans, R. C., Jr., Blasingame, B. P., and Clementson, G. C.:
     The Pulse Method for the Determination of Aircraft Dynamic
     Performance. Jour. Aero. Sci., vol. 17, no. 1, Jan. 1950,
     pp. 22-38.

119. Greenberg, Harry: A Survey of Methods for Determining
     Stability Parameters of an Airplane from Dynamic Flight
     Measurements. NACA TN 2340, 1951.

120. Shinbrot, Marvin: A Least Squares Curve Fitting Method with
     Applications to the Calculation of Stability Coefficients from
     Transient-Response Data. NACA TN 2341, 1951.

TABLE I. - TABLE FOR CALCULATING OSCILLATORY STABILITY BOUNDARIES

Computation Procedure

1. Fill in values for the known geometric and mass characteristics and flight conditions (constants (1) to (11)).

2. Determine values of the tail-off stability derivatives (constants (28) to (35)) by methods presented in the text.

3. Select and enter in column (36) values of the independent variable C_{n_β} to cover the range for which the boundary is required.

4. Work out columns (37) and (38) to obtain values of $C_{Y_{\beta_{tail}}}$.

5. From these values of $C_{Y_{\beta_{tail}}}$, determine the tail contribution to the stability derivatives (columns (39) to (44)) by methods presented in the text.

6. Perform the operations indicated for constants (12) to (27) and columns (45) to (90) to obtain the values of Routh's discriminant R.

7. Solve for values of l_β the quadratics formed by setting the values in column (90) equal to zero (column (91) and (92)).

8. Solution of columns (93) and (94) gives the values of C_{l_β} required for neutral oscillatory stability for the values of C_{n_β} in column (36).

TABLE II.- REFERENCES CONTAINING USEFUL INFORMATION FOR ESTIMATING LATERAL STABILITY DERIVATIVES

Derivative	Subsonic		Supersonic (All are theoretical estimation methods.)						
	Estimation methods	Related data	▭	⬡	⬭	△	△	△	△
c_{Y_β}	1,25,26,27,28,29,30,31,32,33,34,35,36	37,38,39,40,41,42,43,44,45,46,47,48,49,50,51,52,53,54,55,56,57,58,59,60,61,62,63,64,65	95			96,97,98,99,100	99	101	
c_{n_β}	1,25,26,27,28,29,30,31,35,36,66,67,68,69,70	37,38,39,40,41,42,43,44,45,46,47,48,49,50,51,52,53,54,55,56,57,58,59,60,61,62,63,64,65,71,72,73,74,75,76,77,78	95,102,103		102,103	96,97,98,99,100,102,103	99,102,103	101	102
c_{l_β}	1,25,26,29,36,58,66,67,79	30,35,37,38,39,40,41,42,43,44,45,46,51,52,53,54,55,56,57,59,60,61,62,63,64,65,74,75,77,80	95,103,104		103,104	96,97,98,99,103,104	99,103,104		104
c_{Y_r}	25	58,59,60,65	95			96,97,99	99		
c_{n_r}	1,25,66,70,81,82,83,84	58,59,60,65	95,103		103	96,97,99,103	99,103		
c_{l_r}	1,25,26,66,85	58,59,60,65	95,103		103	96,97,99,103	99,103		
c_{Y_p}	25,26,36,86,87	65	95			96,97,99	99	105,106	
c_{n_p}	1,25,26,36,66,79,86	65	95,103		103	96,97,99,103	99,103	105,106	
c_{l_p}	1,25,26,36,66,79,87,88,89,90	57,65,86,91,92,93,94	95,103,107,108	107,109	103,110	96,97,99,103,107,108,110,111,112	99,103,107,112	107,112,113,114	110,112,115

NACA
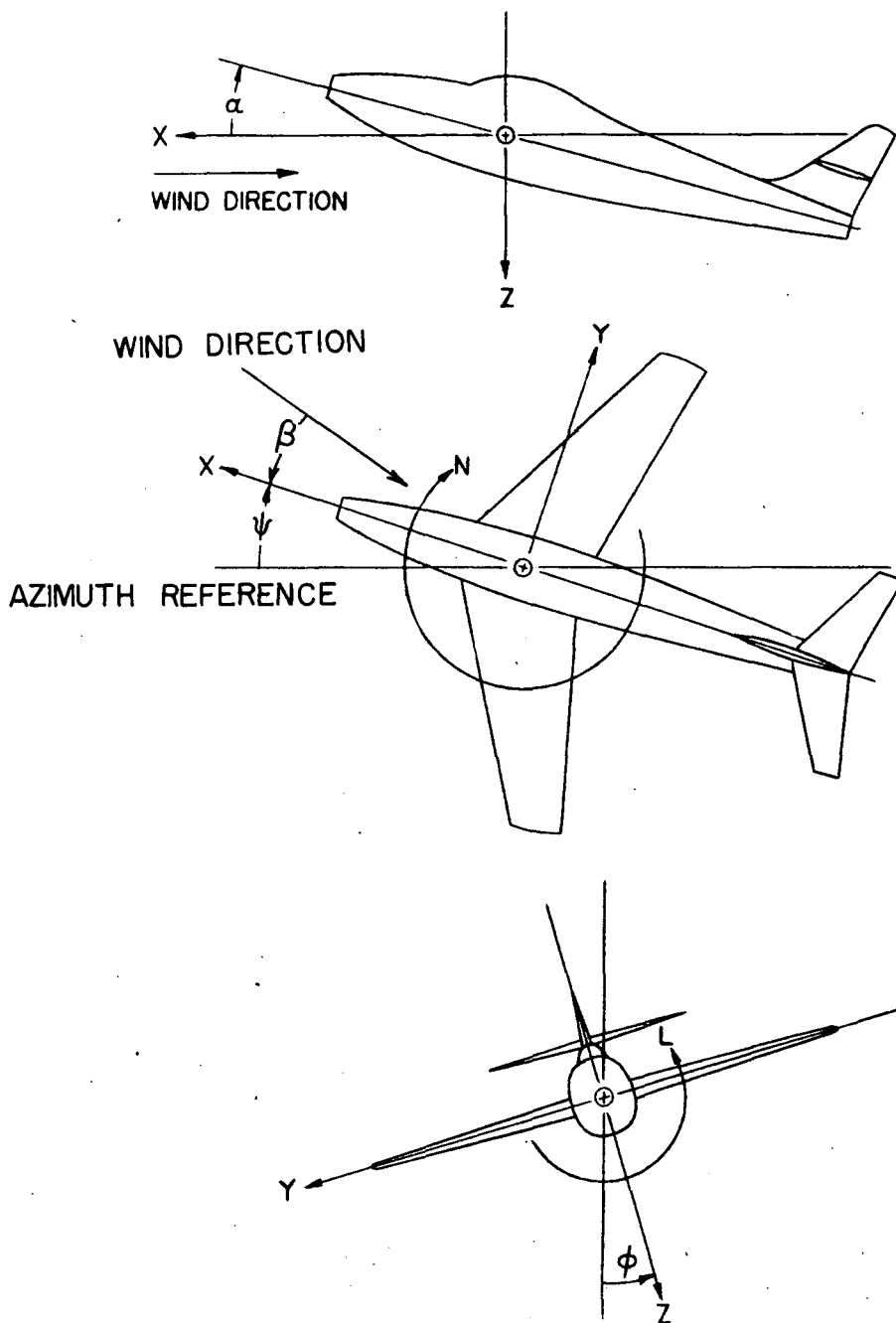
Figure 1.- The stability system of axes. Arrows indicate positive direc-
tions of moments, forces, and angles. This system of axes is defined
as an orthogonal system having the origin at the center of gravity and
in which the Z-axis is in the plane of symmetry and perpendicular to
the relative wind, the X-axis is in the plane of symmetry and perpendi-
cular to the Z-axis, and the Y-axis is perpendicular to the plane of
symmetry. At a constant angle of attack, these axes are fixed in the
airplane.
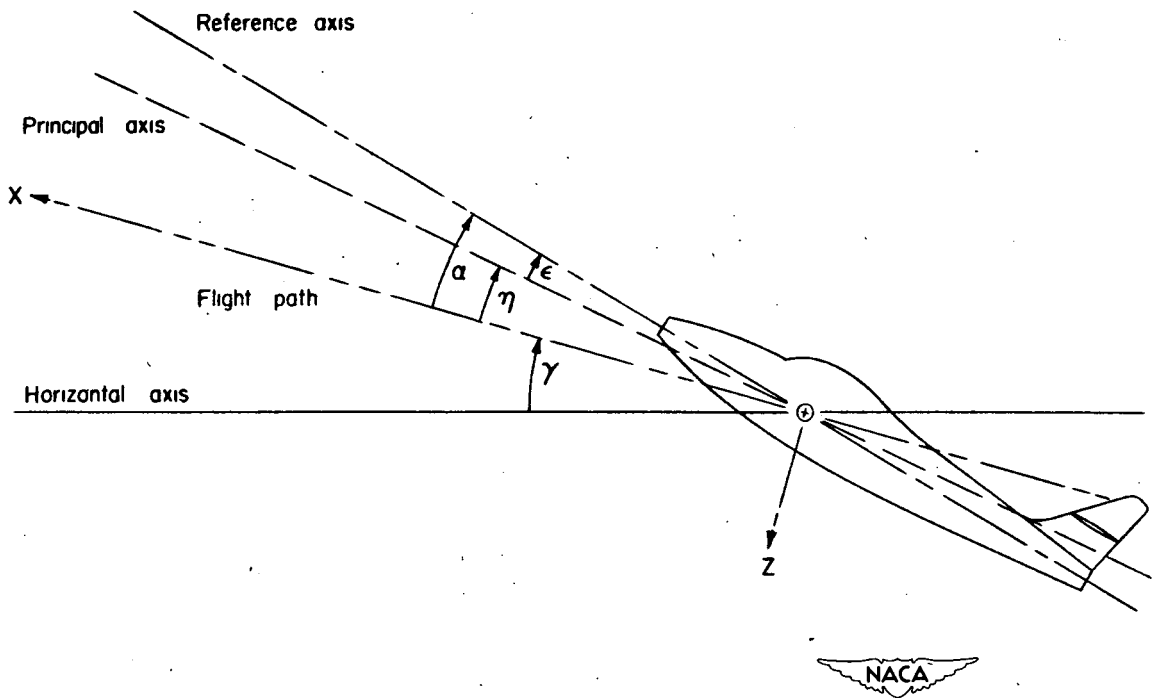
Figure 2.- System of axes and angular relationship in flight. Arrows indicate positive direction of angles. $\eta = \alpha - \epsilon$.

(a) Gust disturbance

(b) Control manipulation

(c) Gust disturbance and corrective control manipulation
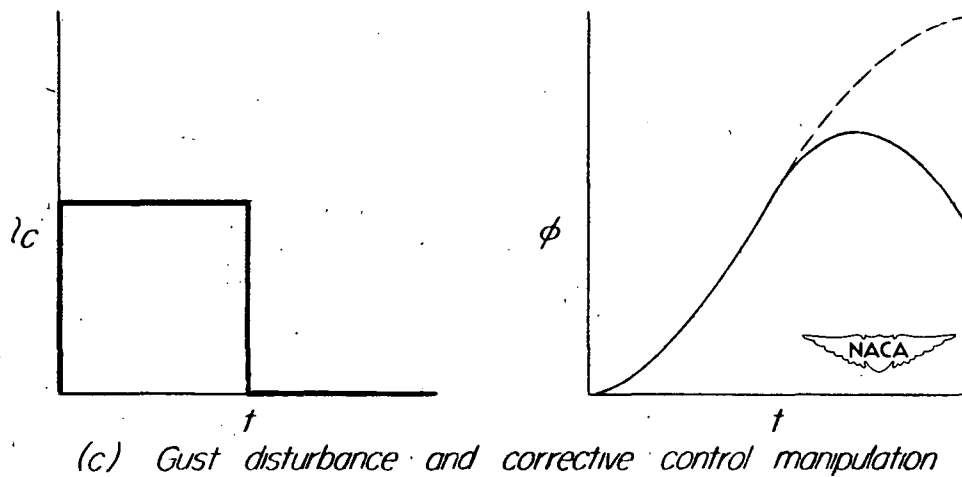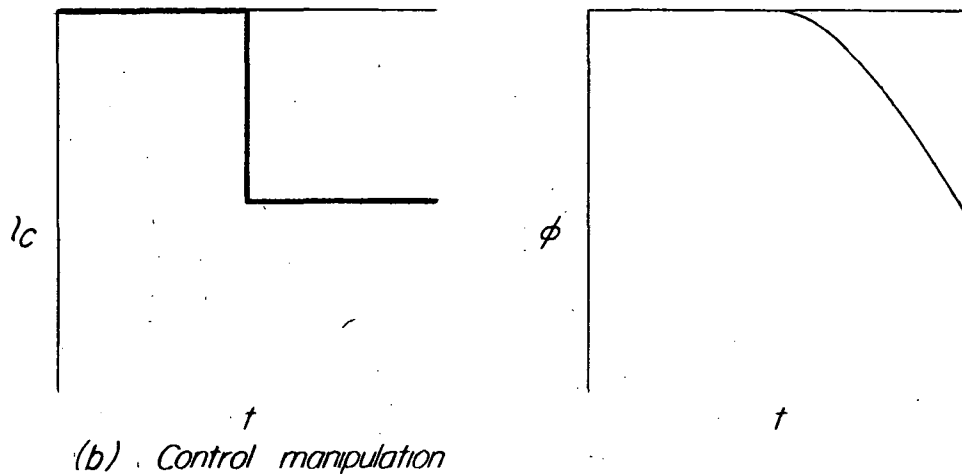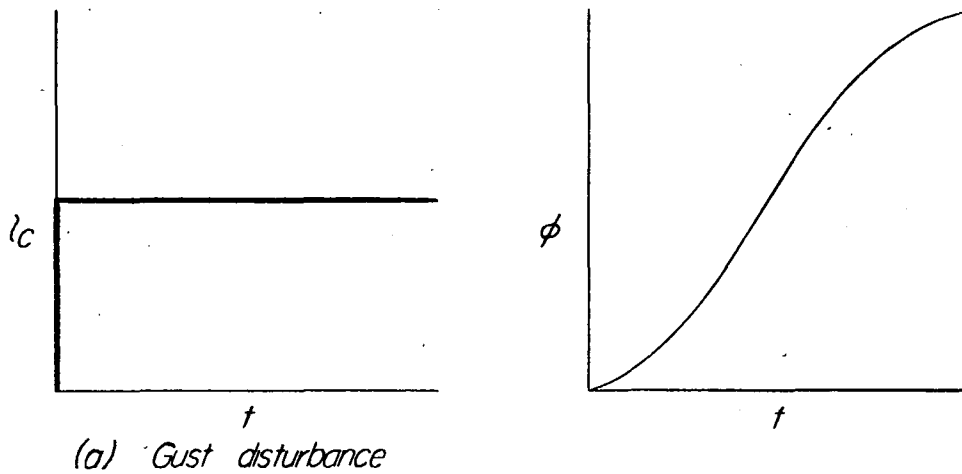
Figure 3.- Illustration of superposition of motions to determine effect
of arbitrary disturbances.
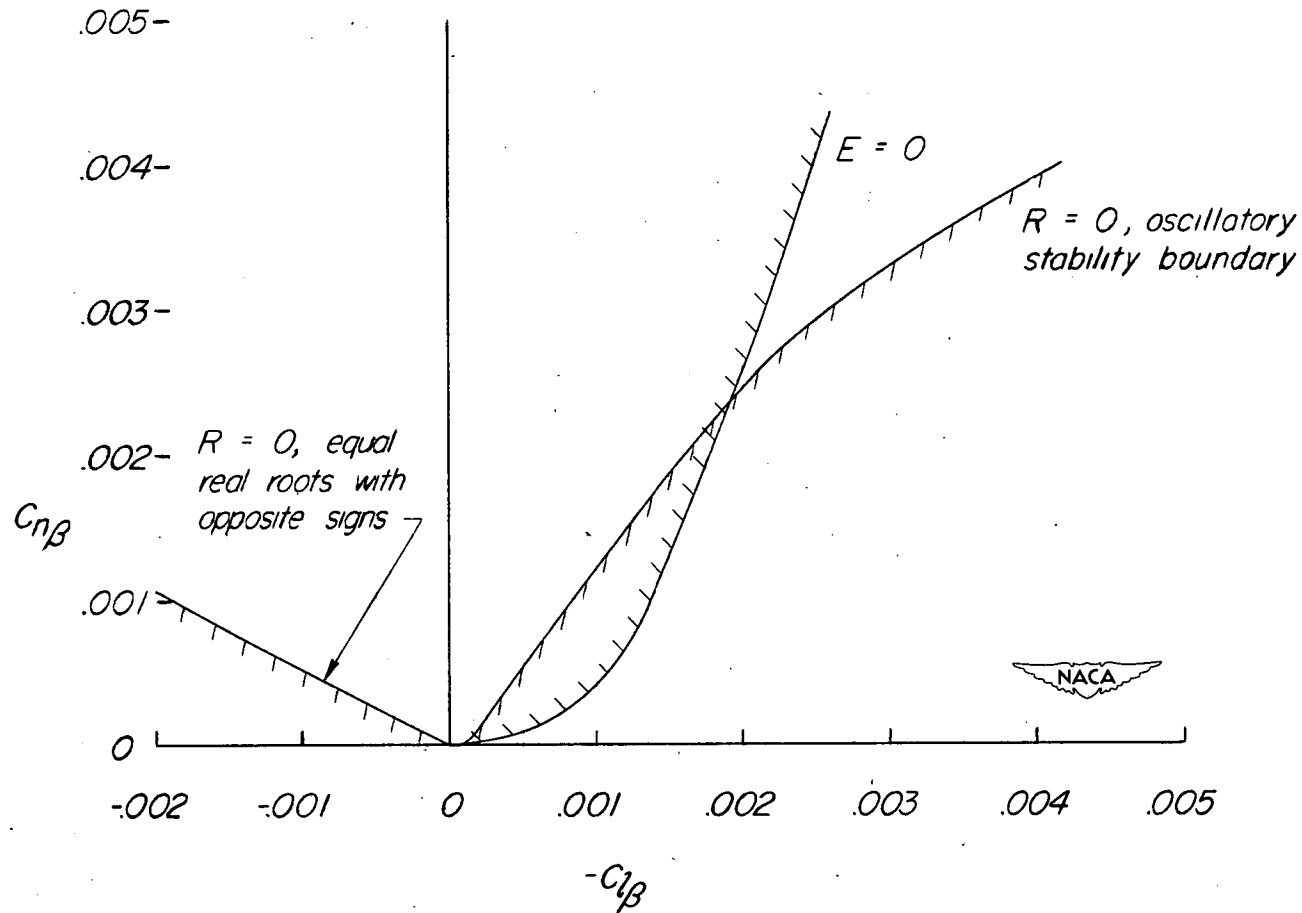
Figure 4.- Lateral-stability boundaries calculated in table I. C_{l_β} was the dependent variable. C_{n_β} was the independent variable. C_{n_β} was actually varied by changing $C_{Y_{\beta_{tail}}}$. Varying C_{n_β} in this manner caused changes in the tail contribution to all the other derivatives.
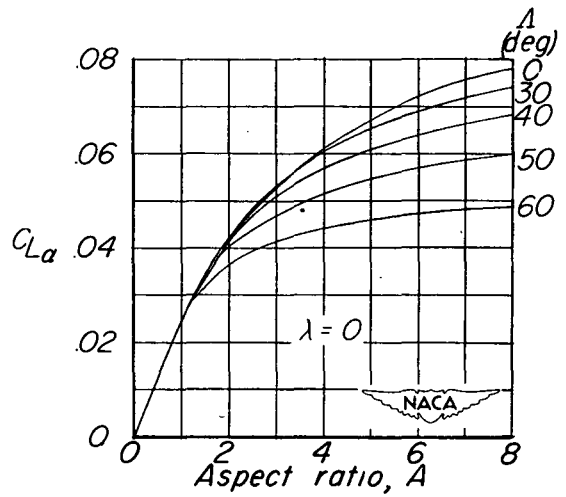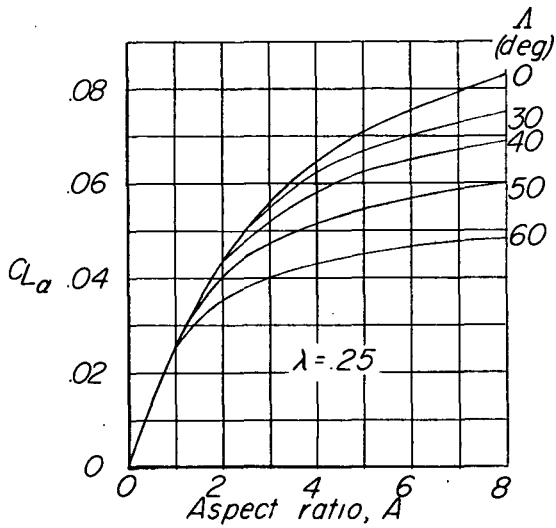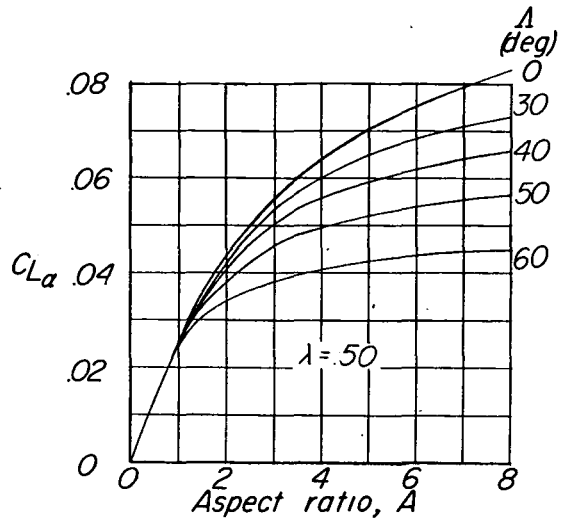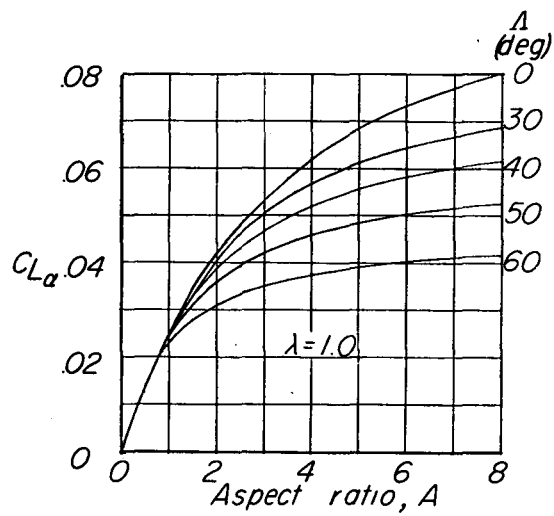
Figure 5.- Variation of lift-curve slope with aspect ratio, taper ratio, and sweepback for the case of subsonic incompressible flow. $a_0 = 0.11$. Values from reference 34.
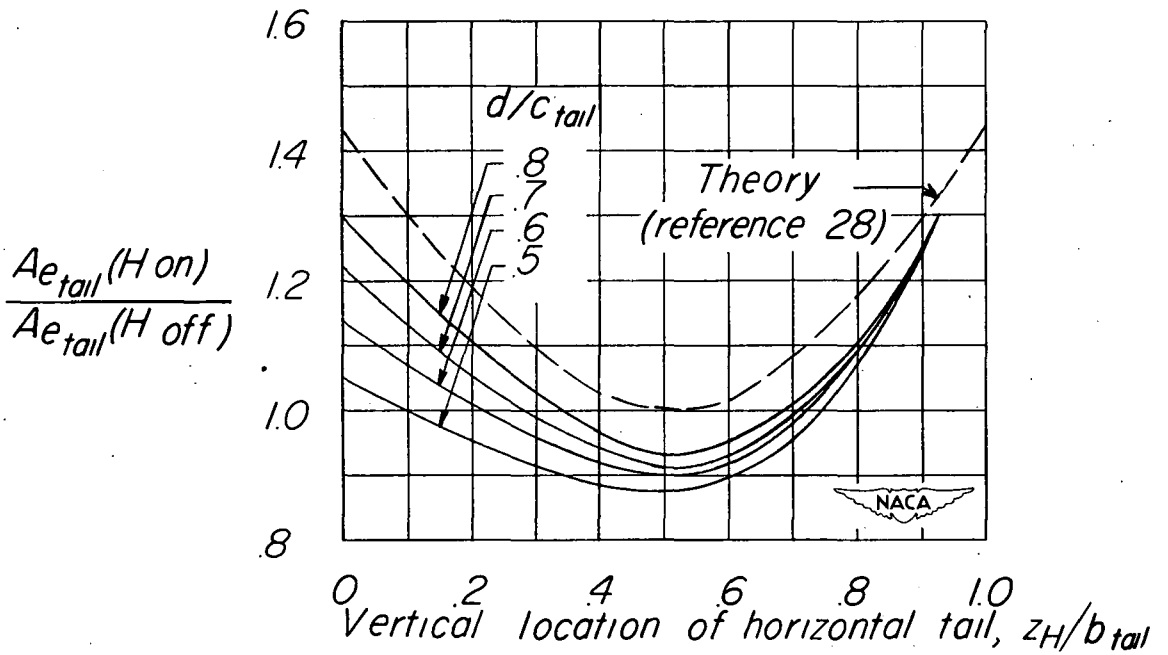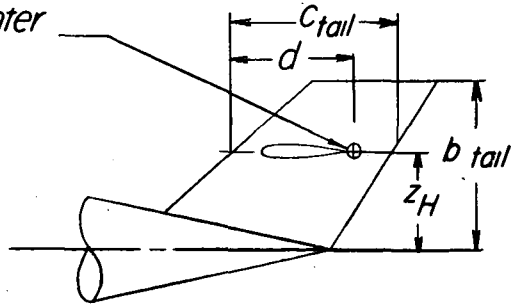
Figure 6.- Effect of horizontal-tail location on the effective aspect
ratio of the vertical tail $\left(Ae_{tail}\right)$ for the case of subsonic incom-
pressible flow. $\alpha = 0^o$. Taken from reference 35.
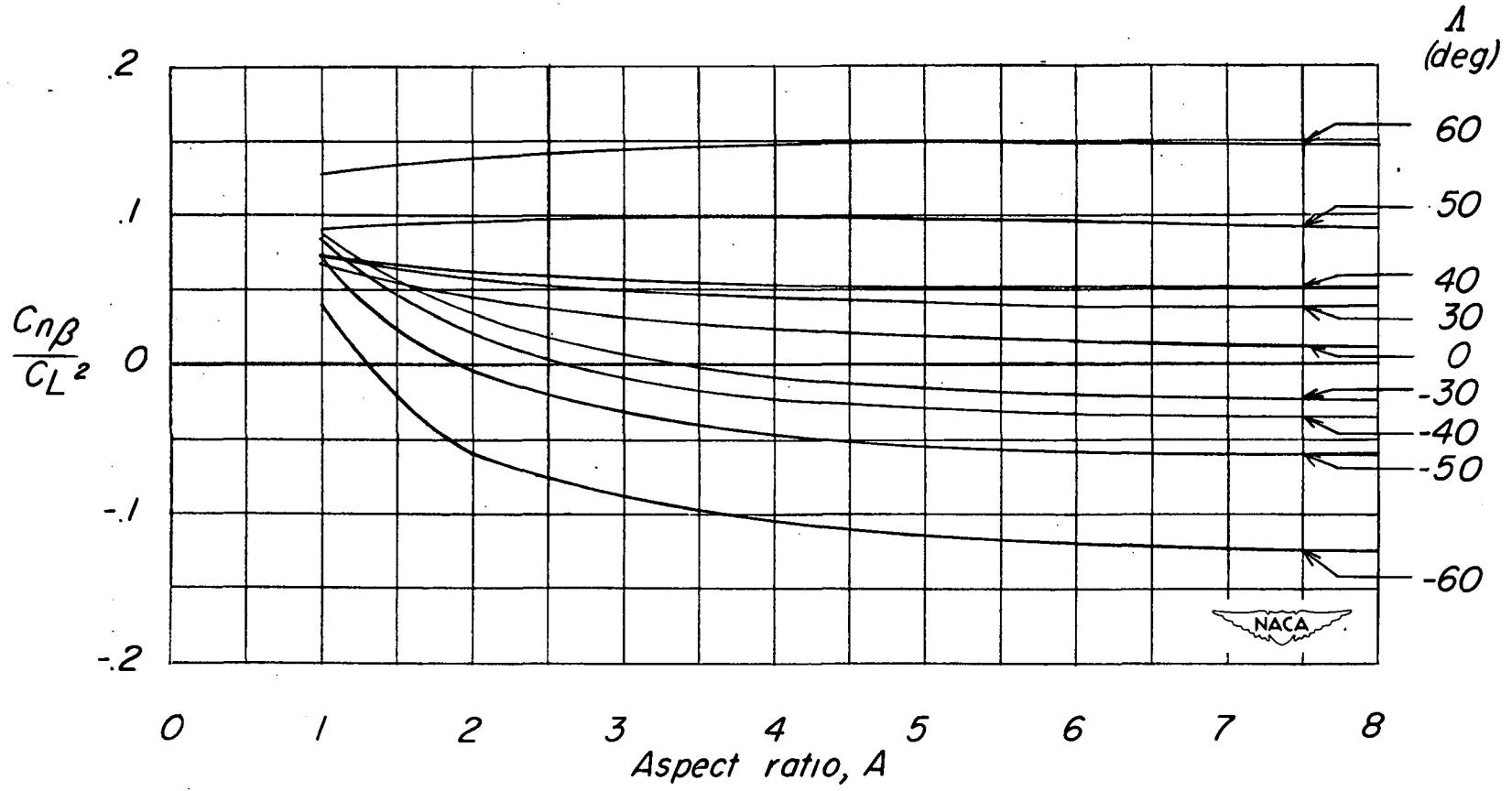
Figure 7.- Variation of C_{n_β}/C_L^2 with aspect ratio and sweep for the case of subsonic incompressible flow. $\lambda = 1.0$; $\frac{\bar{x}}{\bar{c}} = 0$. Taken from reference 25.
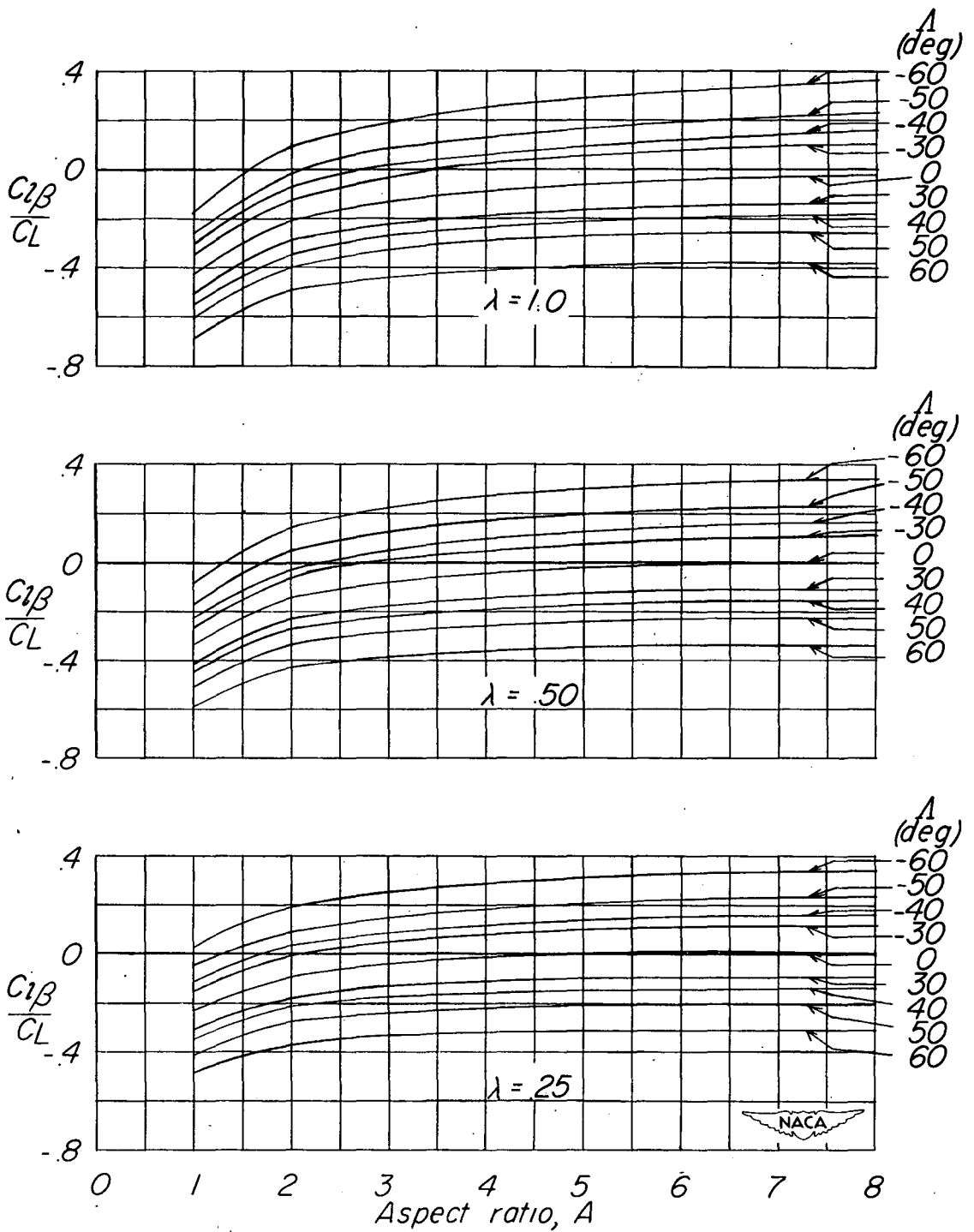
Figure 8.- Variation of C_{l_β}/C_L with aspect ratio, taper ratio, and

sweep for the case of subsonic incompressible flow. Based on method
of reference 25.
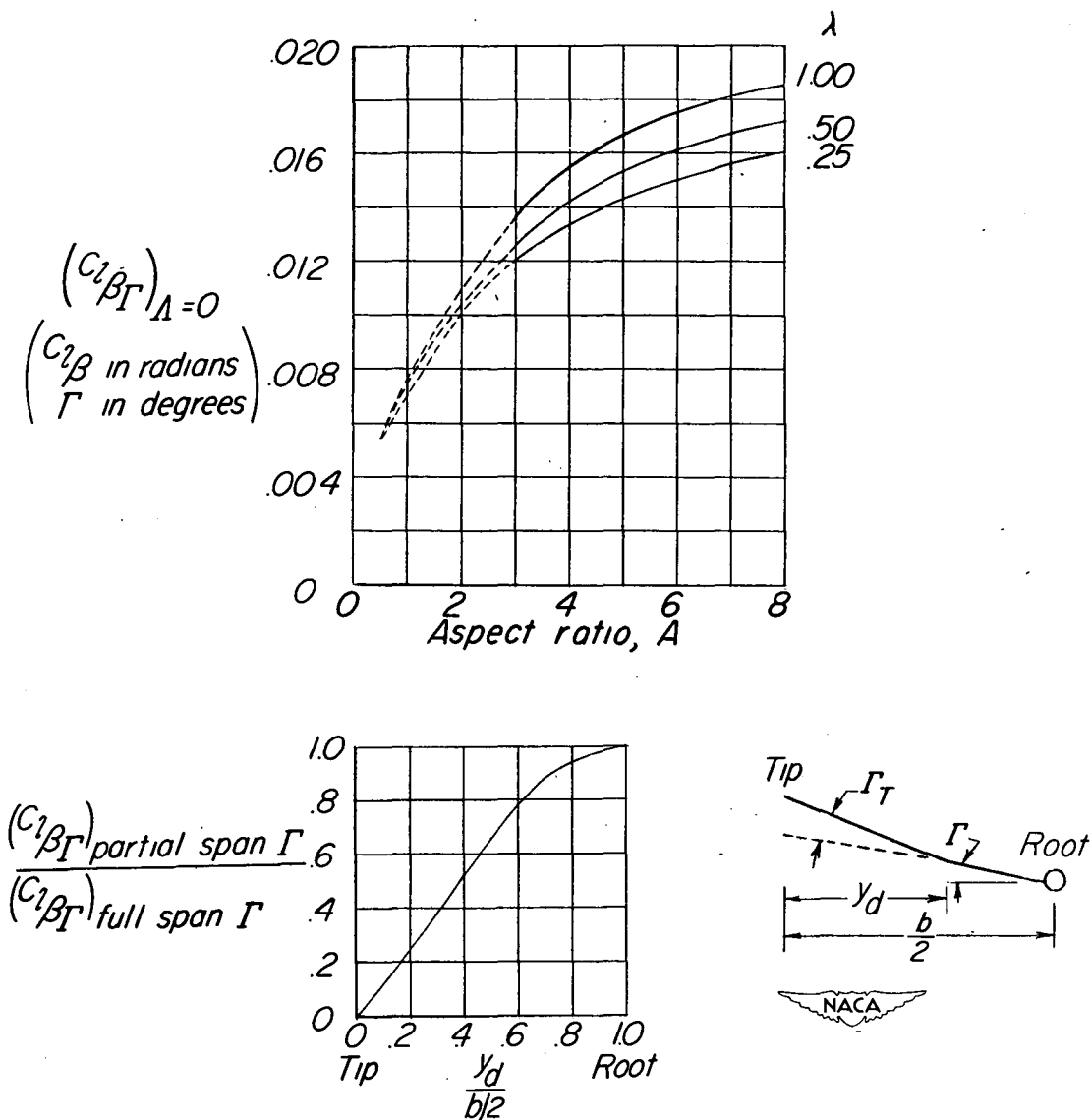
Figure 9.- Effect of dihedral angle on C_{l_β} for the case of subsonic incompressible flow. Taken from reference 58 and 66.

$$C_{l_\beta} = C_{l_{\beta_\Gamma}} \left[\Gamma - \frac{\left(C_{l_{\beta_\Gamma}}\right)_{\text{partial span }\Gamma}}{\left(C_{l_{\beta_\Gamma}}\right)_{\text{full span }\Gamma}} \Gamma_T \right]$$

where

$$C_{l_{\beta_\Gamma}} = \frac{(A + 4)\cos \Lambda}{A + 4 \cos \Lambda} \left(C_{l_{\beta_\Gamma}}\right)_{\Lambda=0}$$
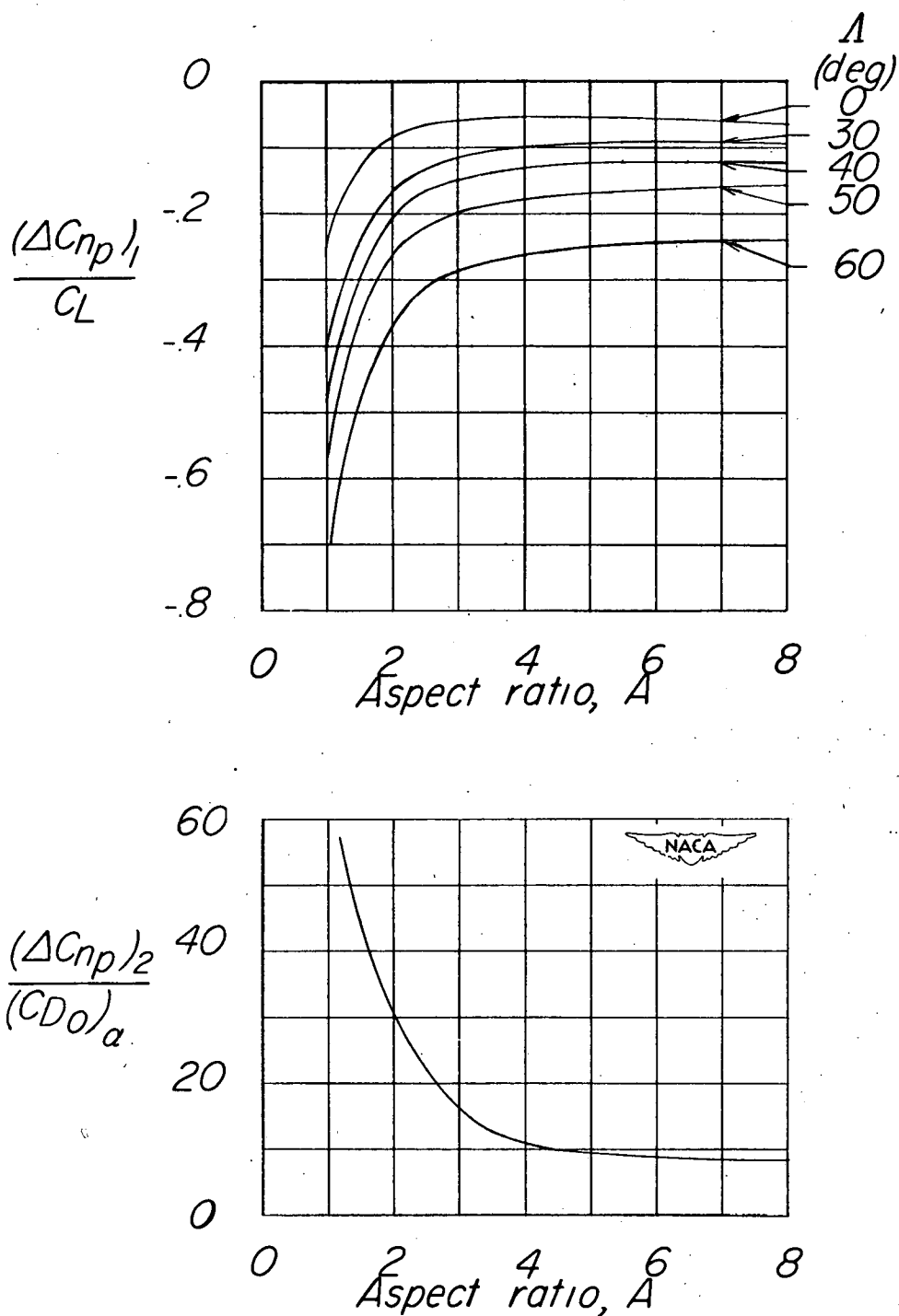
Figure 10.- Variation of $\left(\Delta C_{n_p}\right)_1 / C_L$ and $\left(\Delta C_{n_p}\right)_2 / \left(C_{D_o}\right)_\alpha$ with aspect ratio for the case of subsonic incompressible flow. $\lambda = 1.0$. Taken from reference 96.

$$C_{n_p} = \frac{\left(\Delta C_{n_p}\right)_1}{C_L} C_L + \frac{\left(\Delta C_{n_p}\right)_2}{\left(C_{D_o}\right)_\alpha} \left(C_{D_o}\right)_\alpha$$
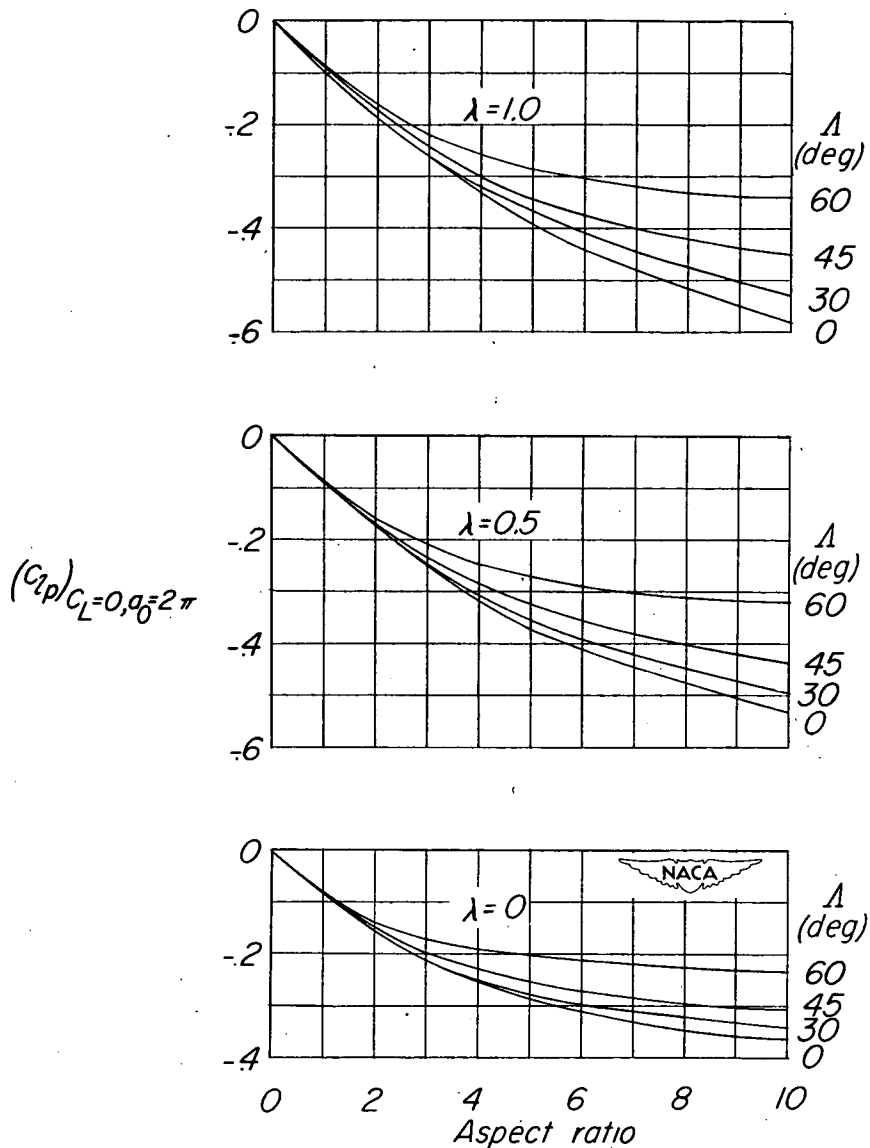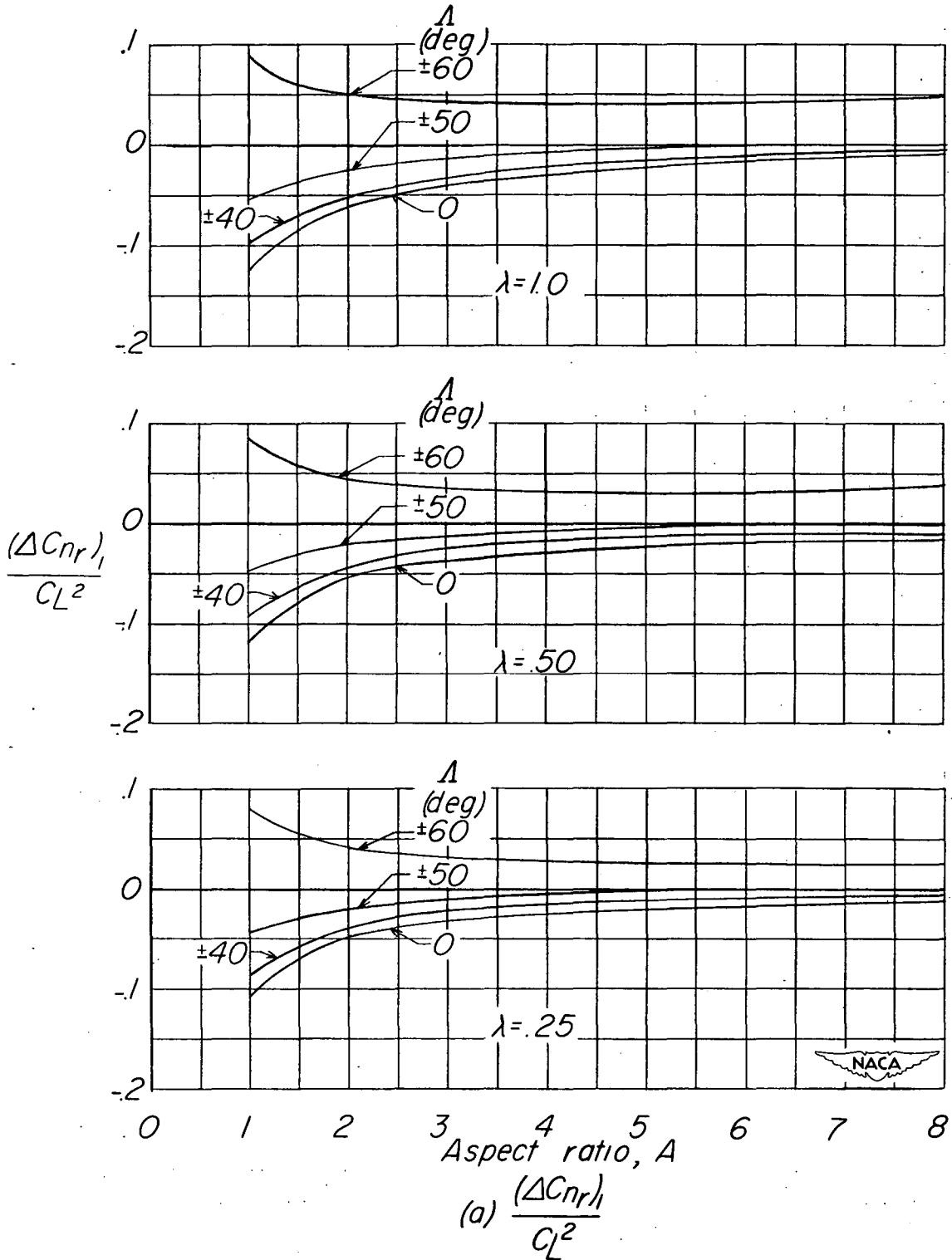
Figure 11.- Charts and formulas for estimating C_{l_p} for the case of subsonic incompressible flow. Taken from reference 89.

$$C_{l_p} = \left(C_{l_p}\right)_{C_L=0} \frac{\left(C_{L_\alpha}\right)_{C_L}}{\left(C_{L_\alpha}\right)_{C_L=0}} - \frac{1}{8} \frac{C_L^2}{\pi A \cos^2\Lambda} \left(1 + 2 \sin^2\Lambda \frac{A + 2 \cos \Lambda}{A + 4 \cos \Lambda}\right) - \frac{1}{8}\left(C_D - \frac{C_L^2}{\pi A}\right)$$

where

$$\left(C_{l_p}\right)_{C_L=0} = \left(C_{l_p}\right)_{C_L=0,a_0=2\pi} \frac{A + 4 \cos \Lambda}{\left(\frac{2\pi}{a_0}\right)A + 4 \cos \Lambda}$$

Figure 12.- Charts and formula for estimating C_{n_r} for the case of subsonic incompressible flow. Taken from reference 25.

$$C_{n_r} = C_L{}^2 \frac{\left(\Delta C_{n_r}\right)_1}{C_L{}^2} + C_{D_o} \frac{\left(\Delta C_{n_r}\right)_2}{C_{D_o}}$$
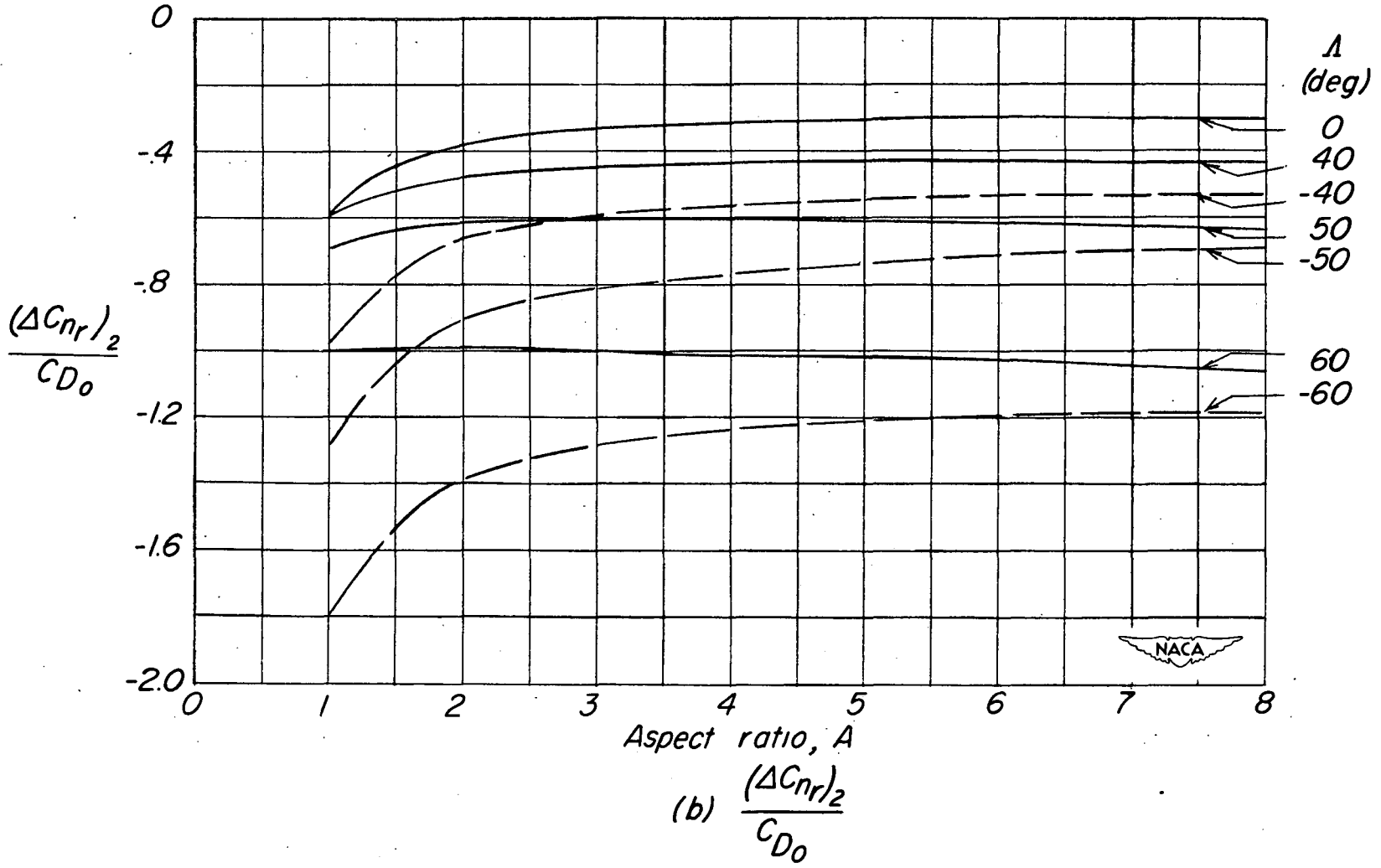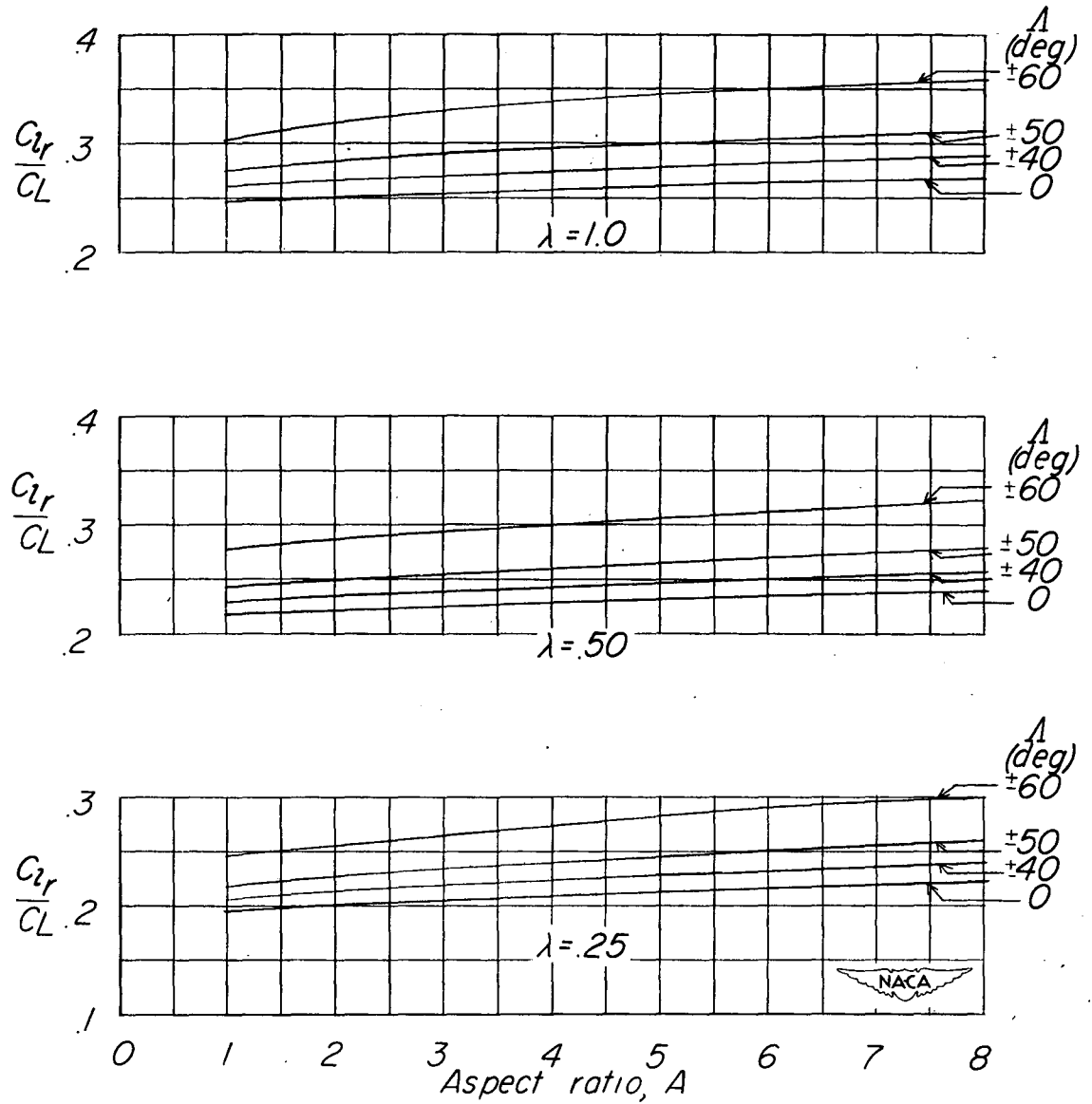
(b) $\dfrac{(\Delta C_{n_r})_2}{C_{D_0}}$

Figure 12.- Concluded.

Figure 13.- Charts and formula for estimating C_{l_r} for the case of subsonic incompressible flow. Taken from reference 85.

$$C_{l_{r_{wing}}} = C_L \left(\frac{C_{l_r}}{C_L}\right)_{theory} + C_L \left(\frac{C_{l_\beta}}{C_L}\right)_{theory} - C_{l_{\beta_{exp}}}$$
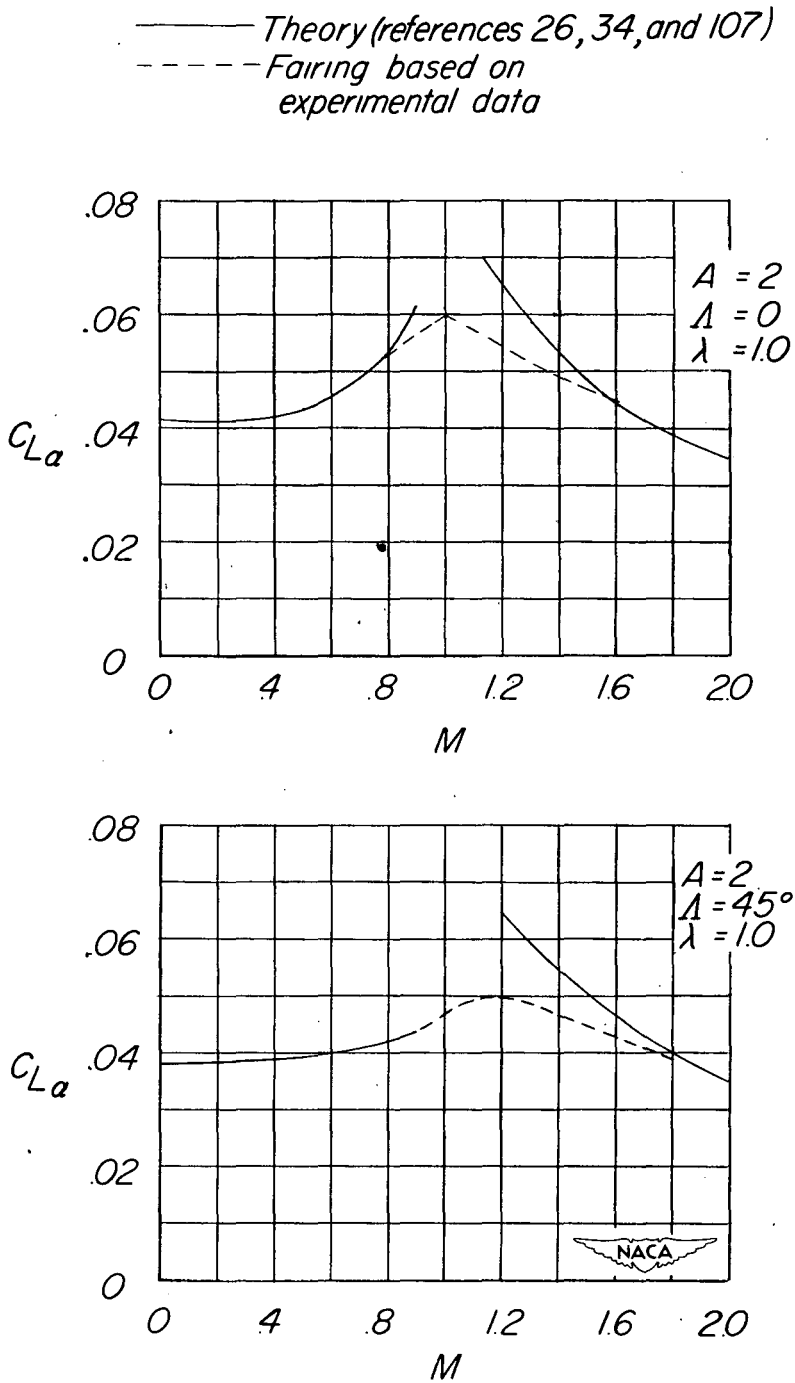
Figure 14.- Examples of suggested fairing of theoretical values of lift-
curve slope for use in estimating values for the vertical tail in the
transonic range.